DEFENSE TECHNICAL INFORMATION CENTER

Information for the Defense Community

DTIC® has determined on _4/16/2010_ that this Technical Document has the Distribution Statement checked below. The current distribution for this document can be found in the DTIC® Technical Report Database.

☒ **DISTRIBUTION STATEMENT A.** Approved for public release; distribution is unlimited. Per ERDC-CERL-IL

☐ **© COPYRIGHTED**; U.S. Government or Federal Rights License. All other rights and uses except those permitted by copyright law are reserved by the copyright owner.

☐ **DISTRIBUTION STATEMENT B.** Distribution authorized to U.S. Government agencies only (fill in reason) (date of determination). Other requests for this document shall be referred to (insert controlling DoD office)

☐ **DISTRIBUTION STATEMENT C.** Distribution authorized to U.S. Government Agencies and their contractors (fill in reason) (date of determination). Other requests for this document shall be referred to (insert controlling DoD office)

☐ **DISTRIBUTION STATEMENT D.** Distribution authorized to the Department of Defense and U.S. DoD contractors only (fill in reason) (date of determination). Other requests shall be referred to (insert controlling DoD office).

☐ **DISTRIBUTION STATEMENT E.** Distribution authorized to DoD Components only (fill in reason) (date of determination). Other requests shall be referred to (insert controlling DoD office).

☐ **DISTRIBUTION STATEMENT F.** Further dissemination only as directed by (inserting controlling DoD office) (date of determination) or higher DoD authority.

Distribution Statement F is also used when a document does not contain a distribution statement and no distribution statement can be determined.

☐ **DISTRIBUTION STATEMENT X.** Distribution authorized to U.S. Government Agencies and private individuals or enterprises eligible to obtain export-controlled technical data in accordance with DoDD 5230.25; (date of determination). DoD Controlling Office is (insert controlling DoD office).

REPORT DOCUMENTATION PAGE

Form Approved
OMB No. 0704-0188

The public reporting burden for this collection of information is estimated to average 1 hour per response, including the time for reviewing instructions, searching existing data sources, gathering and maintaining the data needed, and completing and reviewing the collection of information. Send comments regarding this burden estimate or any other aspect of this collection of information, including suggestions for reducing the burden, to Department of Defense, Washington Headquarters Services, Directorate for Information Operations and Reports (0704-0188), 1215 Jefferson Davis Highway, Suite 1204, Arlington, VA 22202-4302. Respondents should be aware that notwithstanding any other provision of law, no person shall be subject to any penalty for failing to comply with a collection of information if it does not display a currently valid OMB control number. **PLEASE DO NOT RETURN YOUR FORM TO THE ABOVE ADDRESS.**

1. REPORT DATE *(DD-MM-YYYY)*	2. REPORT TYPE	3. DATES COVERED *(From - To)*
03/31/2010	Final Report	06/25/2008 – 09/24/2009

4. TITLE AND SUBTITLE

Production of JP-8-Based Hydrogen and Advanced Tactical Fuels for the U.S. Military

5a. CONTRACT NUMBER

5b. GRANT NUMBER

W9132T-08-2-0014

5c. PROGRAM ELEMENT NUMBER

6. AUTHOR(S)

Zygarlicke, Christopher, J
Aulich, Ted, R
Wocken, Chad, A
Pflughoeft-Hassett, Debra, F
Buckley, Tera, D
Hurley, John, P
Jiang, Junhua

5d. PROJECT NUMBER

5e. TASK NUMBER

5f. WORK UNIT NUMBER

7. PERFORMING ORGANIZATION NAME(S) AND ADDRESS(ES)

University of North Dakota
Energy & Environmental Research Center
15 North 23rd Street, Stop 9018
Grand Forks, ND 58202-9018

8. PERFORMING ORGANIZATION REPORT NUMBER

2010-EERC-03-08

9. SPONSORING/MONITORING AGENCY NAME(S) AND ADDRESS(ES)

U.S. Army Corps of Engineers
Engineer Research and Development Center
2902 Newmark Drive
Champaign, IL 61822-1076

10. SPONSOR/MONITOR'S ACRONYM(S)

ERDC-CERL/ONR

11. SPONSOR/MONITOR'S REPORT NUMBER(S)

N/A

12. DISTRIBUTION/AVAILABILITY STATEMENT

Defense Technical Information Center
ATTN: DTIC-OCA
8725 John J. Kingman Road, Suite 0944

20100402021

13. SUPPLEMENTARY NOTES

N/A

14. ABSTRACT

The EERC conducted R&D for ERDC–CERL/ONR under Contract W9132T-08-2-0014 to develop fuel cell hydrogen/hydrocarbon fuel technologies to power vehicles and auxiliary power and stationary systems.

In Task 1, a high-pressure (HP) water-reforming process was modified to improve heat transfer to a catalyst bed for converting methane, methanol, ethanol, and sulfur-free jet fuel to H2. HP condensation effectively removed water. Physical absorption effectively captured non-H2 gases, resulting in a HP (6000 psi) gas stream containing 96% H2 when reforming methanol. HP-compatible ESA/electrochemical processes were developed/optimized for HP H2 purification. Testing of an electrically conductive high-surface-density monolithic adsorber from activated carbon at 800 psig showed no excessive heating and an acceptable purification level. Electrochemical H2 separation and purification based on reversible H2 oxidation and reduction reactions (ambient pressure and 140° 160° and 180°C operating temperatures using high-temperature polymer electrolyte

15. SUBJECT TERMS

fuel cell, hydrogen, alternative fuels, renewable jet fuel, coal, biomass, distributed energy systems, gasification, catalysts, thermochemical conversion, electrochemistry

16. SECURITY CLASSIFICATION OF:			17. LIMITATION OF ABSTRACT	18. NUMBER OF PAGES	19a. NAME OF RESPONSIBLE PERSON
a. REPORT	b. ABSTRACT	c. THIS PAGE	UU		
U	U	U			19b. TELEPHONE NUMBER *(Include area code)*

Standard Form 298 (Rev. 8/98)
Prescribed by ANSI Std. Z39.18

EERC DISCLAIMER

TABLE OF CONTENTS

LIST OF FIGURES

LIST OF FIGURES (continued)

LIST OF FIGURES (continued)

LIST OF TABLES

PRODUCTION OF JP-8-BASED HYDROGEN AND ADVANCED TACTICAL FUELS FOR THE U.S. MILITARY COOPERATIVE AGREEMENT NO. W9132T-08-2-0014 FINAL PROJECT REPORT FOR THE PERIOD JUNE 25, 2008 – SEPTEMBER 24, 2009

EXECUTIVE SUMMARY

The University of North Dakota Energy & Environmental Research Center (EERC) worked with the U.S. Army Corps of Engineers Engineering Research and Development Center (ERDC) in Champaign, Illinois, to develop and demonstrate the production of hydrogen and hydrocarbon fuels for use at military installations. In 2005, EERC began the first phase of a multiyear program to develop, optimize, and demonstrate the military viability of an EERC-developed technology for on-demand production of high-pressure hydrogen for fuel cell electric hybrid (FCEH) vehicles. A broad goal of the program was to develop a military logistics fuel-based hydrogen supply scenario that enables battlefield use of hydrogen in highly efficient FCEH vehicles. A second goal was to develop advanced tactical fuels with JP-8 drop-in compatibility and superior hydrogen-reforming properties from domestic or indigenous fossil feedstocks such as coal, natural gas, and petroleum coke and renewable feedstocks such as crop oils and biomass. Herein is a final report for work conducted from June 25, 2008 – September 24, 2009, under the project entitled *Production of JP-8-Based Hydrogen and Advanced Tactical Fuels for the U.S. Military*, under Cooperative Agreement No. W9132T-08-2-0014.

This report describes technical work conducted under Task 1, hydrogen production, purification, and vehicle development and demonstration, and Task 2, the development of alternative (nonpetroleum) feedstock-based technologies for production of advanced tactical fuels with JP-8 drop-in compatibility and improved properties for use as hydrogen feedstocks. Overall project management and select strategic studies are included in Task 3.

Subtask 1.1

Optimization experiments were conducted in an EERC-developed high-pressure hydrogen production unit. The process converts liquid, organic feedstock, and water into a high-pressure, hydrogen-rich gas stream. A modified reactor was developed and demonstrated. This reactor provided improved heat transfer to the catalyst bed. In order to decrease the load on downstream purification equipment, the removal of nonhydrogen gases at high pressure was also investigated via high-pressure condensation and physical adsorption techniques.

High-pressure condensation was not effective at removing nonhydrogen gases. Physical adsorption, however, was effective at capturing nonhydrogen gases, specifically carbon dioxide. Installing the physical adsorption vessel resulted in a high-pressure gas stream (6000 psi) that contained 96 mol% hydrogen.

Subtask 1.2.1

Under this activity, the EERC is evaluating the use of the Oak Ridge National Laboratory (ORNL)-developed electrical swing adsorption (ESA) process for purification of high-pressure hydrogen produced from the HPWR process. If successful, the ESA process has the potential to significantly increase the production efficiency and lower the power costs of purification relative to the standard method used at low pressures: pressure swing adsorption.

The first task was to develop an electrically conductive high-surface-density monolithic adsorber for use in the system. Three routes were pursued, all involving the creation or use of activated carbon as the base adsorber material. In two routes, we attempted to first make very high density carbon monoliths using carbon fibers and/or phenolic resins and then activate the monolith. This technique was not successful because the level of activation of the carbon; i.e., the increase in adsorptivity due to partial oxidation was always much lower than can be found in commercial activated carbons. Therefore, we focused on making monoliths from commercially available powdered activated carbon. This effort was successful in making monoliths with approximately twice the surface area density of the powdered material, an electrical resistivity of 1.2 inch-ohms, and a compressive strength of 3500 pounds per square inch. Adsorptivity of the monoliths was tested by passing a mixture of H_2, CH_4, CO, and CO_2 gases through cylinders of the material at up to 800 psig. These tests demonstrated that the cylinders were very good at providing high-purity hydrogen from a gas mixture. However, significant heating occurred when an electric current was passed through the saturated monoliths during attempted regeneration. Therefore, a method of treating the activated carbon was developed to reduce its electrical resistivity by a factor of 10. The new material will be tested at higher pressures in the pilot-scale test system described below.

Work in this activity also continued with design and construction of the 12,000 psi ESA test system. Before the design of the system was finalized, two project engineers were trained in high-pressure hydrogen technology and safety. A quantifiable risk assessment of the system was performed in order to ensure safe remote operation in an open pilot plant setting. Risk needed to be equivalent to or better than that experienced by workers at a commercial hydrogen-fueling station. One engineer also obtained certification as a hydrogen safety engineer. The system was designed for remote operation, and all electrical components met the National Electrical Code Class 1 Division 2 rating for operation in environments that may contain explosive gases.

The 12,000 psi ESA test system creates simulated reformate gases by blending pure gases from cylinders, which are then compressed to up to 12,000 psi and passed through the adsorber monoliths. Changes in gas composition at the outlet can be continuously measured with a laser gas analyzer, and temperature changes in the monoliths can be monitored by six embedded thermocouples. Electric currents can be passed through the monoliths to determine how well the adsorbed gases are driven off and how temperature changes during that process. The system will be used in future work in this activity to refine operating procedures, determine gas adsorptivity and breakthrough behavior at high pressure, and develop monolith regeneration procedures. As of the end of this phase of work, the 12,000 psi ESA test system was constructed and ready for shakedown and testing.

Subtask 1.2.2

The development of efficient, cost-effective, and scalable hydrogen separation and purification technologies are key requirements for the advancement of a hydrogen economy since ultrapure hydrogen (99.9% H_2) is the ideal fuel for polymer electrolyte membrane fuel cells. Electrochemical hydrogen separation and purification using proton exchange membranes was based on reversible hydrogen oxidation and reduction reactions. It is expected that minimal power should be required to operate the electrochemical process, and the hydrogen purity produced at the cathode is very high. Hydrogen normally produced from hydrocarbons contains a level of CO up to 2%. This high CO level requires the development of an electrochemical hydrogen purification technology based on high-temperature proton-conducting membranes since Pt catalysts can tolerate such high CO levels without significant activity degradation at increased temperature.

The electrochemical hydrogen purification process was investigated using high-temperature polymer electrolyte membranes at ambient and increased pressure. All electrochemical experiments were performed using a 50-cm^2 active area electrochemical cell comprising two metal end plates, two parallel multichannel serpentine flow field graphite plates, and a high-temperature membrane–electrode assembly (MEA). During each run, a simulated gas stream consisting of 76% H_2, 2% CO, 2% CH_4, and 20% CO_2 was supplied to the anode side, and high-purity nitrogen was fed to the cathode side to carry hydrogen purified for gas analysis.

The feasibility of the electrochemical hydrogen purification process was demonstrated, and the electrochemical process was optimized at ambient pressure. At three operating temperatures of 140°, 160°, and 180°C, only hydrogen was produced at the cathode. Moreover, the current efficiency for the hydrogen purification process was higher than 90% at the three temperatures above and at a constant current of 200 mA cm^{-2}. The cell voltage measured at this constant current density was dependent upon the operating temperature. At 140°C, a value of around 0.14 V was obtained. This value was decreased to around 0.06 V when the temperature was increased to 180°C. Moreover, it was found that the cell voltage almost remained constant at controlled constant current polarizations. The purification process was further investigated as a function of process start-up and shutdown. Exclusive hydrogen gas at the cathode, high current efficiency, and stable low cell voltage were reproduced.

Work was initialized on tailoring the process for use at elevated pressure. The next phase of work will focus on the feasibility demonstration and optimization of the high-pressure hydrogen purification processes.

Subtask 2.1

The EERC developed an advanced distributed-scale gasifier that can convert widely available complex waste resources into energy, liquid fuels, or hydrogen. The gasifier accommodates fuel composition variations that attain self-sustained, steady-state gasification in the simplest configuration while maintaining near-zero effluent discharge. The new gasification design was tested for improved performance using a wide range of biomass fuel.

The fuels selected for self-sustained gasification experiments were high-moisture biomass waste (moisture ranging from 35% to 60%), high-moisture PRB coal (26%–30%), and creosote-treated railroad ties–a hybrid fuel having characteristics of woody biomass (base material is oak wood) but with an included creosote (complex mixture of coal tar).

Woody biomass containing moisture greater than 50% was tested during a 24-hour gasification test. Desired variations in syngas composition for application in the liquid synthesis process (high H_2/CO ratio) and electricity production (high CO/H_2) ratio were achieved by varying the gasifier operating condition. The worst-case tar produced in case of wet biomass gasification was 3830 mg/m^3 and 290 mg/m^3 in hot and cold syngas, respectively. The particulate matter concentration determined was 175 and 54 mg/m^3 in hot and cold syngas, respectively.

Tests using high moisture coal as feedstock also showed high H_2/CO and CO/CO_2 ratios in the syngas, which would be excellent syngas quality for hydrogen and liquid fuels production. During 13 hR steady state gasification of 35% moisture wood waste, hydrogen rich syngas composition was produced with an achieved average and highest H_2/CO ratio of 1.51 and 2.26 respectively. Such steady state gasification could be obtained on high moisture biomass for commercial liquid production system.

Tests on the creosote treated railroad ties were primarily concerned with lowering tar generation in the gasification process and removing tars with post-gasification scrubbing. The level of tar during steady-state gasification of railroad tie in the unscrubbed hot syngas and scrubbed syngas was determined to be 822 and 200 mg/m^3, respectively, while the particulate concentration was 353 and 32 mg/m^3, respectively. The cold-side tar contained about 83% toluene and xylenes which are typically used as performance enhancers in internal combustion engines. No tar heaver than naphthalene (only 7%) escaped the syngas polisher. Fine performance adjustments in the syngas polisher can lead to higher than 95% tar capture.

Overall, the performance study revealed that gasification efficiency greater than 80% could be achieved for fuel such as railroad ties and high-moisture biomass. The primary advantage of utilizing waste without requiring predrying is envisaged to be a simple system, and moisture could be used as gasification medium.

Subtask 2.2.1

In order to develop and demonstrate a bench-scale coal-/biomass-to-liquids process, three large batches of an iron-based, Fischer–Tropsch (FT) catalyst, 1 kilogram each, were prepared and evaluated in a lab-scale FT reactor. After the effectiveness of the catalyst was verified, the catalysts were loaded into the bench-scale FT reactor, which was used to convert coal–biomass derived syngas into FT liquids. The liquids were subsequently upgraded into synthetic isoparaffinic kerosene (SPK) that is compatible with military-grade JP-8 jet fuel.

Further tests were conducted on the FT iron catalyst preparation method in order to improve the repeatability of catalyst production and the stability and performance of the catalyst. It was determined that if the catalyst is exposed to atmospheric water vapor for extended periods

of time, activity and selectivity to heavier hydrocarbons will be negatively impacted. Also, the catalyst must be exposed to dry, flowing air during calcining in order to maximize performance.

The FT iron catalyst was promoted with varying amounts of lanthanum oxide to determine potential effects on catalyst productivity and product selectivity. It may be that small amounts of lanthanum help to improve selectivity to heavy hydrocarbons, but too much may negatively impact catalyst performance. The trials were confounded by excessive variation in iron and potassium loading on the catalyst, and the results of the experiment may be due in large part to the ratio of potassium to iron.

Various FT catalysts were received from a commercial catalyst supplier. These catalysts were tested in the small-scale FT reactor. The performance of the catalyst was evaluated and compared to the FT catalyst developed at the EERC. The results were reported back to the supplier to assist in improving the catalyst formulation for future tests.

Subtask 2.2.2

The EERC developed a process to convert plant- or animal-derived fats and oils into hydrocarbon fuels. The fuels produced from this process are chemically identical to their petroleum-derived counterparts.

Under Construction Engineering Research Laboratory (CERL) funding, experiments were conducted to support process scale-up. Laboratory experiments were conducted in continuous process systems, typically run at 0–6 L/hr. Feedstock flexibility was demonstrated. A feedstock-flexible process is less sensitive to specific feedstock prices and, therefore, reduces the economic risks associated with feedstock price volatility. To demonstrate feedstock flexibility, researchers experimented with many different crop oil and fatty acid feedstocks. Feedstock effect on product composition and quality was investigated. The process proved to be extremely feedstock-flexible with the only notable difference, when varying feedstock, being the chain length of the hydrocarbon product.

Operational parameters were also investigated in order to optimize the process and to reduce overall operating costs. Reactor pressure, oil feed rate, and hydrogen feed rate were varied to determine their effect on product quality. The minimum operating condition was found for each variable. Reaction kinetics were also investigated, and a kinetic model was developed to fit the experimental data. This model showed that the reaction was first order with respect to feedstock concentration and a fractional order with respect to hydrogen partial pressure.

Process integration strategies were investigated. The main conclusion from this analysis was that the high-cetane, low-sulfur, renewable hydrocarbon fuel that is produced from the EERC process could be a valuable product for refineries to blend into their existing diesel pool.

Subtask 2.3 Development of Modular Systems for Distributed Fuels and Energy

The EERC performed a brief evaluation of specific renewable technologies focused on the distributed production of fuels and/or energy. Technologies evaluated were biomass gasification

coupled with internal combustion engine, biomass gasification coupled with synthetic natural gas (SNG) production, biomass gasification coupled with the FT process, and catalytic hydrodeoxygenation isomerization (CHI).

Based on previous work on different projects by National Renewable Energy Laboratory, Princeton University, and the EERC, process efficiencies, energy balances, and block diagrams were determined for each process based on a "normalized" input Btu content of the feedstock, and output quantities and makeup were then derived.

Using these results the EERC evaluated these technologies for a specific military facility, Grand Forks Air Force Base (GFAFB) located near Grand Forks, North Dakota. Fuel and energy usage information was provided by GFAFB personnel, and each technology was evaluated to determine the potential to offset current fuels or energy usage.

Based on reasonableness of scale, cost, and feedstock availability, three technologies appear to warrant further study: 1) biomass gasification coupled with SNG production to offset propane usage, 2) diesel production using biomass gasification coupled with FT, and 3) CHI process to offset diesel usage.

Task 3

This task facilitated management of the entire project, Production of JP-8-Based Hydrogen and Advanced Tactical Fuels for the U.S. Military, under Cooperative Agreement No. W9132T-08-2-0014. Task 3 included all project management such as tracking deliverables and budgets, monthly and quarterly reporting, final reporting, internal project meetings, project review meetings with U.S. Army ERDC's CERL staff, and strategic studies.

In the area strategic studies and publications, a special ERDC/CERL technical report was initiated and completed to a draft copy. The technical report is entitled *Development and Demonstration of Hydrogen Production and Purification Systems for U.S. Military Fuel Cell Vehicles*. The report summarizes activities to date related to the development of the high-pressure hydrogen production, purification, refueling, and vehicle demonstration work.

A second major strategic studies effort involved work done to put together a biomass resource and characterization assessment for the contiguous United States. A report was written that gives the current status biomass availability for conversion to power and fuels. Biomass types considered included agricultural and forest residues and energy crops and urban residuals. Primary data consisted of county-by-county biomass resource types and estimates and also included some data on the chemical and physical properties of those sources. The study included some data and information on national land ownership, climate zones, and biomass-growing conditions. One conclusion drawn from the study is that there is no single ideal biomass source. While some sources may have ideal combustion and cofiring properties, such as wood, other sources are optimal feedstocks for fuel production, such as corn or soybeans. In addition, no type of biomass is uniformly available across the United States or even within individual states.

PRODUCTION OF JP-8-BASED HYDROGEN AND ADVANCED TACTICAL FUELS FOR THE U.S. MILITARY COOPERATIVE AGREEMENT NO. W9132T-08-2-0014 FINAL PROJECT REPORT FOR THE PERIOD JUNE 25, 2008 – SEPTEMBER 24, 2009

INTRODUCTION

The University of North Dakota Energy & Environmental Research Center (EERC) has been working with the U.S. Army Corps of Engineers Engineering Research and Development Center (ERDC) in Champaign, Illinois, to develop and demonstrate hydrogen and hydrocarbon fuels production and use at military installations. In 2005, the EERC was awarded a contract under Broad Agency Announcement (BAA) W9132T-04-R-BAA1: PEM Fuel Cell Demonstration and began the first phase of a multiyear program to develop, optimize, and demonstrate the military viability of an EERC-developed technology for on-demand production of high-pressure hydrogen for fuel cell electric hybrid (FCEH) vehicles. The overall goal of the program was to develop a military logistics fuel-based hydrogen supply scenario that enables battlefield use of hydrogen in highly efficient FCEH vehicles, thereby helping to meet the U.S. Army after Next (AAN) objective of a 75% reduction in battlefield petroleum use. Work performed previously under the Cooperative Agreement was documented in annual reports filed with ERDC.

In 2008 a new contract, Cooperative Agreement W9132T-08-2-0014, was awarded to the EERC to provide funding to continue the research and development of hydrogen and fuel production technologies with military relevance. This report includes work conducted under Cooperative Agreement W9132T-08-2-0014 during the reporting period of June 25, 2008, to September 24, 2009.

Cooperative Agreement W9132T-08-2-0014 has since been modified to provide additional funding for continued research and development and extends the Cooperative Agreement period of performance to January 1, 2011.

PREVIOUS KEY ACCOMPLISHMENTS

Since 2006, the following activities have been conducted:

- The EERC preliminarily evaluated the military viability of the high-pressure water reforming (HPWR) concept for on-demand production of high-pressure proton exchange membrane (PEM) fuel cell-quality hydrogen from JP-8, resulting in a positive proof-of-concept assessment.

- The EERC completed the design, fabrication, and shakedown of a pilot-scale (600-standard cubic feet/hour [1.5-kilograms/hour]) HPWR hydrogen production system.

- The EERC completed required facility upgrades for conducting HPWR system optimization activities.

- The EERC initiated partnership arrangements with major catalyst suppliers, including CRI International, Johnson Matthey, and Sud Chemie to enable project access to catalysts and/or catalyst combinations with the best potential for generating maximum hydrogen and minimum coke production in the HPWR system.

- HPWR process optimization testing was conducted using aromatics- and sulfur-free Syntroleum-produced "S-8" fuel as feedstock. Initial results have demonstrated good hydrogen production, as measured by product gas hydrogen concentrations of up to 56% (versus a maximum theoretical concentration of 75%), and indicated the need for increased S-8 "cracking" prior to hydrogen production to achieve a higher overall hydrogen yield.

- ePower designed and built a FCEH forklift to operate in the cold winter and hot summer weather of Grand Forks Army National Guard Base (GFARNGB). The forklift was delivered to GFARNGB and demonstrated for over 1 year before being decommissioned and returned to ePower. Development of an FCEH multipurpose utility vehicle (MPUV) was initiated and then halted after ePower Synergies was unable to meet the performance specification requirements with the first of two Bobcat® MPUVs. Two additional FCEH forklift vehicles were fabricated and delivered to Robins Air Force Base (AFB) for demonstration activities. The FCEH forklift vehicles were delivered to Robins AFB on December 18, 2007, and April 27, 2009.

- In collaboration with Kraus Global Inc. and Airgas, Inc., the EERC designed, fabricated, shook down, and installed at GFARNGB a hydrogen-dispensing system that delivers high-pressure hydrogen. The dispensing system was utilized at GFARNGB to refuel the ePower-designed FCEH forklift and provided an interim hydrogen supply to support FCEH vehicle demonstration activities in advance of a fully integrated HPWR-based hydrogen production, purification, and dispensing system running on JP-8. The EERC and ePower conducted a training session at GFARNGB on October 19, 2006, to provide instruction to base personnel on the proper and safe operation of the hydrogen refueler and the FCEH forklift.

- The EERC investigated options for increasing the density of commercially available activated carbon sorbents without reducing their surface areas. The purpose of this work was to create a high-density electrically conductive monolithic adsorber for purifying hydrogen at very high pressures. The monolithic design is necessary whether electrical, pressure, or thermal swinging is used to regenerate the adsorber. Monoliths have been made using mixtures of granular and powdered activated carbon tested at up to 800 psig. They are effective at adsorbing contaminants from the gas stream, leaving pure hydrogen.

- Tests of the regeneration of the monoliths at up to 800 psig using electric currents have shown significant heating of the monolith, indicating that gas desorption may be due to

the heating and not the electric current alone. However, we are working to make more electrically conductive monoliths which may better show gas desorption due to the electric current before any heating occurs.

- Two engineers have been trained in high-pressure hydrogen technologies and have performed a detailed risk assessment of the operation of a 12,000 psi electric swing adsorption (ESA) system operated in an open-bay area with other workers in the facility. The assessment led to design changes in order to match the safety level equivalent to that of trained operators at a commercial hydrogen-refueling station.

- A 12,000 psi ESA test system capable of purifying 300 scfh of reformed gas was designed and constructed. The system is designed for remote computer-controlled operation and has automatically operated safety procedures in case of a gas leak. Two monolith pressure vessels were installed: one for a 1.5-inch-diameter monolith 24 inches long, the other for a 2.5-inch-diameter monolith 36 inches long.

- In collaboration with U.S. military fuel experts and commercial fuel developers, the EERC developed a process to produce a renewable biomass-derived turbine fuel with JP-8 "drop-in compatibility" (the ability to meet all JP-8 military specifications and "fit-for-purpose" requirements). Theoretical design, chemical modeling, and bench-scale thermocatalytic processing activities were used to produce a crop oil-derived JP-8—an advanced tactical fuel with excellent properties (zero aromatics and sulfur content) for use as a turbine engine fuel or a feedstock for the HPWR hydrogen production process.

- The EERC worked with technology providers and catalyst producers to initiate development of a process for producing a drop-in-compatible alternative JP-8 from nonpetroleum feedstocks, including coal, natural gas, and biomass. Initial work was focused on enhancing the chemical composition of fossil-based Fischer–Tropsch (FT) fuel as required to meet all military JP-8 specification and fit-for-purpose requirements and serve as a superior feedstock for the HPWR hydrogen production process.

- A bench-scale reactor was designed and built to convert syngas to liquid fuels which, upon upgrading, meet key specification requirements of JP-8.

- Three large batches of an iron-based FT catalyst, 1 kilogram each, were prepared and evaluated in the small-scale FT reactor. The large batches were loaded into the large-scale FT reactor, which was used to convert coal–biomass-derived syngas into FT liquids. The liquids were subsequently upgraded into SPK (synthetic paraffinic kerosene) that is compatible with JP-8 jet fuel.

- Further tests were conducted on the FT iron catalyst preparation method in order to improve the repeatability of catalyst production and the stability and performance of the catalyst. It was determined that if the catalyst is exposed to atmospheric water vapor for extended periods of time, activity and selectivity to heavier hydrocarbons will be negatively impacted. Also, the catalyst must be exposed to dry, flowing air during drying and calcining in order to maximize performance.

3

- The FT iron catalyst was promoted with varying amounts of lanthanum oxide to determine potential effects on catalyst productivity and product selectivity. Small amounts of lanthanum help to reduce the surface acidity of the alumina support, which improves selectivity to heavy hydrocarbons. However, it appears that too much lanthanum negatively impacts catalyst productivity.

- Various FT catalysts were received from a commercial catalyst supplier. These catalysts were tested in the small-scale FT reactor. The performance of the catalyst was evaluated and compared to the FT catalyst developed at the EERC. The results were reported to the supplier to assist in improving catalyst formulation for future tests.

PROGRAM OBJECTIVES

The EERC program is designed to address the following key objectives:

- To develop and optimize the HPWR concept for on-demand production of high-pressure PEM fuel cell-quality hydrogen from JP-8 and other feedstocks.

- To develop advanced tactical fuels with JP-8 drop-in compatibility and superior hydrogen-reforming properties from domestic or indigenous fossil feedstocks such as coal, natural gas, and petroleum coke and renewable feedstocks such as crop oils and biomass.

- To advance the development of FCEH vehicles through demonstration of fuel cell-powered vehicles and hydrogen dispensing and refueling systems at military installations.

These objectives are addressed through the performance of multiple tasks and activities. Specific objectives for the individual tasks and activities include the following:

1) Complete optimization of the HPWR hydrogen production system.

2) Complete optimization of the ESA hydrogen purification system.

3) Initiate design and fabrication of a fully integrated HPWR–ESA-based system for on-demand production, purification, and dispensing of high-pressure PEM fuel cell-quality hydrogen from JP-8.

4) Initiate demonstration at GFARNGB of an FCEH MPUV manufactured by ePower.

5) Optimize a bench-scale FT reactor.

6) Optimize catalyst production.

7) Develop a proof-of-concept system for novel EERC-designed two-stage gasifier.

8) Continue development of modular distributed energy and fuel production systems.

9) Design and fabricate a laboratory-scale ESA system for process optimization, and initiate ESA optimization, with the goal of advancing the technology sufficiently to enable purification of HPWR-generated hydrogen to PEM fuel cell-quality.

Objectives 1–3 and 5–8 have been achieved during the period of performance covered in this report. Objective 4 could not be achieved since a working MPUV was not delivered by ePower; work continues on Objective 9.

PROJECT RESULTS

The EERC program consists of three tasks:

Task 1 – Integrated Demonstration of JP-8-Based Hydrogen Production and Dispensing

Task 2 – Fuel Production from Alternative Feedstocks

Task 3 – Project Management and Reporting

Under Tasks 1 and 2, several activities were performed to achieve the stated program objectives.

Task 1 – Integrated Demonstration of JP-8-Based Hydrogen Production and Dispensing

Task 1 subtasks and activities comprise HPWR-based hydrogen production process optimization and ESA-based hydrogen purification process development and optimization. It is anticipated that an integrated hydrogen production, purification, and dispensing system and vehicle demonstration will be conducted at Grand Forks Air Force Base (GFAFB) under a subsequent contract following completion of the design and fabrication of a deployable HPWR–ESA-based hydrogen-refueling system.

Subtask 1.1 – Hydrogen Production Process Optimization

Experimental

The EERC previously developed a high-pressure hydrogen production system to reform liquid organic feedstocks and water at operating pressures up to 12,000 psi. The advantages of the EERC system include 1) elimination of energy-intensive hydrogen compression, 2) a smaller process footprint, and 3) elimination of gaseous or liquid hydrogen transport. The objective of the gas cleanup work conducted under Subtask 1.1 was to decrease the load on downstream gas cleanup equipment that will further purify the reformate gas to PEM fuel cell quality. To accomplish the subtask objective, the existing EERC system was optimized through a series of

reactor modifications. Thermodynamic modeling was used to determine expected carbon dioxide removals and shakedown, and multiple test runs were conducted.

Results and Discussion

A new reactor was designed and constructed to provide better heat transfer to the catalyst bed. The reforming reactions are endothermic, and cold-spots are possible if there is inadequate heat transfer. A high-pressure condensation vessel was also installed downstream of the reactor as a means to remove water and carbon dioxide from the product gas. Shakedown activities were conducted with the new, reconfigured high-pressure reforming system. The unit was run at an increased capacity of approximately tenfold the original system, indicating that the process can be readily scaled up. Typical reactor conditions are shown in Table 1. Typical reformate gas composition is shown in Table 2.

Table 1. Typical High-Pressure Reformer Conditions During Experiments

Feedstock	Methanol
Temperature, °C	350–400
Pressure, psig	7500–8500
Methanol flow, lb/hr	2
Water flow, lb/hr	9

Table 2. Typical Reformate Gas Composition from the High-Pressure Reformer

	Without CO_2 Absorber, vol% [R50]	With CO_2 Absorber, vol% [R56]
Hydrogen	74.6	83.1
Carbon Dioxide	19.1	11.1
Carbon Monoxide	2.0	1.7
Methane	1.8	1.0
Other Light Hydrocarbons C_xH_y)	0.4	0.2
Water	1.1	0.1

Thermodynamic modeling indicated that it should be possible to condense liquid carbon dioxide simply by cooling the high-pressure gas stream. In laboratory tests, however, condensation of carbon dioxide to liquid was not achieved in the cold, high-pressure condensate vessel. To increase the cold surface area in the condensate vessel, steel packing was inserted. Even with the additional condensation area provided by the steel packing, the carbon dioxide concentration of the reformate gas remained unchanged. An alternate approach to removing carbon dioxide from the high-pressure reformate stream involving physical absorption of the carbon dioxide into a proprietary liquid solvent was investigated. Results in Table 2 indicate that the physical absorption column was moderately effective at removing carbon dioxide and water from the reformate gas stream. To prevent the absorption vessel solvent from becoming saturated with contaminants, the solution was constantly circulated to a flash drum, where pressure was

dropped and contaminant gasses were flashed off. Clean absorbent solution was then circulated back to the working absorption vessel. A flow diagram of the system is shown in Figure 1.

To increase gas–liquid contact time, a taller absorption column was constructed and installed to investigate the effect of increased contact time between reformate gas and absorption liquid on carbon dioxide absorption. This modification did not have a discernible effect on reformate gas composition, compared to the shorter absorption column. The experiment indicated that the contact time between the absorbent and reformate gas stream was not limiting carbon dioxide removal, further indicating that the absorption solvent itself may be the limiting factor. It was hypothesized that better carbon dioxide removal would be achieved with an improved absorption solvent. This hypothesis was supported when an improved absorption media was utilized. Results from tests using the improved absorption media, a methanol feed rate of 1.25 lb/hr, water feed rate of 6.25 lb/hr, and a pressure of 6000 psi are shown in Table 3.

Accomplishments

Work during this period of performance focused on optimization of the high-pressure production system. The reactor vessel was modified for higher hydrogen production and proof-of-concept testing was conducted for various high-pressure gas cleanup systems. The high-pressure carbon dioxide absorption experiments conducted resulted in promising proof-of-concept data for the high-pressure physical absorption technique of removing carbon dioxide and water. The absorption system will substantially reduce the load on downstream gas purification equipment.
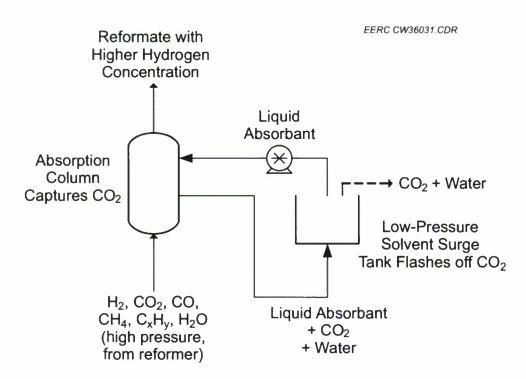
Figure 1. Liquid absorbent circulation system to remove carbon dioxide and water from a high-pressure reformate gas stream.

Table 3. High-Pressure Reformate Gas Composition Upstream and Downstream of an Absorption Column Designed to Remove Carbon Dioxide

Reformate Gas Component	Concentration (vol%) Upstream of Absorption Column	Concentration (vol%) Downstream of Absorption Column
Hydrogen	76	96
Carbon Dioxide	20.8	0.07
Methane	1.5	2.1
Carbon Monoxide	1.5	1.8

A peer-reviewed journal article titled "On-demand Hydrogen via High-Pressure Water Reforming for Military Fuel Cell Applications" was published as a technical brief in the November 2008 issue of the *Journal of Fuel Cell Science and Technology*. A copy of the journal article is included in Appendix A.

Subtask 1.2 – High-Pressure Hydrogen Purification Process Development and Evaluation

Multiple activities were included in Subtask 1.2

Activity 1.2.1 – ESA Process Development

Experimental

The HPWR process concept consists of converting JP-8 to a hydrogen-rich gas stream at pressures ranging from 3200 to 12,000 psi. To maximize the benefit of generating hydrogen at high pressure, a purification process that can work efficiently at these pressures without significantly reducing the pressure of the hydrogen is required. Separation membranes produce hydrogen with a pressure less than its partial pressure in the HPWR reformate stream. Conversely, adsorption systems produce hydrogen at pressures slightly less than the total gas pressure of the reformate. By producing and purifying hydrogen at the dispensing pressure, the need for high capital cost and energy-intensive hydrogen compression is eliminated. Currently, pressure swing adsorption (PSA) is the most common hydrogen purification technology in commercial use. In PSA, a pressure drop is used to desorb contaminants from an activated carbon sorbent, and clean hydrogen is used to purge the contaminants from the PSA vessel. Because effecting large pressure variations with hydrogen is expensive, the use of PSA at high pressure is unlikely to be economical. ESA represents a plausible alternative to PSA for hydrogen purification at high pressure, since ESA relies on electrical current variation rather than pressure variation to effect sorbent purging. Under this activity, the EERC evaluated the use of Oak Ridge National Laboratory (ORNL)-developed ESA for purification of hydrogen produced from the HPWR process.

Granular activated carbon is a common sorbent used in both PSA and ESA, but the high intergranular porosity and macroporosity of typical granular activated carbon sorbents (about 80%) necessitates the use of large volumes of hydrogen to purge the mass of contaminated gas

present within the pore structures. Additionally, granular carbon beds are poor electrical conductors. To address these technical issues, this activity focused on development of an electrically conductive adsorber with a significantly higher density than granular beds. Development of a dense electrically conductive monolithic activated carbon adsorber was accomplished through the use of powdered activated carbon and binder which was then compressed to create a monolith with a density approximately twice that of the bulk density of powdered activated carbon. Absorptivity of the monoliths was tested by passing a mixture of H_2, CH_4, CO, and CO_2 gases through small cylinders of the material. Delays and breakthroughs of each gas in the mixture were evaluated. The gas-mixing system and pressure vessel are shown as a schematic in Figure 2.

In addition to developing a dense electrically conductive monolithic activated carbon adsorber, a 12,000 psi ESA system capable of testing the purification technology on a stand-alone basis, separate from the HPWR system, was designed and built.

Results and Discussion

High-density electrically conductive activated carbon monoliths were formed using both powdered and granular activated carbons and various binders. Approximately eight different types of activated carbons and five different types of binders were tested. The best first-generation monoliths had an electrical resistivity of approximately 1.2 inch-ohms. Refinements in the methodology to produce the monoliths resulted in an increase in density and a decrease in electrical resistance. After the development of activated carbon treatments to reduce resistance, a
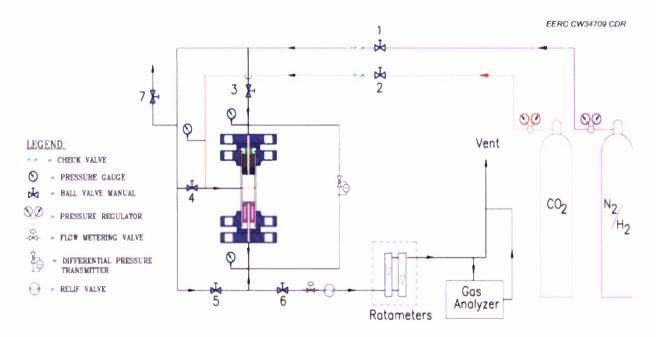
Figure 2. Schematic of the gas-mixing system and pressure vessel used for testing the adsorber monoliths at pressures up to 1000 psig.

second-generation monolith with resistivity of approximately one-tenth that of the first generation was developed. The lower resistivity reduces the amount of heating that occurs while driving off the gas.

Efforts were also made to produce activated carbon fiber composite monoliths. The composite material had an even higher density and lower resistivity than the pressed powdered activated carbon monoliths. As reported in last year's quarterly reports, efforts to activate the carbon fiber composites focused on physical activation using compressed carbon dioxide or steam. These attempts were unsuccessful because the pressure vessels could not reach a sufficiently high temperature for activation. In these experiments, chemical activation using potassium hydroxide and potassium carbonate was investigated for the carbon fiber monoliths. The chemical activation was more successful than the previous physical activation; however, the adsorptivity of the chemically activated carbon fiber was significantly lower (1/7) than the powdered activated carbon. As a result, the remainder of the testing focused on the monoliths made of the compressed powdered activated carbon.

Testing of the monoliths with a mixture of H_2, CH_4, CO, and CO_2 to simulate a reformate stream was performed. The order of breakthrough of the gases is H_2, CO, CH_4 and, finally, CO_2. Figure 3 shows a graphical depiction of typical results. The original concentrations of the different gases in the simulated reformate stream are signified by the horizontal lines in the graph. The data show the breakthrough times for the gases when passed through a 4-inch-long cylinder of the monolith at a flow rate and pressure of 1.5 scfh and 200 psig. The light blue line in the graph shows the breakthrough of oxygen which had been adsorbed on the carbon from the
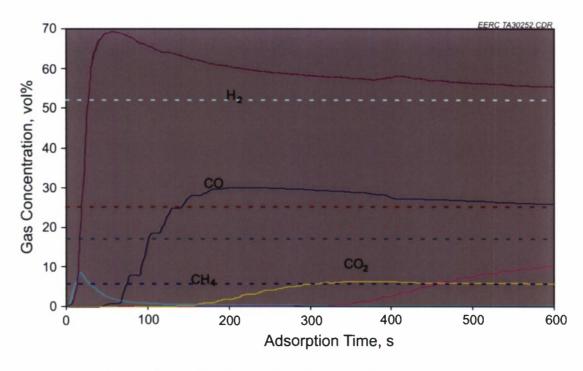
Figure 3. Gas breakthrough curves for a monolith tested at
200 psig with a simulated reformate gas stream.

10

air before testing. Nitrogen was not measured directly but can be calculated by difference. Adsorptivity tests were also performed at 300 and 800 psig. Breakthrough results were similar at the higher pressure.

Regeneration of the first-generation monoliths was evaluated at up to 800 psig using electric currents. During the regeneration, significant heating of the monolith was noted, potentially indicating that gas desorption may be due to the heating and not the electric current alone. Regeneration testing of the second-generation monoliths has not yet been performed but will be performed in future work under this activity.

Work in this activity continued with design and construction of the 12,000 psi ESA test system. Before finalizing the design of the system, project engineers were trained in high-pressure hydrogen technology. Design parameters required a quantifiable risk assessment of the system to ensure safe operation in an open pilot plant setting. Risk needed to be equivalent to that experienced by workers at a commercial hydrogen-fueling station. One engineer was certified as a hydrogen safety engineer.

A schematic of the 12,000 psi ESA test system is shown in Figure 4. It is designed to allow mixing of simulated reformate gases from gas cylinders. The gas is then compressed to an operating pressure of 12,000 psi. The system will be used in future work in this activity to refine operating procedures, determine gas adsorptivity and breakthrough behavior at high pressure, and develop monolith regeneration procedures. The system was designed for remote operation, and all electrical components meet the National Electrical Code Class 1 Division 2 rating for
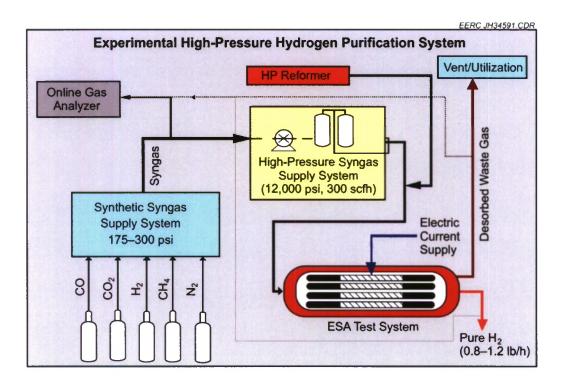
Figure 4. Schematic of the 12,000 psi ESA test system.

operation in environments that may contain explosive gases. A detailed risk assessment of the system was performed, and the system design modified as needed, to meet the suggested safety requirements of a commercial hydrogen refueling station. The 12,000 ESA test system was constructed and is ready for testing.

Figure 5 shows the two pressure vessels that will house the purification monoliths and valves and a meter for controlling gas flow during the adsorption and desorption cycles. Two monolith pressure vessels were installed: one for a 1.5-inch-diameter monolith 24 inches long and the other for a 2.5-inch-diameter monolith 36 inches long. The smaller vessel will be used in early development of operating procedures in order to reduce gas usage.

Figure 6 shows the air-purged box in which all electronic controls and data acquisition connections are made. The gas cylinders will be held in the rack along the right side.

Figure 7 shows the gas compressor and the back of the board holding gas-blending valves and regulators. The system is capable of blending up to five gases and compressing them from 175 to 300 psi inlet to up to 14,500 psi with a flow rate of up to 500 scfh. However, the standard operation will be for 175 psi inlet, outlet of 12,000 psi, and a flow rate of up to 300 scfh.

The EERC technology for producing and purifying hydrogen at high pressures offers several advantages over systems that produce the hydrogen at low pressures and then compress

Figure 5. Monolith pressure vessels and valves and regulators that control gas flow during adsorption and desorption testing. The open pilot plant setting can be seen behind the test system.

12
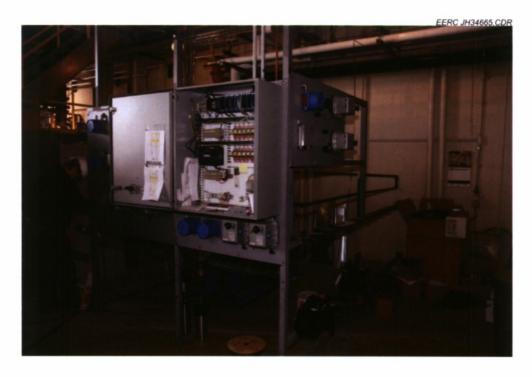
Figure 6. The air-purged electronics box in which all electronic connections are made.

Figure 7. The gas compressor and the back of the board holding
gas-blending valves and regulators.

it. The advantages include a smaller footprint, lower cost, lower operation noise, lower weight, and lower energy requirement.

Accomplishments

Activated carbon monoliths were prepared and tested for potential use in the 12,000 psi ESA system.

For the ESA 12,000 psi system, all equipment and parts were received and installed, and computer programs have been written for remote operation and automatic shutdown in case of system failures or leaks.

A technical presentation entitled "High-Pressure Hydrogen Purification Using Electrical Swing Adsorption" was given at the American Institute of Chemical Engineers spring national meeting in Tampa, Florida, in March 2008.

Also during this reporting period, a request was sent to the Construction Engineering Research Laboratory (CERL) contract specialist for permission to purchase a gas analyzer for use in the purification method development work. Permission to make the purchase was granted, and the analyzer was purchased and received. The analyzer supported hydrogen purification work performed under Task 1.2.1 to determine the selectivity, capacity, and regeneration activity of the gas purification system.

Because of delays in delivery of equipment and required additional work related to safety issues, system shakedown and testing were postponed.

Subtask 1.2.2 – Electrochemical Hydrogen Purification Process Development

Experimental

Electrochemical hydrogen purification process development work was investigated using simulated reformate gas mixtures and two modified fuel cells with each comprising two metal end plates, two graphite flow field plates, and a high-temperature membrane–electrode assembly (MEA) based on high-temperature polymer proton-conducting membranes. The component development and process optimization were carried out in an electrochemical cell with 5 cm^2 active area and using a single channel serpentine flow field. The process scale-up research was performed in an electrochemical cell with 50 cm^2 active area and using a parallel multichannel serpentine flow field. The two electrochemical cells have a similar structure which is indicated in Figure 8. Figure 9 shows the images of the two electrochemical cells. During the electrolysis, currents and potentials were controlled by an Autolab potentiostat/galvanostat integrated with a 20-A booster (Figure 10).

The gas streams were supplied directly from commercially available tanks without external humidification, except where humidification is noted. The external humidification was controlled by a water bath held at 60°C, resulting in approximately 3% relative humidity at 160°C, 6% at 140°C, and 10% at 120°C. The pressure was not regulated and open to the atmosphere. All tests

14
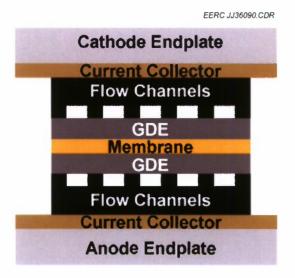
Figure 8. Schematic diagram of an electrochemical cell.
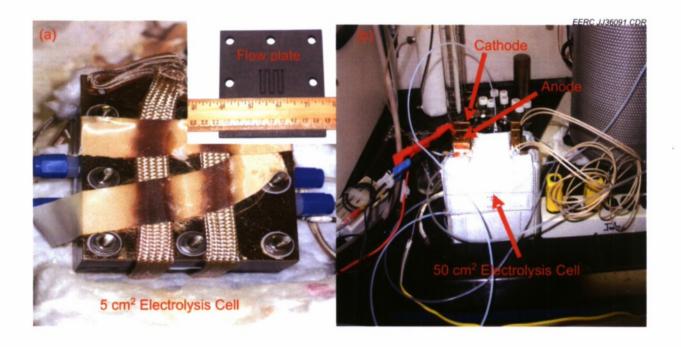
Figure 9. Images of electroelectrolysis cell with an active cell area of 5 cm^2 (a) and 50 cm^2 (b).
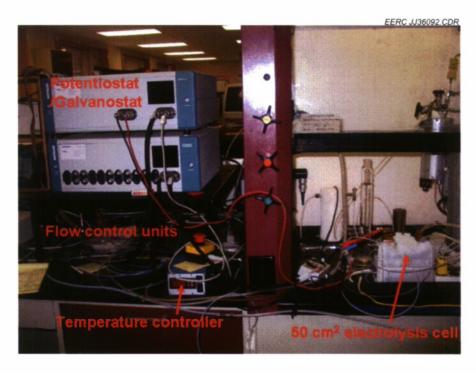
Figure 10. A controlling system for electrochemical hydrogen purification process which comprises an Autolab potentiostat/galvanostat, mass flow controllers, and temperature control.

were performed in the temperature range of 140° ~ 180°C. The fuels included pure hydrogen and simulated reformate gas (76% H_2, 2% CO, 2% CH_4, and 20% CO_2). High-purity nitrogen was fed to the cathode side to carry hydrogen purified for gas analysis using an Agilent 7890A gas chromatograph (GC).

Gas diffusion electrodes with a platinum loading of 1.0 mg/cm^2 were used as the cathode. The MEAs were fabricated by hot-pressing a piece of membrane between the two Kapton-framed electrodes. The MEA was then assembled into a single cell testing hardware.

Results and Discussion

Electrochemical Hydrogen Purification Using 5-cm^2 Electrolysis Cell. Initial proof-of-concept work was performed by feeding simulated reformate gas and pure nitrogen gas through the anode chamber and cathode chamber, respectively. Under open-circuit potential (OCP) and at atmospheric pressure and 140°C, hydrogen permeated the polymer membrane, and CO_2 crossover was too low to be detected by GC analysis. In a constant-current electrolysis mode, only H_2 was detected as an exclusive cathode product, and no CO, CH_4, or CO_2 was detected. For the purpose of comparison, pure H_2 was fed to the anode side in replace of the simulated reformate gas, the similar results were obtained with H_2 produced at the cathode side. The production rates of H_2 from pure H_2 and the simulated reformate were similar under the same constant current conditions. These results indicated the viability of the proposed electrochemical hydrogen purification method at ambient pressure.

The optimization of the hydrogen purification process focused on the MEAs for decreased cell voltage and increased electrochemical reaction rate. The prepared MEAs were evaluated as a function of reaction temperature based on the measured potential-current curves with hydrogen as reactant input through both anode and cathode chambers of a modified fuel cell. At temperatures relevant to the purification process operating conditions, a typical cell voltage is around 0.2 V at a constant current density of 200 mA cm^{-2}, with dry H_2 as the input. This cell voltage was decreased to 0.15 V at the same current density when dry H_2 was switched to wet H_2. This decrease in the cell voltage is mainly caused by the increase in electrolyte membrane conductivity in the presence of moisture. It is expected that the cell voltage could be further decreased at a controlled current density via further optimization of the MEAs and operating conditions.

Two approaches were used to improve performance of MEAs for increased current density and decreased cell voltage. Because the high-temperature gas diffusion electrodes used were designed for aqueous electrolyte-based electrochemical processes, there are no developed three-dimensional net channels for ion conduction inside the electrodes themselves. Since the electrochemical reactions occur only at the interfacial area between the electrode and the polymer electrolyte membrane, the total electrochemical reaction areas were expected to be low. Because the polyelectrolyte solution is not commercially available, a one-step synthesis of the high-temperature polymer electrolyte was developed. The synthesized polymer solution was used to impregnate the electrode layers for improved reaction areas. The second approach evaluated was the optimization of the hot-pressing process for the preparation of MEAs.

Electrochemical Hydrogen Purification Using a Scaled-Up Electrolysis Cell. The optimization of the electrochemical hydrogen purification process at atmospheric pressure was completed. The optimized process was demonstrated using a high-performance, high-temperature MEA with highly developed solid electrolyte and electrode interfaces and dry simulated reforming gas comprising 76% H_2, 2% CO, 2% CH_4, and 20% CO_2. At three operating temperatures of 140°, 160°, and 180°C, only hydrogen was produced at the cathode. The current efficiency for the hydrogen purification process was greater than 90% at the test temperatures noted and at a constant current of 200 mA cm^{-2}. The cell voltage measured at this constant current density was dependent upon the operating temperature. At 140°C, a value of approximately 0.14 V was obtained. This value decreased to approximately 0.06 V when the temperature was increased to 180°C. The cell voltage remained nearly constant at controlled constant current polarizations (Figure 11). The purification process was further investigated as a function of process shutdown and restart. Pure hydrogen gas was produced at the cathode. High current efficiency and stable low cell voltage were reproduced. The progress made at atmospheric pressure enabled initialization of work to tailor the process for use at elevated pressure.

EERC JJ36093.CDR
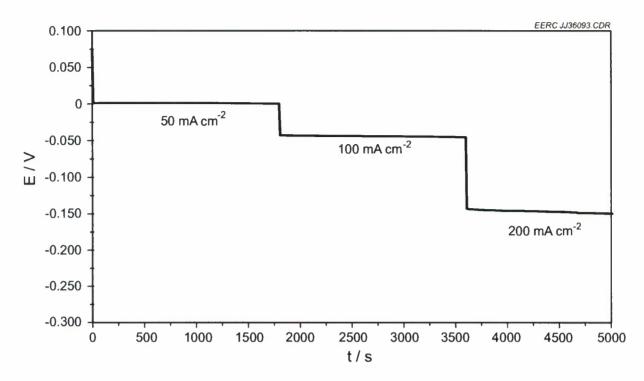
Figure 11. Dependence of cell voltage as a function of reaction time under controlled constant current conditions at 140°C.

Electrochemical Hydrogen Purification Using a Pressurized Scaled-Up Electrolysis Cell

The design and construction of a pressurized electrochemical cell were initialized, and the integration of the controlling system was initiated.

Accomplishments

The feasibility of electrochemical hydrogen purification process was demonstrated, and the electrochemical process was optimized at ambient pressure. Low cell voltage, high reaction rate, and high current efficiency were achieved for the purification process. Work was initialized on tailoring the process for use at elevated pressure.

The next phase of work will focus on the feasibility demonstration and optimization of high-pressure hydrogen purification processes.

Subtask 1.2.3 – Hydrogen Production and Purification Systems Integration

The system integration design team has completed a draft piping and instrumentation diagram and has begun specifying equipment for the integrated hydrogen production, purification, and dispensing system. Some pressure vessels will be purchased; however, many components of the current reforming system will be utilized in the new integrated system. The

18

system, when modified, will include hydrogen production, purification, and dispensing in a continuous, integrated process.

Subtask 1.3 – Hydrogen Dispensing and Use

The objective of this subtask is to advance the development of FCEH vehicles through demonstration of fuel cell-powered vehicles and hydrogen dispensing and refueling systems at military installations.

Experimental

With respect to hydrogen as a tactical fuel, the increased efficiency of an FCEH vehicle (running on onboard-stored hydrogen) versus a comparable-power internal combustion (IC) engine vehicle is well documented. The work performed under this subtask was designed to quantify the actual efficiency increase achievable in specific military applications and develop vehicle performance and maintenance data. The vehicle performance and maintenance data are critical to assessing the military viability of FCEH vehicles for mobility applications, including applications whereby multiple power-generating assets can be combined, thereby reducing the number of power generators and the complexity of maintaining and operating those assets.

Results and Discussion

Technical work focused on ensuring that vehicle design, use, and refueling operations were compatible with hydrogen production and dispensing operations. Systems and vehicles developed under this activity are described below.

Mobile Hydrogen Refueler. In collaboration with Kraus Global and Airgas Inc., a high-pressure (5000 psi) hydrogen-dispensing system was designed and fabricated by the EERC based on the use of delivered cylinders of 6400 psi hydrogen (see Figure 12). The refueling station was operated extensively for over 12 months in cold winter and hot summer weather at GFARNGB.

FCEH Forklift Truck. A 5000-pound-capacity FCEH forklift truck was designed and manufactured by ePower Synergies and demonstrated at GFARNGB. This vehicle represented an early application of an electric forklift and plug-and-play fuel cell pack using commercially available off-the-shelf technology. The standard battery pack was removed from a Hyster 50 forklift and replaced with a fuel cell pack produced by General Hydrogen. The General Hydrogen Model FS-0002 Hydricity Fuel Cell Pack consisted of a Ballard 80-V 9-kW fuel cell stack, 5000 psi hydrogen tank capable of holding 1.79 kg of hydrogen and an ultracapacitor system to provide energy storage and transient power. Beginning in 2006, the FCEH forklift and refueling station were operated extensively for over 12 months in cold winter and hot summer weather. In December of 2007, a second forklift was assembled by ePower and delivered to Robins AFB for subsequent use and demonstration.

Figure 12. Mobile hydrogen refueler.

Hyster Forklift Truck. In 2009, a third FCEH forklift was assembled based on the Hyster 50 platform (see Figure 13). A Hydrogenics HyPX-1-33 fuel cell pack was used to replace the battery pack of the forklift. The Hyster 50 and Hydrogenics fuel cell pack were delivered to the EERC and assembled prior to being shipped to Robins AFB. The FCEH forklift provided equivalent performance to a standard forklift and had several features that improved operability over the previous forklifts demonstrated in 2006 and 2007. The fuel cell pack possessed a 12-V battery in addition to the ultracapacitors. The 12-V battery works similarly to the battery of an automobile, providing start-up power even when the forklift sat unused and the ultracapacitors lost their electrical charge. The Hydrogenics HyPX-1-33 fuel cell provides plug-and-play capability with the Hyster 50 forklift. The only custom fabrication modification performed by the EERC was fabrication and installation of a steel plate under the fuel cell to increase the vehicle weight to that of the original battery-powered vehicle. This increase in weight maintained the forklift lift capacity consistent with the stock battery-powered Hyster 50. This vehicle will continue to be utilized at Robins AFB under the direction of the Advanced Power Technology Office (APTO).

Bobcat Toolcat. Following the completion of two FCEH forklift vehicles, ePower worked with GFARNGB and APTO personnel to develop design specifications for a MPUV based on the Bobcat Toolcat vehicle platform. The vehicle was designed and fabricated with a hub motor for each wheel and significant upgrades to the frame and suspension to meet the tow requirements of an aircraft tug vehicle. The Toolcat was delivered to Robins AFB and evaluated by APTO personnel and then shipped to the EERC where staff conducted a detailed inspection in
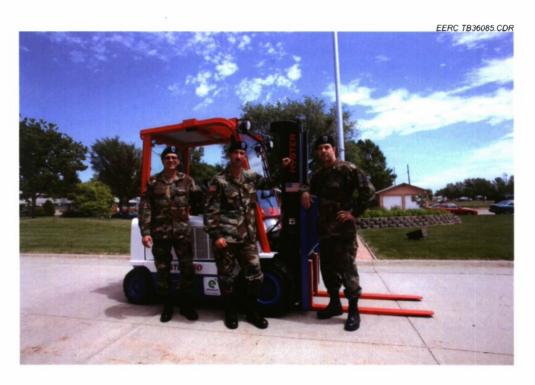
Figure 13. FCEH Hyster forklift.

which the systems were reviewed and documented in a series of as-built drawings. Evaluation of the vehicle by APTO personnel and EERC staff determined that the Toolcat was not well suited for use as an aircraft tug. Further design modifications were identified that, if implemented, would allow the vehicle to have performance capabilities similar to a standard diesel-powered Bobcat Toolcat. The vehicle has undergone several modifications in an effort to achieve this standard level of performance using the hydrogen-powered fuel cell system. In its current configuration (shown in Figure 14), the Bobcat Toolcat utilizes a hydraulic drive system powered by the fuel cell. The vehicle is fully functional but lacks the efficiency and power that could be achieved with a fully electric drive system. Future work is anticipated in which improvements to the drive system and component integration will take advantage of the efficiency benefits of a hydrogen-powered fuel cell.

Accomplishments

Several vehicles and a hydrogen-refueling system were designed, built, and tested under a range of hot to cold weather conditions. The refueling system remains in service at GFARNGB. Two hydrogen-powered forklift trucks remain in service at Robins AFB, and the Bobcat Toolcat is fully functional after modifications; however, additional modifications are planned.

Task 2 – Fuel Production from Alternative Feedstocks

Work performed under Task 2 included development of alternative (nonpetroleum) feedstock-based technologies for production of advanced tactical fuels with JP-8 drop-in compatibility and improved properties for use as hydrogen feedstocks.

21

Figure 14. Current configuration of the Bobcat Toolcat.

Subtask 2.1 – Advanced Gasifier Development for Clean Syngas Generation

Gasification is one of several thermochemical conversion technologies capable of providing advanced fuels and energy to the military using domestic feedstocks such as biomass, coal, municipal solid waste, or field waste. The activities conducted under this subtask were focused on testing an advanced gasifier, designed and fabricated at the EERC, capable of producing a variety of syngas compositions from a range of feedstocks with diverse physicochemical properties. The objective of this effort was to demonstrate the operational flexibility of the advanced gasification system to accommodate numerous feedstocks to produce different syngas compositions ideally suited for applications such as power generation in IC engine generators, distributed hydrogen production, and liquid fuel synthesis reactions such as FT.

One of the greatest challenges to commercial deployment of distributed gasification systems has been the inability to effectively gasify a variety of fuels with different physical and chemical characteristics. The EERC's advanced gasifier addresses this challenge by providing exceptional operational control allowing the system to accommodate a wide variety of fuels and associated char reactivity while still providing self-sustained steady-state gasification and providing near-complete carbon conversion.

Advanced Gasifier System Description

The gasifier design philosophy is based on the production of clean syngas with high conversion efficiency and achieving near-zero effluent discharge from the overall system. The

production of clean syngas is achieved by converting the complex organics in the hot zones of the gasifier. The near-zero effluent discharge is achieved by recycling the trace amount of unconverted organics in the syngas into the gasifier hot zones such that the syngas (composition) production is favored.

The main components of the gasifier system include a fixed-bed downdraft gasifier reactor, a fuel feed system, a syngas scrubbing and polishing system, a syngas exhaust system, an auxiliary fuel feed system, a residue extraction system, an induced-draft (ID) fan, and an instrumentation and control system. The process flow diagram of the gasification system is shown in Figure 15, and a photograph of the system is shown in Figure 16. A 3-dimensional representation of the gasifier is shown in Figure 17. The system is classified for Class 1, Division 2, Group B for the operation of electrical components in explosive gas environments.

Chipped fuels are screw-fed from the top of the gasifier. The syngas is removed from the reactor outlet at the bottom of the gasifier. The nominal throughput of the biomass is 33 lb/hr; however, maximum capacity can reach 100 lb/hr depending on the type and size of the fuel, its reactivity, and gasifier operating parameters. The fuel hopper can store about 200 lb of biomass or 400 lb of coal. Gasification air is injected from the top of the gasifier under the suction caused by the ID fan located downstream of the syngas scrubber system. The fuel bed is ignited with the help of a hot air generator which is specially adapted for the system. After ignition, the reaction front propagates and attains the steady-state exothermic heat profile necessary for maintaining gasification reactions. Steady-state gasification can be achieved within 30 minutes of ignition, depending on the fuel moisture content and fuel reactivity. Specially designed vertical augers are used to extract solid residue and provide the added function of supporting the bed.

Clean syngas is produced in the hot zone of the gasifier by staging the oxidizer to combine devolatilization, partial oxidation, and reduction reactions. The reactor geometry in the upper zone of the gasifier is designed to allow a smooth flow of the chipped fuel and gasification air. The air injection occurs in this zone. The air injection is balanced by forced-draft and ID fans such that the overall gasifier operating pressure is maintained slightly below atmospheric pressure. The ID fan located downstream of the syngas cleanup system is sized to overcome the system pressure drop (of about 30–40 inches of water column) at a rated flow rate. The pressure sensor at the inlet controls the forced-draft fan used for injecting gasification air through a preheater. To improve the conversion and thermodynamic efficiency of the system, extractable sensible heat from the syngas is recycled back into the gasifier by using gasification air as a heat carrier fluid.

In order to achieve near-zero effluent discharge and improve the composition of syngas, the effluent from the scrubber section is injected into the gasifier. The condensed tar and particulate matter along with a small fraction of water are injected into the reactor hot bed such that the hydrodynamics or the reactor temperature profile is not affected. The inert inorganic residue removed from the gasifier is the only disposable material generated from the system.

Syngas, after exiting the reactor, is scrubbed in a two-stage water scrubber and syngas polisher. The first section cools the hot syngas and removes the condensable tars. The second stage effectively scrubs the remaining tars that are typically formed only under high tar loading

Gas Composition

	CH4 (%)	CO (%)	CO2 (%)	H2 (%)	H2O (%)	N2 (%)	HHV (MJ/kg)
Syngas at Gasifier Outlet (I-A.1)	0.40	21.16	11.08	18.86	6.16	42.35	4.79
Syngas at Wet Scrubber Outlet (I-A.5)	0.42	22.19	11.62	19.78	1.57	44.42	5.07

I. Process Piping	DESCRIPTION	ACTUAL FLOW (kg/h)	TEMP (°C)	PRESSURE (atm)	SENS HEAT (kW)	CHEM ENERGY (kW)
A. Syngas						
I-A.1	Outlet of Gasifier	55.0	730.00	1.00	18.32	73.2
I-A.2	Outlet of scrubbers	52.0	20.00	1.00	0.35	73.2
I-A.3	Inlet to polisher	52.0	20.00	1.00	0.35	73.2
I-A.4	Outlet of polisher	52.0	5.00	1.00	0.35	73.2
I-A.5	Inlet to exhaust flare	52.0	5.00	1.00	0.00	73.2
B. Water						
I-B.4	Inlet to water pump	4,000.0	18.00	1.00	0.00	
I-B.5	Outlet of water pump	4,000.0	18.00	4.40	0.00	
I-B.6	Inlet to nozzle b/ manifold	4,090.0	18.00	4.40	0.00	
I-B.13	Scrubbers drain	2.1	30.00	1.00	0.04	
I-B.14	Water tank drain	3.1	30.00	1.00	0.04	
D. Feed						
I-D.1	Biomass feed	20.0	25.00	1.00	0.00	96.5
E. Solvent						
I-E.1	Used solvent to tank	375.0	5.00	1.00	0.36	
I-E.2	Solvent pump outlet	375.0	5.00	3.00	0.00	
I-E.4	Inlet to polisher	375.0	5.00	1.00	0.00	
I-E.5	Solvent tank drain	Variable				
F. Air						
I-H.1	Outlet of HX-200	0.9	20.00	1.61	0.00	
I-H.2	Air supply to flare	67.5	15.00	1.00	0.00	

Item No.	Description	Capacity (hp)
M	Motor	
M-200	Biomass Feed Auger	3
M-201	Solids extraction auger	0.5
M-300	Wet scrubber water circulation pump	7.5
M-350	Solvent circulation pump	2
M-353	Coolant supply	0.5
M-600	Syngas ID fan	5

Item No.	Description	Fluid	Temp (in/out)
F	Fan		
F-600	Exhaust fan	Syngas	5°C

Item No.	Description	Fluid	Temp
P	Pump		
P-300	Wet scrubber water circulation pump	Water	18°C
P-350	Solvent circulation pump	Solvent	0°C

EERC

P & ID : Pilot-Scale
The Gasification System

Drawn By:	K. Palmisano
BSS Check:	B. Moe
Design:	
Manager:	N. Patel
Approved:	N. Patel
Revision: 0	D. Hajicek
	6/4/09

Figure 15. General process flow diagram of the advanced pilot plant gasifier.

Advanced Pilot-Scale Gasifier

EERC NP35002

Third Level

Scrubber System – Second Level

Vent System

Polisher System – First Level

Gasifier Feed – Second Level

Gasifier – First Level

Advanced Pilot-Scale Gasifier

Figure 16. Photographs of commissioned advanced fixed-bed gasifier pilot plant.

Figure 17. Three-dimensional view of the pilot plant gasifier
depicting the major components of the system.

conditions attained during severe conditions such as high throughput or high fine loading, etc. The final syngas polisher removes carryover tar with a liquid solvent. This syngas polishing system can be bypassed depending on the syngas quality required. Both scrubbing systems are closed-looped in order to facilitate determination of condensable and soluble organic and inorganic components of the syngas. The solids removed in the scrubbing mediums can be removed in the filteration system.

The flow rate of the syngas and gasification air is measured using orifice flowmeters. The syngas flowmeter is located downstream of the blower; the gasification injection air is measured upstream of the gasifier.

The clean syngas is routed through the enclosed combustor and flared at an elevation of 16 feet from the roof height. The flare in the pilot system has a hot surface igniter; the combustion air is induced by the ejector effect caused by the flow of syngas. A gas-sampling port is available for determining flare emissions.

The clean syngas composition is determined using an online gas analyzer capable of measuring CO, CO_2, O_2, N_2, H_2, CH_4, and higher hydrocarbons. A quasi online GC is used for determining trace hydrocarbon gases in the syngas. Additional sample ports are available for conducting isokinetic sampling of syngas to measure tar and particulate matter according to the modified European tar protocol (1) and EPA Method 5. These samples can be obtained from the syngas both before and after syngas cleanup unit operations.

The bed and syngas temperatures are measured at several locations to provide both process control and operational monitoring.

Fuel Selection

The gasification experiments were conducted on five fuels considered most challenging, but having commercial interest in being utilized without requiring any preprocessing, including drying or screening fines. Since these preprocessing efforts are capital-intensive and are not practical for distributed applications because of economic or environmental reasons, the experiments were conducted on the fuels as received. These fuels included high-moisture wood waste, Powder River Basin (PRB) coal, and creosote-treated railroad ties. Figure 18 shows direct photos of fuel samples used in the pilot plant test. The writing pen shown along with the fuel is to provided an estimation of the relative size of the fuels and the fraction of fines.

A summary of the results from proximate and ultimate analaysis of these fuels is provided in Table 4. Additionally, for the purposes of comparison, data from a typical oak wood and oakwood charcoal have been included in Table 4.

EERC NP32560.AI

12.5% Moisture Creosote-Treated Railroad Ties

35% Moisture Pine Wood

26.5% Moisture PRB Coal

48.5% Moisture GF Municipal Wood Waste

Figure 18. Sample of fuels used in the pilot plant test.

Table 4. Comparative Fuel Analysis of Woody Biomass Wastes, Oak and Pine Wood, PRB Coal, and Oak Wood Charcoal Used in the Experiments

Fuel	Oak Wood	35% Moisture Pine Wood*		Railroad Tie 2		Railroad Tie 4		Marcel Wood Chips		GF Municipal Wood Waste		PRB Coal		Oakwood Charcoal	
	From Literature	As-Received	Moisture, Ash-Free	As-Received	Moisture, Ash-Free	As-Received	Moisture, Ash-Free	As-Received	Moisture, Ash-Free	As-Received	Moisture, Ash-Free	As-Received	Moisture, Ash-Free	As-Received	Moisture, Ash-Free
Proximate Analysis, wt%															
Moisture	–	9.2	–	31.9	–	23.7	–	33.5	–	43.6	–	22.7	–	5	–
Volatile Matter	81.28	76.99	84.97	56.95	85.83	65.73	87.22	51.17	77.47	39.57	71.43	25.6	35.98	19.68	21.1
Fixed Carbon	17.2	13.66	15.03	9.38	14.17	9.58	12.78	14.26	22.53	15.84	28.57	45.97	64.02	73.58	78.9
Ash	1.52	0.15	–	1.76	–	0.99	–	0.17	–	0.99	–	5.48	–	1.74	–
Ultimate Analysis, wt%															
Hydrogen	5.38	6.58	6.13	7.85	6.49	7.83	6.9	8.27	6.89	8.34	6.31	5.5	4.78	3.21	2.85
Carbon	49.28	44.67	49.3	40.29	60.72	49.23	65.33	34.45	52.15	32.43	58.55	54.91	76.4	77.93	85.53
Nitrogen	0.035	0.15	0.016	0.27	0.41	0.44	0.59	0.16	0.25	0.28	0.51	0.75	1.04	0.38	0.41
Sulfur	0.01	0.2	0.22	0.12	0.18	0.21	0.27	0.19	0.19	0.01	0.02	0.56	0.77	0	0
Oxygen	43.13	48.26	44.19	49.71	32.19	41.29	26.9	40.23	40.51	57.94	34.61	32.35	17	1.74	0
Heating Value,															
MJ/kg	19.42	17.33	19.12	15.79	23.80	18.34	24.34	12.71	19.25	11.85	21.40	21.16	29.44	21.16	34.18
Btu/lb	8349	7451	8223	6790	10,233	7888	10,468	5467	8277	5097	9200	9098	12,659	9098	14,697
C/H Ratio	9.16		8.04		9.36		9.47		7.57		9.28		15.98		30.01
C/O Ratio	1.14		1.12		1.89		2.43		1.29		1.69		4.49		–
C/C (oak)	1.00		1.00		1.23		1.33		1.06		1.19		1.55		1.74
CV/CV (oak wood)	1.00	0.98		1.23		1.25		0.87		0.97		1.33		1.55	

* Pine wood fuel was prepared to achieve a 35% moisture content as processed by the gasifier. The reported 9.2% moisture represents an as-received value only

28

35% Moisture Pine Wood

This fuel consisted of chipped pine lumber collected from a residential roof truss plant in Grand Forks, North Dakota. The average moisture content of the batch of fuel received was about 9.2%. The moisture in the pine wood waste was increased to 35% by adding water to the batch of 1000 lb in order to match with the typical moisture content of the fuel stored in the exposed piles outside the plant premises to determine gasifier performance on actual fuel.

Railroad Ties

Creosote-treated railroad ties were also identified as a fuel of commercial interest. This is a complex gasification feedstock containing hardwood and coal-derived creosote used as a treating agent. The creosote is a mixture of different distillation fractions of hard coal tar. The main compounds in the creosote are polycyclic aromatic hydrocarbons (PAHs) and heteroaromatic compounds such as naphthalene, quinoline, acenaphthene, dibenzofuran, fluorene, phenanthrene, anthracene, fluoranthene, and pyrene. To further complicate railroad tie chemistry, this feedstock is exposed to changing environmental conditions, and the ties are often coated with lubricants and fuel. Proximate and ultimate analyses were conducted on rail ties from two different sources and reported in Table 5. The differences observed from these two samples can be attributed to differences in creosote used to treat the railroad tie as well as different environmental conditions over the service life of the railroad tie. Tie 2 was obtained from a source in the United States, while Tie 4 was obtained from Kamloops, British Columbia, Canada.

Marcel Wood Chips

This wood waste was obtained from legacy piles or landfill located near a sawmill situated in Marcel, Minnesota. The moisture content of the fuel determined was 33.5% which is about 1.5%–25% lower than fuel processed during the gasification test.

Grand Forks Municipal Wood Waste

The composition of the municipal waste wood in Table 4 shows 43.6% moisture on an as-received basis. However, additional moisture analysis was conducted on this feedstock during testing to gather representative data on fuel chemistry as it was fed to the gasifier. Moisture data collected over the course of two test days show a range of moisture content from 51.0%–60.6%

Table 5. Grand Forks Municipal Waste Wood Moisture

	Units	10/1/2009	10/12/2009
Sample 1	%	59.6	51.0
Sample 2	%	58.2	53.1
Sample 3	%	61.6	52.2
Sample 4	%	62.9	54.4
Average	%	60.58	52.68
Standard Deviation	%	2.09	1.44

from a single 1500-pound batch of waste wood. Data from the gasification of this fuel were obtained on October 12, 2009, and represent a waste wood fuel possessing, on average, 52.69% moisture.

PRB Coal

Coal feedstock, one of the fuels of interest for distributed hydrogen production, contained of about 25% moisture. The coal was Montana subbituminous, commonly known as PRB coal.

Comparative Fuel Analysis of Railroad Ties, Wood, and PRB Coal

Composition data collected for the various fuels were compared to oak wood which is the type of wood typically used in making railroad ties. Volatile matter was the highest in the two railroad tie feeds; however, similar volatile matter was measured in the oak wood, pine wood, and railroad ties ranging from 81.28 to 87.22 wt% on a moisture- and ash-free basis. The volatile matter of the waste wood chip samples was slightly lower than that of the other wood samples and the PRB coal had the lowest volatile matter, about 35% on an ash- and moisture-free basis.

Fuel volatile content is an important parameter in gasification. The fuel particle size and associated heating rate typically determine the yield and devolatilization rate in the gasifier. However, fuels with high volatile contents such as railroad ties, can achieve higher devolatilization rates leading to higher tar concentration in the syngas. A high devolatilization rate may have the effect of reducing gas-phase residence time of volatile product, therefore limiting opportunity to crack the tars in the high-temperature zone. Additionally, the higher devolatilization rate can reduce the gasifier bed temperature because of excessive heat loss caused by convection or endothermic organic devolatilization. The EERC's advanced gasifier has been designed to accommodate fuel with high volatile content, and through proper process control, railroad ties have been gasified while demonstrating improved syngas composition, increased gasification efficiency, and reduced tar formation.

The comparative data of C/H and C/O ratio of the fuels are shown in Table 4. The C/H values of woody fuels ranged between 7.57 and 9.28, while the values for ties are in a higher range, 9.36 to 9.47, indicating the presence of carbon-rich organics typically found in coal tar or creosote. The C/H of coal and oak charcoal are 15.98 and 30.01 respectively. At these elevated C/H ratios typical fixed-bed gasification would typically produce a CO-rich syngas.

The concentration of oxygen in the fuel is critical in estimating the required oxidizer-to-fuel ratio to attain the desired gasification operation and syngas quality. The ability to adjust process inputs, such as feed or air, ensures effective feed conversion and low tar formation. The C/O ratio of the wood biomass fuels ranged from 1.12 to 1.69. In contrast to these fuels, the values for railroad ties range from 1.89 to 2.43, and PRB coal had a C/O ratio of 4.5. In response to these feedstock characteristics, a higher oxidizer feed rate was used when testing fuels such as railroad ties and coal.

The comparison of the carbon content of the different fuels is presented in Table 4 as a ratio of fuel carbon to that present in oak wood. The carbon content in railroad ties is 23% to

30

33% higher than oak wood, while in PBR coal, it is about 55% higher than oak wood. The calorific value of the ties and coal are about 25% and 33% higher than oak wood, while the oak wood charcoal is about 55% higher than dry, ash-free wood.

Oakwood Charcoal Gasification

During gasifier start-up, charcoal was used as the bed fuel for ignition and reactor heatup. Data were collected during start-up and, for a short period of time, at steady-state operation. The results of the charcoal gasification test are presented in order to compare the variations in gas composition and bed temperature observed during railroad tie gasification with low-volatile-fraction charcoal. The test results shown in Figure 19 depict syngas composition and bed temperature variation with time for three phases of gasification (ignition, devolatilization, and carbon gasification).

A steady-state bed temperature is observed to have been attained soon after sustained ignition occurred. The oxygen concentration reduced to near 0%, while the concentration of combustible syngas species (H_2, CO, and CH_4) increased. Since the char contains volatiles
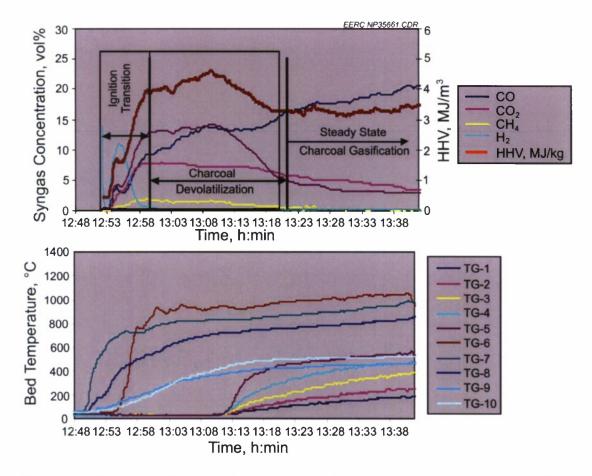

Figure 19. The charcoal gasification test results depicting syngas composition and bed temperature variation with time obtained during ignition, devolatilization, and carbon steady-state gasification.

31

during the initial gasification phase, the concentration of H_2 and CH_4 species attains peak values. In this batch mode charcoal gasification experiment, the fuel volatiles depleted rapidly, resulting in reduced H_2 and CH_4 concentrations. Subsequent carbon gasification resulted in an increase in CO concentration, peaking at about 21%. The CO_2 concentration decreased during this gasification phase until complete conversion of carbon in the bed occurred. A CO/CO_2 ratio greater than 10 obtained in the gasifier is attributed to the ability of the gasifier to maintain bed temperature profiles such that near-complete conversion of carbon is possible under self-sustained (without external heating) gasifier operation.

35% Pine Wood Gasification

This test was conducted with the aim of acquiring steady-state operational data for a full day of operation while operating on high-moisture fuels. The feedstock for this test was a 35% moisture content pine wood. The system was operated for a total of 14 hours, 13 hours of which pine wood fuel was being gasified. The gasifier operating condition was unaltered during the test run except for small variation in fuel moisture levels typical of woody biomass stored in open space.

Results from gasifying 35% moisture pine wood waste are shown in Figure 20. The test was ended voluntary after approximately 13 hours of operation on pine wood fuel. The fuel conversion rate was 61 lb/hr. Besides high moisture content, this fuel consisted of about 10% to 15% fines, an unacceptably high concentration for commercial downdraft gasifiers. The fuel was continuously injected at a constant rate, and the bed height remained constant. The syngas was cleaned in the pilot plant scrubber system. Fuel ash content was low; therefore, the residue dump system was not operated during the test. The gasifier produced water at a rate of 8.1 L (2.14 gallon/hour). The clean syngas was flared.

A summary of syngas composition and higher heating value is provided in Table 6. The average H_2/CO ratio achieved was 1.51; the highest ratio achieved was 2.26. The high concentration of CO_2 was primarily due to water–gas shift reaction. It would be possible to produce a syngas with lower CO_2 concentrations in the current gasifier design using different operating conditions.

The average CH_4 and higher hydrocarbons (C_xH_x) concentration in the syngas was 1.5% and 0.5%, respectively. The highest CH_4 concentration measured was 2.2%, with a higher hydrocarbon value of 1.2% for a total of 3.4% total hydrocarbons. These values were observed for a duration of only 3 to 4 minutes during the test. Since instantaneous tar concentration is not possible to measure, the CH_4 concentration was used as an indicator of tar production. Generally, a CH_4 concentration greater than 2% is indicative that heavier tars are being formed.

The bed temperature profile shows a significant variation in the high-temperature zone of the gasifier. The average bed temperature achieved was 850°C which is desired for attaining carbon gasification and is indicated by consistent CO and H_2 concentration in the syngas. The upper bed temperature was below 250°C. Evaporation and devolatilization occur in this upper cold zone prior to ignition of the particles in the bed. The bed depth was found to be greater
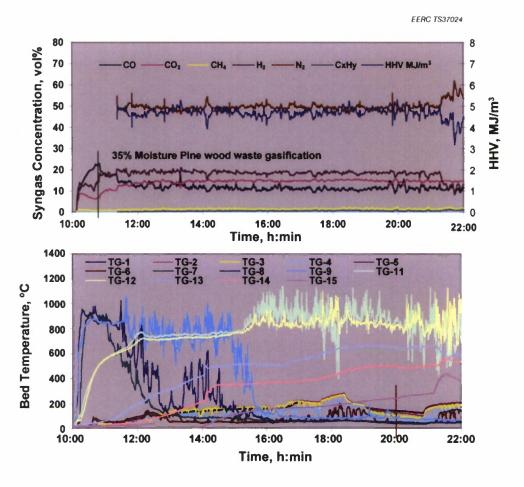
Figure 20. The 35% moisture pine wood waste gasification test results depict syngas composition and bed temperature variation with time obtained during steady-state gasification.

Table 6. Average Syngas Composition and HHV of the Syngas and Standard Deviations

	CO, %	CO_2, %	CH_4, %	H_2, %	N_2, %	C_xH_y, %	HHV, MJ/m^3
Average Syngas Composition	12.1	14.1	1.5	17.2	50.3	0.5	4.7
Standard Deviation	2.2	1.8	0.4	2.8	2.6	0.2	0.3

(from TG-3 to TG-9) as an effect of higher moisture content in the test fuel. In contrast to this, the upper bed depth for drier fuels such as charcoal and predried tie consisting of 5% was small TG3 – TG5 (see Figure 20). This feature of the expansion of the cold zone can be compared to the effect of moisture on single particle ignition delay as earlier observed by Patel et al. (1996) in the case of single particle combustion studies performed on distillery effluents consisting of moisture ranging from 0% to 45%.

The syngas production to biomass feed ratio was 2.57. The flow rate remained almost constant during the experiment. The average higher heating value (HHV) of the gas was

33

4.7 MJ/m^3, which is acceptable for IC engine operation for electrical generation applications. Inorganics from the fuel did agglomerate into small deposits less than 1 inch in diameter; however, the bed temperature distribution helped maintain the solid movement and avoid formation of larger deposits.

Conversion of fuel volatiles in the gasifier is critical for the production of clean syngas. Production of small amounts of low-molecular-weight hydrocarbon in the syngas is an important qualitative indication of achieving higher volatile conversion and low concentration of condensable tars. The trace gas composition, determined by a quasi online GC, is shown in Figure 21. The concentration of trace gaseous hydrocarbons consisting of ethylene, ethane, propane, and propylene were an order of magnitude lower than the methane concentration (right-hand abscissa). The variation in the trace hydrocarbon concentration is nearly proportional to the variation in the methane concentration. The H$_2$S and COS concentration time profile shown in Figure 21 shows no direct relationship with the variation in hydrocarbon concentration.

Table 7 shows mass and energy balance and average gasification efficiency based on measured gasification parameters. The gasifier is designed to achieve complete carbon conversion; therefore, except to remove inorganic residue, the extraction screw is not operated.
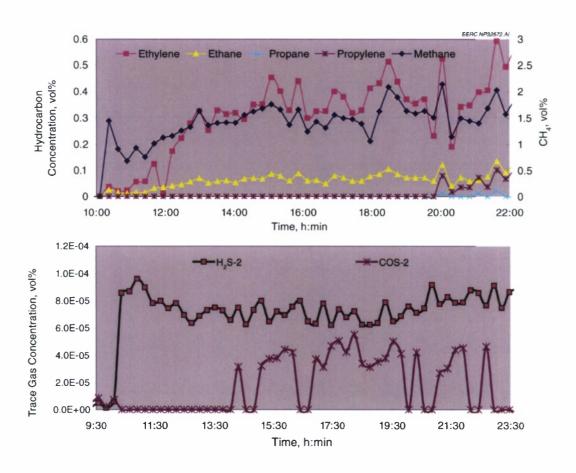
Figure 21. Concentration of hydrocarbon and sulfur containing gases vs. time history obtained during gasification of 35% moisture pine wood waste.

34

Table 7. Gasifier Performance: Test 1

Gasifier Performance	
Test Duration	787.00 minutes
Biomass Throughput	27.94 kg/h
Additional Char Consumed	1.64 kg/h
Air Flow Rate	46.48 kg/h
Biomass Moisture	35.00%
Biomass Calorific Value	12.84 MJ/kg
Thermal Input (tie)	99.65 kW
Char Moisture	3%
Char Calorific Value	31.30 MJ/kg
Thermal Input (char)	13.82
Net Thermal Input	113.46 Wth
Syngas: Thermal Output	
Higher Heating Value	4.65 MJ/m^3
Flow Rate	72.60 m^3/h
Gas Density @18°C	0.99 kg/m^3
Thermal Output (syngas), HHV	92.84 MJ/m^3
Gasification Efficiency, HHV	81.8%

In order to obtain energy balance, the energy content of the net charcoal consumed during the entire duration is added as an input which increases the net thermal input. The cold gasification efficiency, which is the ratio of chemical (unconverted thermal) energy in the syngas to the thermal energy input based on HHV, is 81.8%. Higher gasification efficiency is an indication of higher conversion of the organics present in the fuel and one of the distinct feature of the advanced gasifier. This conversion of volatile compounds is critical to effective gasifier operation because it increases conversion efficiency of fuel to syngas and reduces tar loading to syngas cleanup systems.

Grand Forks Municipal Wood Waste Gasification

During the previous test in which 35% pine waste wood was gasified, hydrogen-rich syngas was produced by promoting the water–gas shift reaction in the gasifier bed. A hydrogen-rich syngas is desirable in some fuel and energy applications; however, when syngas is used for power production in IC engine generators, a CO-rich syngas is preferred. It is possible to adjust operational conditions of the gasifier to reduce N_2 and CO_2 dilution, thereby further increasing hydrogen yield. In order to test the ability of the gasifier to produce H_2-rich syngas or CO-rich syngas, gasifier operating conditions were varied over the course of the 24-hour period.

A 24-hour test was conducted to gather data on long-term operation of the gasification system and to demonstrate the production of both a hydrogen-rich and a CO-rich syngas. During

the 24-hour gasifier operation, two fuels were tested: 1) Grand Forks municipal wood waste and 2) Marcel sawmill wood waste. During the first half of this 24-hour, test Grand Forks municipal wood waste possessing an average moisture content of 52.68% was gasified.

Figure 22 shows the syngas composition and bed temperature vs. time measured. The desired bed temperature was maintained; however, the start-up charcoal bed assisted in maintaining temperature in the lower gasifier zone. The average syngas composition is depicted in Table 8. Table 9 shows the trace gas concentration determined by colorimetric tubes.

The syngas composition profile shown in Figure 23 provides a plot of CO and H_2 concentration with time. Although these concentrations vary over the course of the test, the sum of these two gases remains fairly constant. Further, since CO and H_2 have similar calorific values on a volume basis, the syngas calorific value remained constant. The CO/CO_2 ratio throughout the test remained between 2.5 and 5.5, indicating good CO_2 and char conversion. The fuel injection was constant during the experiment, and the pressure drop across the bed was consistent during the entire 24-hr operation. Although this test was successful in achieving the desired syngas composition at the pilot scale, better performance could be obtained by optimizing heat transfer in the reacting packed bed.
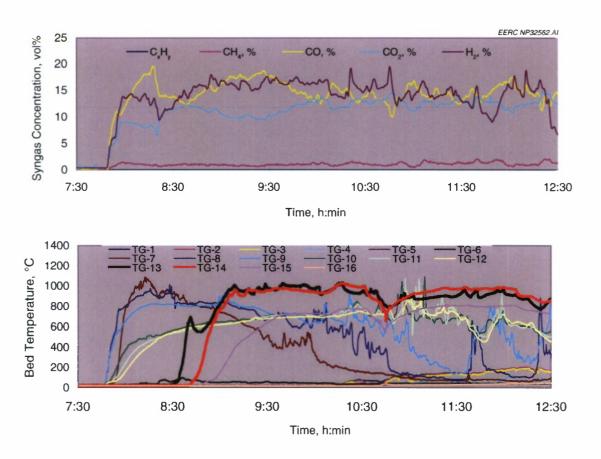
Figure 22. The 52.6% moisture pine wood waste gasification test results depicting syngas composition and bed temperature variation with time obtained during steady-state gasification.

Table 8. Average Syngas Composition and HHV of the Syngas and Standard Deviations

	CO, %	CO$_2$, %	CH$_4$, %	H$_2$, %	N$_2$, %	C$_x$H$_y$, %	HHV, MJ/m^3
Average Syngas Composition	1.3	14.7	12.0	14.5	57.5	4.5	1.3
Standard Deviation	0.5	2.1	1.7	2.5	3.1	0.4	0.5

Table 9. Trace Gas Concentration Determined Using Colorimetric Tubes

	Cold Side Test Time 9:06 – 10:10 ppmv
Toluene	400.0
COS	Not detected
SO$_2$	0.5
Xylene	2.5
HCN	0.8
NH$_3$	Not detected
H$_2$S	11.0

Gasification of High-Moisture Marcel Sawmill Wood Waste

The fuel used during the second half of the 24-hour test was obtained from the Marcel sawmill. This waste wood was gasified containing an average moisture content of 33.5%. During gasification of this fuel, tests were conducted to better understand the range of H$_2$/CO ratio achievable in the advanced fixed-bed gasifier. Short-duration, steady-state experiments were conducted during the test to observe the range of H$_2$ and CO achievable. Table 10 shows single measurement values.

Figure 24 shows the syngas composition and bed temperature vs. time measured during the gasification of Marcel sawmill waste wood. This fuel was gasified for about 5 hours with a throughput of 56.8 lb/hr. Several gasifier operating conditions were tested in order to estimate conditions for attaining desired syngas composition. As can be seen, the average bed temperature at the gasifier operating condition could gasify the wet biomass, and it was possible to increase bed temperature as desired. The gasifier could be operated at two steady-state conditions such that the syngas composition with either high CO or high H$_2$ concentration could be obtained (H$_2$/CO ratio of 0.25 and 1.8). The bed temperature profiles were adjusted with the help of air staging in the advanced gasifier. This special feature allows production of distinct steady-state syngas compositions. The gasifier operating condition, selected for long-duration testing, was a high H$_2$/CO ratio applicable to liquid synthesis applications.

Table 11 shows that the trace gas concentration in the hot syngas was determined by calorimetric tubes. The COS and NH$_3$ were not detected; however, trace concentrations of HCN, SO$_2$, xylene, and H$_2$S were determined. The toluene concentration was lower than expected. These short point tests are indicative and could be used for planning scrubbing strategies.
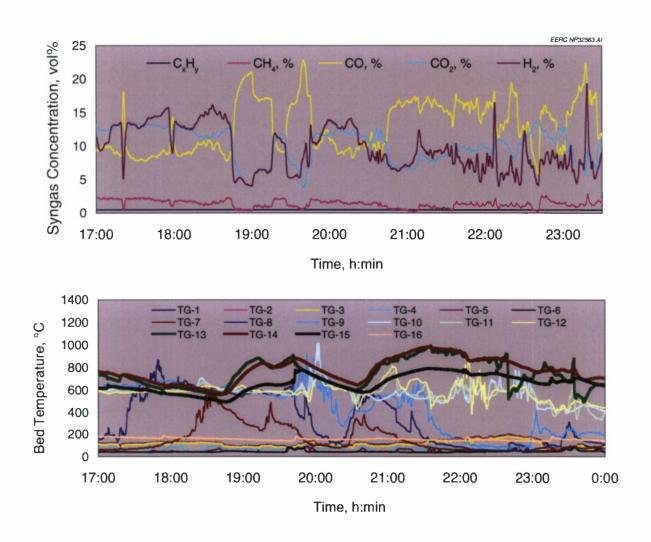
Figure 23. The 52.6% moisture Grand Forks municipal wood waste gasification test results depict syngas composition and bed temperature variation with time obtained during testing to produce CO-rich and high CO/CO_2 syngas.

Table 10. Measured Gas Composition Achievable During Self-Sustained Gasification of 35% Moisture Marcel Sawmill Wood Waste

Test Date: November 11, 2009	CO	CO_2	CH_4	H_2	N_2
Highest Concentration, vol%	22.8	8.4	1.36	37.4	30

The tar and particulate matter concentration in the syngas was determined during the wet wood gasification test. The results of the test are described in a later section.

Railroad Tie Gasification

Railroad ties are a complex fuel for use in gasification because of the presence of wood with complex hydrocarbon mixtures and associated high volatiles content. The comparative

38
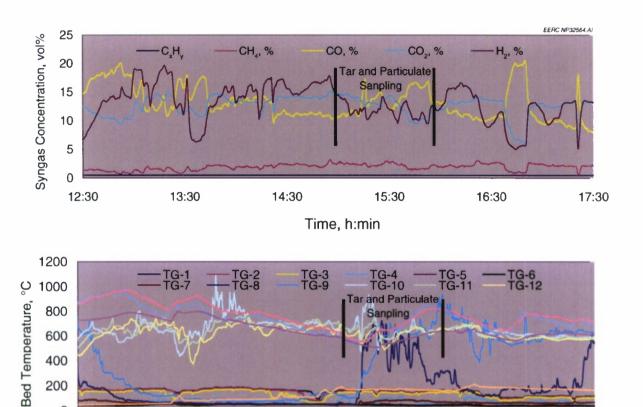
Figure 24. Syngas composition and bed temperature vs. time history of gasification of wet wood received from legacy waste pile from a sawmill located in Marcel, Minnesota. Tar and particulate sampling was conducted during times indicated on the composition and bed temperature plot (24-hr test).

Table 11. Results of Calorimetric Tube Measurement of Trace Syngas Components Obtained During Gasification of Sawmill Wood Waste from Marcel

	Hot Side Test Time 12:49–13:50 ppmv
Toluene	33.3
COS	Not detected
SO_2	1.0
Xylene	1.7
HCN	0.8
NH_3	Not detected
H_2S	2.0

composition of two different railroad ties is shown in Table 4. Railroad Tie 2 was obtained from a source in the United States, and Railroad Tie 4 was obtained from British Columbia, Canada. Tie 2 was used in both tests. These ties were predried to 12.6% moisture in order to be tested with the advanced gasifier; for comparison, 35% moisture pine wood was also tested.

The railroad tie feedstocks were not modified for the experiment. The variation in syngas composition including variation in trace hydrocarbon gases and reactor bed temperature with time were recorded.

During the first phase of operation, 35% moisture pine wood was gasified for a period of 10.6 hr at the rate of 56 lb/hr. Railroad Tie 2 was next fed to the gasifier for 3 hours at the rate of 62 lb/hr. The test results are presented in Figures 25 and 26.

The gasifier performance with pine wood chips was similar to the previous test (see Figure 20). The gas composition and temperature profile were similar until the injection of railroad ties at approximately 18:30. A new steady state for railroad tie was attained as observed with the distinct lowering of the H_2/CO ratio from greater than 1 to less than 1. In contrast to the
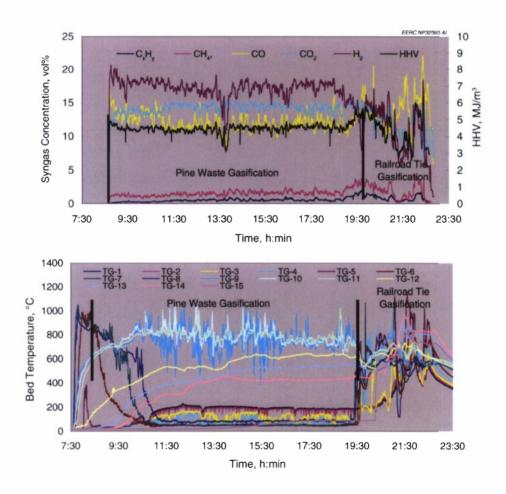
Figure 25. Syngas and bed temperature vs. time history of pine wood waste and railroad tie gasification at 54.5- and 56.1-lb/hr throughput, respectively.

40
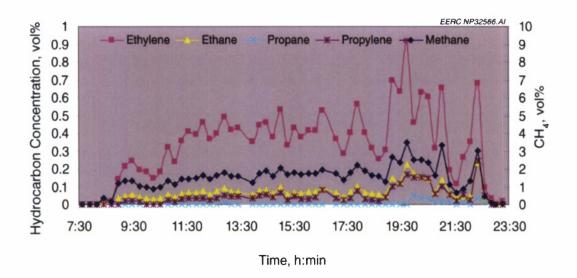
Figure 26. Concentration of hydrocarbon gases obtained during
gasification of 35% moisture pine wood waste.

pine wood gasification, the bed temperature during the tie gasification spread into the upper zones of the gasifier such that the reacting bed depth increased, resulting in a higher conversion rate. The observable shift in bed temperatures to the upper zone of the gasifier could be attributed to comparatively lower moisture (approximately 12.5%) and higher volatile content of the railroad tie fuel. The higher volatile content likely resulted in a higher devolatilization rate which, in turn, caused flaming and temperature fluctuations in the bed.

Besides lowering of H_2/CO ratio, the CO_2 concentration also dropped when railroad ties were injected to the gasifier. CO_2 concentration decrease is a direct effect of increased bed temperature and decrease in feed moisture, consistent with the properties of the railroad tie fuel. The H_2/CO ratio dropped because of a decrease in H_2 concentration as an effect of fuel composition, including low fuel moisture content. A distinct increase in the trace hydrocarbon gas concentration was also observed with the railroad tie fuel.

The second test using Railroad Tie 2 was designed to evaluate the effect of maintaining higher average bed temperatures as compared to the bed temperature in the first test on carbon conversion and the fate of organic material during gasification. The gasifier was operated at its nominal design throughput of 33 lb/hr. Table 12 shows average syngas composition, HHV, and standard deviation obtained during tie performance test. The heating value of the syngas was higher than syngas from pine wood waste. The lower CH_4 concentration as compared to previously observed concentrations greater than 2.5% is an indication of relatively better organic conversion. The syngas flow rate was 33.0 scfm and remained constant during steady-state gasifier operation. The tie carbon conversion was complete, and in addition, the bed char above the grate converted at a rate of about 2.4 lb/hr (1.09 kg/hr) (7% of the tie throughput). In the gasification efficiency calculation, the thermal energy contribution of the char is added to the net thermal input to the gasifier. It was observed that, because of the higher bed temperature, a large

41

Table 12. Average Syngas Composition, HHV, and Standard Deviation Obtained During Performance Test 2

	CO, %	CO_2, %	CH_4, %	H_2, %	C_xH_y, %	HHV, MJ/m^3
Average Syngas Composition	17.4	11.1	1.8	14.8	1.1	5.29
Standard Deviation	2.1	1.5	0.9	5.2	–	1.06

fraction of fuel moisture was converted to syngas. The gasification efficiency calculated as a ratio of thermal energy output in the syngas and input in the tie and char was about 80% to 85% (Table 13).

Figure 27 shows variation of syngas composition, HHV bed temperature, and syngas flow rate variation with time. As was observed, the variation in the syngas composition is due to fuel injection timing, which is consistent with previous observations and characteristic of the fuel. However, the variation in bed temperature was not coupled with fuel injection and maintained an almost constant profile. This effect is primarily due to reduction in the fines (compared to the fines in Test 1) in the fuel and a stable reacting char bed.

Table 13. Gasifier Performance: Tie Test

Gasifier Performance	
Test Duration	82.00 minutes
Tie Throughput	14.60 kg/hr
Additional Char Consumed	1.09 kg/hr
Air Flow Rate	37.31 kg/hr
Tie Moisture	12.60%
Tie Calorific Value	20.17 MJ/kg
Thermal Input (tie)	81.80 kW
Char Moisture	5%
Char Calorific Value	31.30 MJ/kg
Thermal Input (char)	9.48
Net Thermal Input	91.28
Syngas: Thermal Output	
Higher Heating Value	5.29 MJ/m^3
Flow Rate	56.00 m^3/h
Gas Density @ 18°C	0.94 kg/m^3
	52.64 kg/hr
Thermal Output (syngas), HHV	77.35 MJ/m^3
Gasification Efficiency, HHV	84.74%
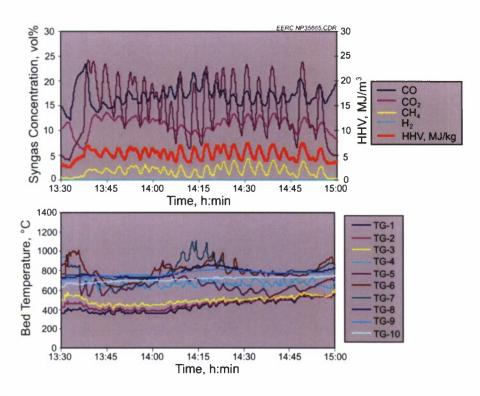
Figure 27. Syngas, bed temperature, and flow rate vs. time history of Tie 2
gasification at 14.6 kg (32.2 lb/hr) throughput obtained during gasifier performance Test 2.

PRB Coal Gasification

A coal gasification test was conducted to evaluate gasifier operation and syngas quality.
The self-sustained gasification test was conducted with a Montana subbituminous coal
commonly known as PRB coal containing 26.5% moisture. The experiment was initiated with
the gasification of wood charcoal consisting of 5% moisture. Syngas composition and bed
temperature data are summarized in Figure 28. The coal conversion began as soon as the coal
reached the hot charcoal reaction front. Moisture in the coal typically reduces bed temperature
and the rate of syngas production (see temperature profile TG-7). Tests conducted with the
advanced gasifier resulted in maintaining bed temperature and gas composition ($CO + H_2$).
However, the axial location of the hot zone moved downstream in the gasifier char bed.

The conversion of the coal-bound moisture increased the the H_2/CO ratio to greater than
1.5: a condition that could be easily maintained for achieving hydrogen-rich syngas. Under this
scenario, coal predrying could be avoided.

The trace gas composition determined by the quasi online GC is shown in Figure 29. The
concentration of trace gaseous hydrocarbons consisting of ethylene, ethane, propane, and
propylene were an order of magnitude lower than methane concentration (right-hand abscissa).
The variation in the trace HC concentration is nearly proportional to the variation in the methane
concentration.
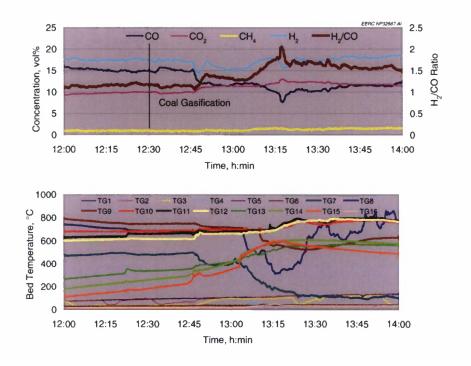
Figure 28. Syngas composition and bed temperature vs. time history of
Montana subbituminous coal gasification in pilot plant gasifier.
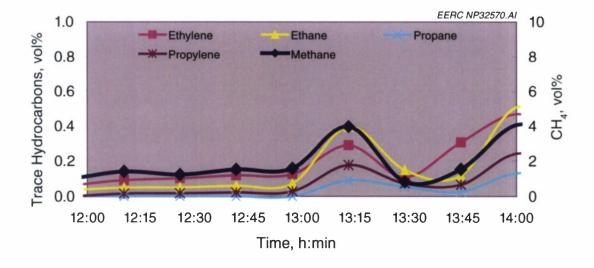
Figure 29. Concentration of hydrocarbon gases obtained during gasification of Montana
subbituminous coal gasification in pilot plant gasifier.

In order to understand the effect of wet coal on the syngas composition, an experiment was conducted in which high-moisture coal was injected during the gasification of dried coal. To simulate this condition, the coal fuel was not fed for a short period of time. During this nonfeed period, the reaction front stabilized on the top surface of the bed, and it was assumed that the moisture was completely evaporated from fuel contained within the gasifier.

$$CO + H_2O \rightarrow CO_2 + H_2$$

$$CO_2 + C_2 \rightleftharpoons CO$$

The syngas composition measured during the dry coal gasification phase is shown in Figure 30. The CO/H_2 ratio was less than 1; however, the production of CH_4 is a clear indication that coal was being gasified and not the char which is devoid of volatiles. When high-moisture coal was again fed to the gasifier, a sharp increase in H_2 occurred. This change is primarily due to the water–gas shift reaction (first reaction). The increase in CO_2 coupled with a decrease in CO is a clear indication of the water–gas shift reaction. The condition of dry coal gasification

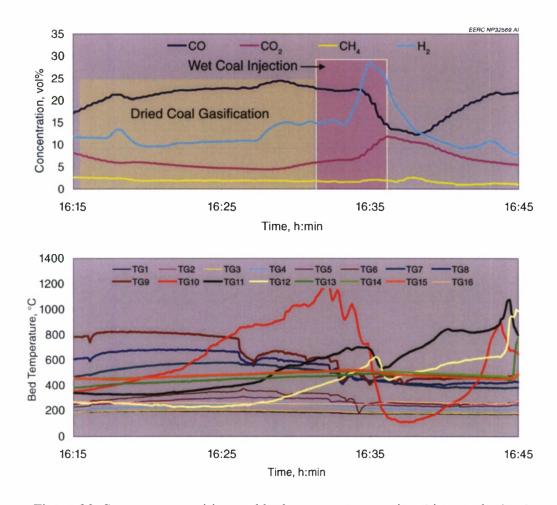Figure 30. Syngas composition and bed temperature vs. time history obtained during gasification of PRB coal – effect of injection of wet coal on dry coal bed.

45

was recovered once the feeding of wet coal was stopped. The sharp decrease in the local bed (TG-10) is an indication of the localized cooling of the bed because of injection of wet coal.

The bed temperature during the dry coal gasification was favorable for the Boudouard reaction (second reaction); therefore, the resulting CO_2 concentration in the syngas was a relatively low value of about 5% (CO/CO_2 ratio was about 5). The pilot plant gasifier is capable of operating at conditions such that rates of both these reactions are high to maintain high H_2/CO and CO/CO_2 ratios. This is desirable for applications requiring production of pure hydrogen and liquid fuel synthesis. These results demonstrate preliminary proof-of-concept for utilizing high-moisture coal as a feedstock for distributed application utilizing air as gasification medium.

Tar and Particulate Measurement

One of the important performance characteristics of the gasifier is determined by quantifying the tar and particulate matter in the syngas. The condensable tars typically heavier than benzene are considered problematic in the applications such as power generation in the IC engine for distributed application. Toluene and xylenes could be considered as engine performance enhancers; however, the engine manufacturers have yet to characterize the engine performance as a function of the effect of these components. Similarly, the effect of heavier components in the catalytic synthesis of FT liquids or methanol is not clearly understood.

A low concentration of gaseous hydrocarbons in syngas is a qualitative indication of the presence of low contaminants (tar and particulate matter) in the syngas. In practical applications, tar and particulate matter are not determined. As an effort to evaluate the gasifier's ability to minimize production of these contaminants as well as the capability of the scrubber system to effectively remove them from the syngas, tar and particulates were determined during the gasification of railroad ties and Marcel sawmill waste wood.

Elaborate tar- and particulate-sampling and analysis procedures have been developed and implemented. A general outline of the procedures is found in the European Tar Protocol (1). Figure 31 depicts tar and particulate sampling system in pilot plant gasifier. Tar and particulate matter concentrations in the hot (unscrubbed gas) and cold syngas were measured to determine the effectiveness of the upstream scrubber system. The syngas was isokinetically sampled and passed through heated thimbles (see Figure 31, Module 2) used for capturing particulate. The tar-laden syngas was passed through a series of impinger bottles (Module 3 and 4) filled with dichloromethane (DCM) in which the tar is captured by dissolution. DCM is an excellent solvent for capturing and analyzing tar by gas chromatographic techniques. Gravimetric tar determination was achieved by evaporating the solvent.

The total volume of sampled syngas was measured using a gas flowmeter in Module 5. This module consists of a pump, a rotameter, a gas flowmeter, stainless steel needle and ball valves, and pressure and temperature indicators to accurately determine the sample gas volume. The gas leaving Module 5 is then vented to the flare.

Tables 14 and 15 show the differences between the tar concentrations in Test 1 (railroad tie gasification) and Test 2 (Marcel sawmill waste wood), respectively. The optimized gasifier

46
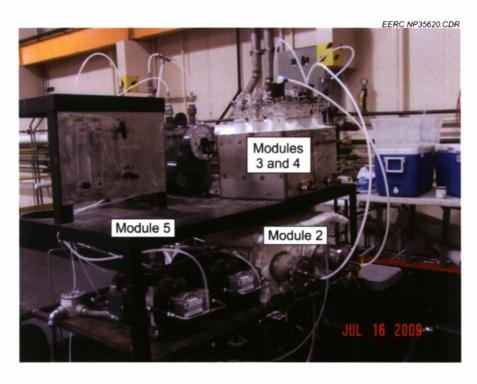
Figure 31. Tar and particulate sampling system in pilot plant gasifier.

Table 14. Summary of the Gravimetric Analysis of Tar (heavier than benzene) and PM Sampled from Hot and Cold Side – Railroad Tie Gasification with Syngas Polisher

Test No.	Contaminants		Total Flow Syngas Volume, Nm^3	Concentrations in Producer Gas	
	Particulate Filters, mg	Tar Heavier than Benzene, mg		Particulate, mg/Nm^3	Tars, mg/Nm^3
2 (hot side)	230	534	0.65	353.3	822
2 (cold side)	21	134	0.65	32.3	200

Table 15. Summary of the Gravimetric Analysis of Tar (heavier than benzene) and PM Sampled from Hot and Cold Side – 33.5% Marcel Wood Waste

Test No.	Contaminants		Total Flow Syngas Volume, Nm^3	Concentrations in Producer Gas	
	Particulate Filters, mg	Tar Heavier than Benzene, mg		Particulate, mg/Nm^3	Tars, mg/Nm^3
2 (hot side)	106	2317	0.605	175.2	3829.8
2 (cold side)	31	168	0.579	53.5	290.2

operation, with higher uniform bed temperatures, produced a syngas with tar concentrations to 822 mg/m³ (see Figures 24 and 27) on the hot side (uncleaned syngas). In the case of biomass gasification, the tar and particulate sampling was conducted at lower bed temperatures in order to

understand the worst-case concentrations on the hot side and the ability of the scrubbing section to remove the condensable tar. Wet biomass was directly fed to the relatively cold char zone (630°C). The CH_4 concentration was about 2.5%–2.9% which is about 1%–1.5% higher than that observed during higher bed temperature steady-state gasification of wet biomass. This demonstrates that higher CH_4 concentration may provide an indication of higher tar concentration in the syngas.

The scrubber successfully removed all condensable tars heavier than naphthalene from syngas produced with railroad ties, and all condensable tars heavier than acenaphthalene from syngas produced from biomass. It was determined that, in the case of railroad ties, about 93% of the naphthalene was removed in the scrubber. Out of the total 200 mg/m^3 of tar in the tie syngas, the organics (about 83%) are typical engine performance enhancers, and the remaining condensable tars can be removed in the syngas polisher by adjusting the operation of the system.

Method 5 measurements determined that the installed scrubber system was capable of removing about 85%–96% of the particulate matter, and it is possible to achieve even higher efficiency.

Near-zero carbon conversion could be achieved in the gasifier bed except for a small fraction of carbon recovered during the test in order to determine its gas adsorption capacity.

Accomplishments

In order to reduce the gasifier start-up transient period and reduce tar levels during this phase, ignition tests were conducted on cold, warm, and hot charcoal beds. The hot bed had the shortest ignition delay and produced combustible syngas almost instantaneously. The baseline charcoal gasification tests were conducted to understand the difference in syngas composition and temperature vs. time profiles.

A CO/CO_2 ratio greater than 10 is typically achieved during charcoal gasification, while for high-moisture biomass, the value ranged between 2.5 and 5 in this gasifier design. This shows the ability of the gasifier to attain self-sustained gasification conditions with high CO_2 and carbon conversion.

During the 13-hr steady-state gasification of pine wood, hydrogen-rich syngas composition was produced with an achieved average and highest H_2/CO ratio of 1.51 and 2.26, respectively. Such steady-state gasification could be obtained on high-moisture biomass for a commercial syngas-to-liquid production system.

Cold gasification efficiency greater than 80% for high-moisture biomass and railroad ties was achieved. Higher gasification efficiency is an indication of higher conversion of organics present in the fuel and near-complete carbon conversion.

Woody biomass containing moisture greater than 50% was tested, and desirable syngas composition was achieved for applications of either liquid synthesis process (high H_2/CO ratio) or electricity production (high CO/H_2).

48

A proof-of-concept utilizing high-moisture coal as feedstock for distributed application such as production of pure hydrogen and liquid synthesis was demonstrated. It was established that the advanced gasifier is capable of operating at conditions such that high H_2/CO and CO/CO_2 ratios in the syngas, as required by these applications, could be produced.

The level of tar during steady-state gasification of railroad tie in the unscrubbed hot syngas and scrubbed syngas was determined to be 822 and 200 mg/m^3, respectively, while the particulate concentration was 353 and 32 mg/m^3 respectively. The cold-side tar contained about 83% toluenes and xylenes, which are typically used as performance enhancers in IC engines. No tar heavier than naphthalene (only 7%) escaped the syngas polisher. Operational adjustments to the syngas polisher can lead to higher than 95% tar capture.

The worst-case tar produced in the case of wet biomass gasification was 3830 mg/m^3 and 290 mg/m^3 in hot and cold syngas, respectively. The particulate matter concentration determined was 175 and 54 mg/m^3 in hot and cold syngas, respectively.

The gas cleanup system of the advanced gasifier was able to reduce hydrocarbon levels from 3830 to 290 mg/m^3 and reduce particulate from 175 to 54 mg/m^3.

Subtask 2.2 – Process Development for Advanced Alternative Fuels

Subtask 2.2.1 – FT Process Development

In earlier work, a small-scale FT reactor (Figure 32) was designed and built to test FT catalysts (Zygarlicke et al., 2009). The FT reaction typically requires iron- or cobalt-based catalysts, but previous efforts to acquire commercial FT catalysts had failed. Therefore, work under this activity included development of an FT catalyst in order to demonstrate the
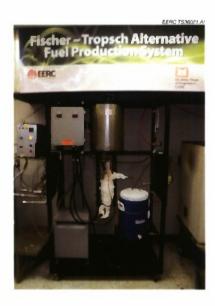
Figure 32. Small-scale FT reactor system for testing
small quantities of catalyst with synthetic syngas.

technology. As iron FT catalysts are cheaper and more suitable for converting coal/biomass-derived syngas, it was chosen as the basis for catalyst development. The iron was precipitated onto an alumina pellet for support, and various promoters such as potassium, copper, and lanthanum were added to improve catalyst performance. Several iterations of catalyst formulations, activation procedures, and operating conditions were tested until satisfactory catalyst productivity and product selectivity were achieved.

As part of a separate project, a large-scale FT reactor (Figure 33) was built capable of testing up to 2 kg of catalyst. The reactor was installed in proximity to various coal and biomass gasifiers and was available for use in this activity. Syngas cleanup units to remove contaminants and catalyst poisons were available as well. To fill the large FT reactor with catalyst, the EERC needed to scale up the iron catalyst production process and prepare at least 3 kg of catalyst.

While a suitable iron catalyst formulation had been developed, further avenues for catalyst optimization were pursued. In particular, it was observed in a repeat test, delayed 4 months after the original test on the same batch of catalyst, that the catalyst activity had declined significantly during storage in the laboratory. The factors that caused this deactivation were investigated. It was also known that lanthanum oxide improved catalyst performance by reducing the surface acidity of the alumina support. The optimum level of lanthanum had not yet been researched, so this variable was also studied more closely.

Continued efforts during this reporting period to acquire FT catalyst from a commercial supplier finally yielded results. A relationship was built with a particular company from another
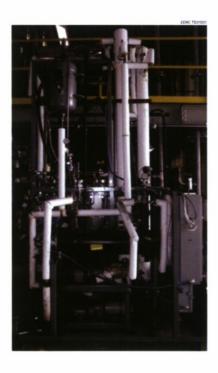
Figure 33. Large-scale FT reactor for testing large
batches of catalyst with coal- or biomass-derived syngas.

project, and the company agreed to submit small quantities of cobalt- and iron-based FT catalysts. These catalysts were tested in the small-scale reactor, and the results were used primarily as a baseline reference to compare the effectiveness of the EERC FT catalyst.

Coal- and Biomass-to-Liquids Process Demonstration

Because of the difficulty in obtaining large quantities of commercial FT catalyst from vendors with exclusive contracts or closely guarded intellectual property positions, the EERC developed an in-house, iron-based, supported catalyst formulation for initial testing. This catalyst was developed, tested, and optimized in a laboratory-scale FT reactor using bottled gases to simulate coal-derived syngas. Following successful demonstration of the in-house catalyst formulation, a large batch of the catalyst formulation was prepared for loading into a large bench-scale FT reactor system and testing on actual coal-derived syngas from a bench-scale high-pressure fluid-bed gasifier.

Production of EERC iron-based FT catalyst was scaled up using the methodology described in more detail in an earlier report (Zygarlicke et al., 2009). The porous alumina pellets that were promoted with lanthanum were soaked in a solution of iron nitrate, copper nitrate, and urea. Under vacuum, the solution fills the pores of the catalyst rapidly. The excess solution was drained, and the catalyst pellets were heated slowly up to 280°C. The urea decomposed into ammonia, which then reacted with the iron and copper compounds to precipitate inside the pores of the support.

Three separate, large batches of catalyst were prepared for the large-scale reactor. The iron loading for each batch was targeted to be 10% by total weight of the catalyst. The lanthanum weight fraction target was 1%, but significant variation was noted between batches (Table 16.) A small sample of approximately 7 g was loaded into the small FT reactor. The catalyst was activated under flowing carbon monoxide at a temperature of 300°C. After several hours, the temperature of the reactor was reduced to 260°C, and synthetic syngas was introduced to the catalyst with a hydrogen to carbon monoxide ratio of 1:1.33. The flow rate of the syngas was adjusted so that approximately 15% to 20% of the CO was converted. Each catalyst batch was

Table 16. Catalyst Composition, CO Conversion, and Product Selectivity Data for Three Large Catalyst Batches

		AP11A	AP11B	AP11C
Iron	wt%	11.2	9.4	10.1
Copper	wt%	0.29	0.20	0.38
Potassium	wt%	0.22	0.30	0.24
Lanthanum	wt%	0.84	1.7	2.9
CO Conversion Fraction	% Feed	17.6	17.4	16.2
CO Conversion Rate	mol CO/kg cat-hr	12.7	13.8	12.4
Light Gas Selectivity	% CO to HC	18.1	16.1	16.2
Liquid/Wax HC Productivity	g HC /kg cat - hr	60	72.9	60.3

tested for a minimum of 250 hours to allow for steady-state catalyst observations. Liquid and wax product were periodically collected, weighed, and analyzed. Exit gases were also collected and analyzed to determine CO conversion rates and light hydrocarbon gas production.

No major differences were observed in catalyst productivity or selectivity for the three test batches, and although the catalysts did not exhibit performance equivalent to the commercial FT catalyst, they were successful in producing significant amounts of liquid and wax hydrocarbons. It was noted AP11B had a slightly higher CO conversion rate and better selectivity to heavier hydrocarbons. Based on this result, it was determined that investigation into the effect of lanthanum on catalyst performance was warranted.

The catalysts were loaded into the large FT reactor. Pressurized syngas exiting the gasification and syngas cleanup systems was routed to the large FT reactor with an estimated maximum liquid production rate of 4 liters (1 gal) per day per reactor bed. The FT reactor system meters up to 100 slpm (3.5 scfm) per bed of clean, pressure-regulated syngas from the gasifier through a preheater and then into a set of downflow parallel packed shell-and-tube reactor beds. Two reactor beds are currently installed on the system, with room for expansion to four. The reactor beds can operate at up to 70 bar (1000 psig) and 300°C (570°F), providing flexibility for the potential of methanol or mixed-alcohol synthesis in future tests.

For the initial start-up of the reactor system, the shell-and-tube reactor beds were heated to temperature using a countercurrent flow of Dowtherm oil through the external (shell-side) tube. Syngas passing through the beds was then slowly brought to operating pressure, initiating the exothermic FT reaction. As pressure builds and the beds begin to heat under exothermic reaction, the Dowtherm heater is turned down, and the Dowtherm begins to function as a coolant. Product gas exiting the beds is recycled through preheater coils to the bed inlets. Incoming syngas is diluted which promotes higher overall conversion efficiencies. Liquid exiting the bottom of the packed beds was collected in a heated wax trap before passing through a set of water-cooled condensers to remove lighter organic material and water. Hot liquid in the wax trap can be recycled to the top of the reactor to provide further syngas dilution and catalyst cooling, thus bringing the inlet to the packed beds closer to outlet conditions. This design allows the packed beds to function similarly to slurry bed designs more commonly used in large-scale FT synthesis. Unrecycled product gas is depressurized and measured through a dry gas meter, and a slipstream is passed to a laser gas analyzer to provide online comparison of inlet syngas and outlet product gas composition.

Because the entire unit is compact and skid-mounted, it can be readily moved to any of the different gasification systems located at the EERC, or it can be loaded into a truck and coupled to an off-site gasifier. This design flexibility in terms of recycle ratio, operating conditions, heat load or heat removal, and placement makes the FT reactor system a valuable tool for testing catalysts under a wide variety of scenarios.

To produce syngas from coal and biomass, a bench-scale fluid-bed gasifier was used that is capable of feeding up to 9.0 kg/hr (20 lb/hr) of pulverized coal or biomass at pressures up to 70 bar absolute (1000 psig). The externally heated bed is initially charged from an independent hopper with silica sand or, in the case of high-alkali fuels, an appropriate fluidization media.

Independent mass flow controllers meter the flow of nitrogen, oxygen, steam, and recycled syngas into the bottom of the fluid bed. Various safety interlocks prevent the inadvertent flow of pure oxygen into the bed or reverse flow into the coal feeder.

Coal feed from a K-tron® system drops through a long section of vertical tubing and is then pushed quickly into the fluid bed through a downward-angled feed auger as seen in Figures 34 and 35. Syngas exiting the fluid bed passes through a cyclone before flowing into a transport reactor that uses regenerable sorbent to remove sulfur from the syngas stream. The syngas then passes through a hot candle filter to remove fine particulate before entering a series of fixed beds. One bed is a polishing bed of ZnO that removes all remaining traces of sulfur from the syngas. Other beds can be loaded with water–gas shift catalyst, heavy metal sorbent, a chlorine guard, or other sorbents and catalysts. The clean, shifted syngas, still hot and pressurized, is then routed through a series of water-cooled condensers to remove volatile organics and moisture. Syngas can be sampled upstream of the condensers for hot tests. The clean, dry syngas exiting the condensers is then recycled through a compressor to the bottom of the fluid-bed gasifier, and a portion is vented through a control valve to maintain system pressure. The syngas exiting the system passes through a dry gas meter for mass balance. A slipstream of this depressurized, dry
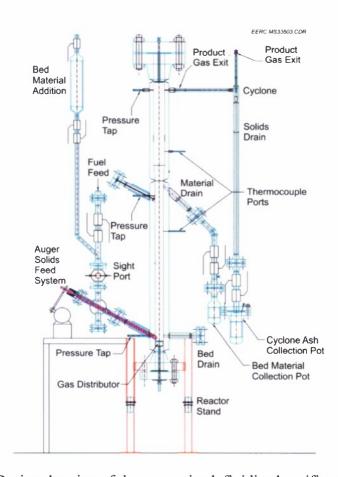
Figure 34. Design drawing of the pressurized, fluidized gasification reactor.
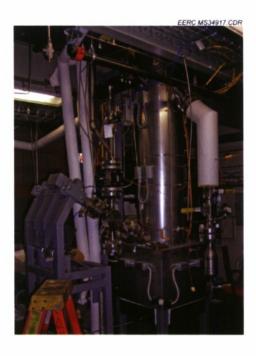
Figure 35. Photograph of the lower section of high-pressure fluid-bed gasifier. Visible at left is the feed auger angled downward into the bed.

gas is also fed to a laser gas analyzer and a GC for online analysis of major gas components and for low-level (ppb) analysis of sulfur species. In addition, operators periodically sample syngas from various points throughout the system using Dräger tubes for H_2S and other trace gases to verify low-level chromatograph data.

Sulfur removal was accomplished by use of two of the fixed beds loaded with regenerable RVS-1® commercial sulfur sorbent. Additionally, two downstream beds were loaded with nonregenerable Actisorb S2® polishing sorbent to capture remaining traces of sulfur compounds from the syngas. Both sorbents were purchased from Süd-Chemie. Each set of fixed beds was operated one-at-a-time so that spent sorbent from one bed could be regenerated or replaced while the system was still running on the second bed.

For the tests described in this section, the gasifier was initially operated using PRB Antelope coal. Target bed temperature was between 816° and 843°C (1500° and 1550°F), target pressure was 21.7 bar (300 psig), and target bed velocity was 0.30 m/s (1.0 ft/s) or less. Coal, oxygen, steam, and recycle flow rates had no specific target flow rates but were adjusted to achieve the desired temperature, pressure, and velocity while sustaining flow to the FT reactor. Laser gas analysis of the syngas composition from the gasifier is shown in Table 17.

After steady-state gasification had been achieved, clean, dry syngas was passed to the FT system. Both fixed-bed FT reactors were loaded with catalyst, but only one fixed-bed reactor was used for this test. This left the other loaded reactor available in the event that the first reactor was overheated or deactivated because of sulfur breakthrough from the upstream sorbent beds. Target operating conditions for the FT reactor system were 18.9 bar (260 psig), 304°C (515°F), 28 slpm (1 scfm) inlet syngas flow, and 140 slpm (5 scfm) recycle product gas flow.

54

Table 17. Steady-State Syngas Composition as Reported by the Laser Gas Analysis

CO	15.1
H_2O	0.13
H_2S^a	0.023
H_2	29.3
N_2	12.9
CO_2	32.7
CH_4	5.1
Hydrocarbons[b]	0.00

[a] H_2S reported by laser gas analysis is due to interference from other gas components.

[b] Hydrocarbons as reported by laser gas analysis is precisely zero due to calibration difficulties. Hydrocarbon composition is lumped with CH_4 to give a total light hydrocarbon gas composition.

During the final 24 hours of testing, the gasifier feed was switched from pure PRB coal to blends of 30% biomass by weight in PRB coal. Several treated biomass blends were tested sequentially, including leached olive pits, leached and torrefied olive pits, leached dried distillers' grains (DDGs), leached switchgrass, and raw (untreated) DDGs.

Table 18 summarizes the average run conditions for the FT reactor skid. The shell-and-tube Dowtherm heat exchanger successfully removed the heat of reaction, allowing the FT reactor to be operated with the coolant only 3°C (6°F) cooler than the catalyst bed. The quench system also performed well, reducing moisture in the exhaust and recycle gas streams to less than 1%. On the front end, problems were observed with the syngas metering system (FI901), which had to be taken offline and cleaned out twice as moisture condensed in the regulator. Flow was also intermittent as brief drops in pressure on the back end of the gasifier would quickly affect the FT reactor supply pressure, since the syngas exiting the gasifier was only slightly higher in pressure than the regulated syngas being metered into the FT reactor (PIR900). A small sample conditioner was installed upstream of the pressure regulator to alleviate these problems. This sample conditioner is a metal cylinder with an inlet dip tube and a gas outlet line located at the top of the vessel. By cooling the cylinder in an ice bath, some residual moisture in the syngas is removed, helping to prevent condensation as the syngas expands and cools through the regulator. Moreover, the volume of pressurized gas in the conditioner vessel provides some buffer to the FT reactor, helping to stabilize supply pressure and, therefore, maintain a steady flow rate. In future tests, it is anticipated that higher gasifier pressures will be used, which will also help to maintain a constant flow into the FT reactor.

The CO and H_2 concentration in the FT reactor product gas decreased substantially after the unit was brought to pressure and temperature. All other gas concentrations increased. Perhaps most notably, the concentration of hydrocarbons larger than methane increased from nondetectable levels in the inlet syngas to well over 1% in the FT reactor product gas. While the increases in CO_2, CH_4, N_2, and water vapor concentrations in the product gas can be partially attributed to the removal of other gas components (H_2 and CO) from the gas stream, the increase in hydrocarbon concentration is apparently due solely to production by FT reaction.

From calibration prior to testing, and also from the gas composition reported by both laser gas analyzers before the catalyst was brought to temperature and pressure, it appears that the

Table 18. Average Run Conditions for the FT Reactor

Description	Instrument	Value
Reactor Temperatures, °F (°C)		
Inlet Syngas Temperature	TIR900	77 (25)
Preheated Feed Gas Temperature	TIR901	387 (197)
Top Bed Temperature	TIR902	473 (245)
Average Hot Bed Temperature	TIR903-909	516 (269)
Wax Trap Inlet Temperature	TIR928	356 (180)
Wax Trap Outlet Temperature	TIR929	309 (154)
Quench System Inlet Temperature	TIR932	280 (138)
Quench System Outlet Temperature	TIR935	92 (33)
Recycle Syngas Temperature (before preheat)	TIR936	88 (31)
Heat Exchange Temperatures, °F (°C)		
Temperature at Dowtherm Heater Inlet	TIR943	502 (261)
Dowtherm Temperature at Reactor Inlet	TIR944	513 (267)
Dowtherm Temperature Exiting Reactor	TIR945	510 (266)
Reactor Pressures, psig (atm)		
Regulated Syngas Pressure	PIR900	276 (19.8)
Reactor Bed Pressure	PIR901	261 (18.7)
Pressure Drops, inches H_2O (kPa)		
Pressure Drop Across Reactor	dPIR901	147 (37)
Pressure Drop Across Wax Trap	dPIR903	N/A
Flow Rates, scfm (slpm)		
Inlet Syngas Flow Rate	FI901	0.88 (25)
Recycle Product Gas Flow Rate	FI905	4.8 (137)
Exhaust Gas Flow Rate	FI907	0.57 (16)
Catalyst Weight, lb (g)		3.048 (1383)

laser gas analyzer unit used to analyze FT product gas composition gave results in agreement with the laser gas analyzer unit used to analyze syngas composition. Thus reporting errors due to variation between the two instruments may be ignored in calculating syngas conversion efficiency. The nitrogen component in the syngas does not participate in either the water–gas shift reaction or the FT reaction, and so its composition in the inlet gas may be taken as a standard to determine relative molar flow rates of product gas components. Calibrating product gas nitrogen to inlet gas nitrogen, the average H_2 and CO conversion efficiencies are both approximately 65%–70% at steady-state. As seen in Figure 36, the overall conversion efficiency was initially low at around 20% (indicating the initial single-pass conversion efficiency) but increased over the course of several hours (perhaps due both to catalyst conditioning and to increasing effect of recycle gas) until it began to reach a plateau.
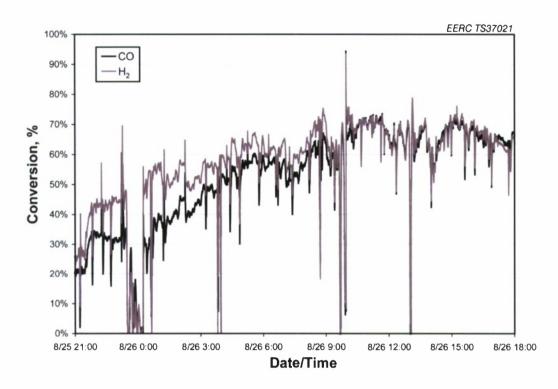
Figure 36. CO and H_2 conversion efficiency during the first 21 hours of FT reactor operation.

Another important factor to consider in FT synthesis is selectivity to light gas. This value is simply the ratio of molar increase in total light gaseous hydrocarbons (hydrocarbons + CH_4) divided by the molar consumption of CO on a CO_2-free basis. Once again using nitrogen as a standard to determine relative molar flow rates, the average light gas selectivity over the course of the run was approximately 20%. This value remained constant throughout the test duration.

The 20% selectivity to light gases is slightly higher than was observed in lab testing. The quench pot system used to condense liquid hydrocarbons and product water from the FT reactor product gas is kept at system pressure and drained through a fully enclosed system into a low-pressure pot, from which product can be safely collected. During product collection, it was observed that gas bubbles would form in the low-pressure drain lines. These gas bubbles were likely light hydrocarbons such as butane and propane that were kept in the liquid phase while inside the pressurized quench pots but then vaporized in the drain line when product was collected. The vent gas exiting the product pot was not analyzed, so the composition of this offgas is unknown. Until a mass balance is completed on the FT reactor, the approximate amount of light gas unaccounted for in the quench system remains unknown.

In addition to the higher light gas selectivity compared to lab test results, wax production was extremely low. Part of this is due to the ineffectiveness of the wax trap to cool the product stream to 150°C to condense and collect the waxes. The wax product accumulated in the cold traps with the liquids hydrocarbons. Even so, a GC–mass spectroscopy (MS) analysis of the liquid hydrocarbons only showed a moderate increase of heavier hydrocarbons. The overall conclusion is that the hydrocarbon product distribution shifted to lighter products.

This shift was attributed to the syngas composition from the gasifier. The iron-based catalyst had been optimized in the small-scale FT reactor that used only H_2 and CO at a 1:1.33 ratio. The syngas composition as reported in Table 17 contained a significant amount of carbon dioxide. Excess amounts if CO_2 can be a problem for iron catalysts. They are typically tasked with producing more hydrogen via the water–gas shift reaction, and the additional CO_2 present can make the water–gas shift reaction thermodynamically unfavorable. Hydrogen will become a limiting reagent, and the concentration of water will increase because it is not being consumed, which will oxidize catalytically active iron sites and render them inactive.

To verify the effect of CO_2 on the catalysts performance in the small-scale FT reactor, the synthetic syngas composition was altered to approximate the syngas composition from the gasifier. It was shown that from a catalyst operating at steady-state conditions under pure CO and H_2, the liquid and wax productivity dropped by nearly 80% when CO_2-laden syngas was introduced. Aqueous productivity dropped somewhat less by 50%, which is a crude indication that more light gases were produced. It was clear that CO_2 can significantly hamper the productivity and selectivity of iron catalysts.

FT "syncrude" product must be upgraded to fungible fuels such as diesel, jet, or gasoline. An accomplishment from earlier work (Zygarlicke et al., 2009) was upgrading FT liquids generated from the small-scale FT reactor to synthetic isoparaffinic kerosene (SPK) compatible with military-grade JP-8 jet fuel. FT liquids are hydro-deoxygenated, dewatered, isomerized, and distilled into appropriate fractions. The same process was used to convert coal- and biomass-derived FT liquids into SPK. Figure 37 is a GC of the raw FT syncrude which contains a variety
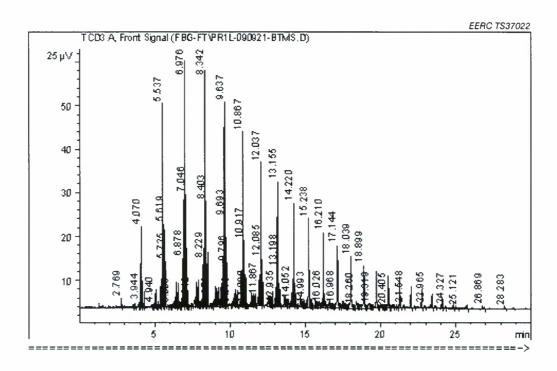
Figure 37. GC of FT syncrude from coal- and biomass-derived syngas.

of hydrocarbons including paraffins, olefins, alcohols, and isomers. Figure 38 is a GC of SPK after the upgrading processes.

Effects of Water on Catalyst Activity and Selectivity

To determine the repeatability of catalyst testing in the small-scale FT reactor, a second sample of AP11B, designated AP11B 2 in Table 19, was loaded into the reactor approximately 4 months after the catalyst was prepared and originally tested. The activity of the catalyst had decreased by 15%, and the selectivity had shifted quite dramatically to lighter hydrocarbons. Selectivity to light gases increased, and wax production decreased by 77%. The ratio of waxes to liquid hydrocarbons collected shifted from 0.79 to 0.27.

After preparation and original testing, the catalyst was not immediately loaded into the large-scale FT reactor, and it was stored in the lab. No special precautions were taken to protect the catalyst from the atmosphere in the lab, so it was hypothesized that water vapor from the air hydrolyzed the iron oxide on the catalyst surface, impacting the properties of the active catalytic sites during activation.

To test this hypothesis, another small sample was loaded into the test reactor (AP11B 3.) Before activation with flowing carbon monoxide, the catalyst was heated to 150°C with flowing nitrogen in order to completely dehydrate the iron oxide. Activation and operating conditions were then continued as before. The activity of the catalyst recovered somewhat, as the CO conversion rate increased by 8% over the previous test. Selectivity to heavier hydrocarbons

Figure 38. GC of SPK after upgrading.

Table 19. Catalyst Productivity and Selectivity Data for Tests on Water Effects

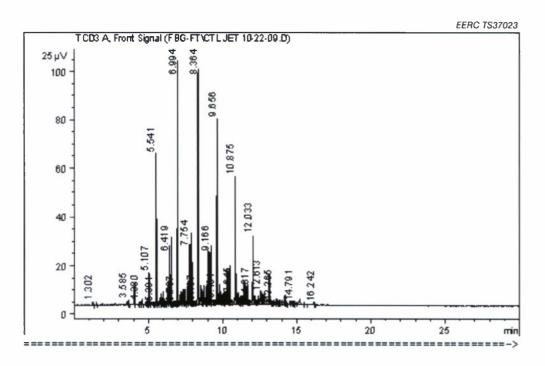|		AP11B	AP11B 2	AP11B 3	AP18	AP22
CO Conversion Fraction	% feed	17.4	13.6	15.5	13.2	14.6
CO Conversion Rate	mol CO/kg cat-hr	13.8	11.7	12.6	12.2	10.7
Light Gas Selectivity	% CO to hydrocarbon	12.7	15.1	14.8	13.5	11.5
Liquid Hydrocarbon Productivity	g hydrocarbon/kg cat-hr	40.7	28.0	35.3	34.1	22
Wax Hydrocarbon Productivity	g hydrocarbon /kg cat-hr	32.2	7.4	12.6	19.2	28.8
Aqueous Productivity	g hydrocarbon /kg cat-hr	104.6	81.9	86.4	83.3	55.0
Ratio Wax:Liquid Hydrocarbon		0.79	0.27	0.36	0.56	1.31

improved slightly as well, but it did not recover fully to the original catalyst's performance. The catalyst may have been permanently compromised by the exposure to water, perhaps in the form of bonding to the alumina support or the loss of surface area by formation of crystallites.

A fresh batch of catalyst was prepared (AP18) to duplicate the results of the original trial of AP11B. The catalyst was loaded into the reactor shortly after preparation was completed. The catalyst was not dried with nitrogen, and the activation and operating conditions were otherwise replicated. Productivity and selectivity were slightly better than the AP11B replication trials, but still did not meet that of the original. A review of lab notes revealed that a potentially important lab procedure had been omitted in the preparation of AP18. Flowing air was used during the drying and calcining steps of AP11B, but was not used for AP18. The flowing air perhaps was facilitating the dehydration of iron oxide.

Another batch of catalyst was prepared with flowing air (AP22). In this case, catalyst activity in terms of CO conversion rate was lowest of all the trials, but selectivity to heavier hydrocarbons was much improved. By weight collected, more waxes than liquid hydrocarbons were produced as the wax to liquid hydrocarbon ratio increased to 1.31. Selectivity to light gases decreased to 11.5% of all hydrocarbons produced.

It is clear from these five trials that the presence of water on the catalyst during activation can influence the activity and product selectivity. The iron oxide must be completely dehydrated during the drying and calcining preparation steps. This is facilitated with flowing air. After preparation, the catalyst should be stored in a desiccated environment to protect it from re-adsorbing water. The water can be driven off after loading into the reactor with nitrogen, but some catalyst activity cannot be recovered, and selectivity to heavier hydrocarbons is compromised. The original results of AP11B trial could not be fully replicated. It was noted that the concentration of iron was slightly higher in AP22 and that of lanthanum was less. The optimum catalyst composition needed further investigating.

Effects of Lanthanum Promotion

After the variables related to the hydrolysis of iron oxides that affect catalyst productivity and selectivity were understood and controlled, the effects of lanthanum on catalyst productivity and selectivity were investigated. It is known that the relatively high surface acidity of alumina supports shifts the product distribution toward lighter hydrocarbons. To counter this effect, some researchers have modified the alumina support by adding lanthanum oxide, which reduces the surface acidity. The EERC incorporated this concept into the catalyst formulation by soaking preformed, porous alumina supports in a lanthanum nitrate solution. The excess solution was drained, and the supports were dried and calcined at a temperature of 600°C for several hours. The lanthanum nitrate decomposes to lanthanum oxide. The deposition of iron, copper, and potassium then proceeds as described elsewhere.

To vary the amount of lanthanum on the alumina support, the concentration of lanthanum nitrate was varied (Table 20). The composition of catalyst was analyzed by inductively coupled plasma (ICP)–MS. Unfortunately, the lanthanum composition between catalyst batches was not as diverse as was hoped, and the composition of iron and potassium varied more than was expected. Even though a significant difference in catalyst performance was observed between batches, it is difficult to determine what variables caused the effect.

AP25 was targeted to have the lowest lanthanum composition, which it did, but the iron composition of 17.2% was much higher than the targeted 10%. AP22 was the midrange lanthanum batch, but the composition was only slightly more so than AP25. While the iron was nearly on target, the fraction of potassium was nearly double that of the other two catalysts. AP24 had the highest level of lanthanum as expected, but a weight fraction of 2% or higher would have been preferred. Iron and potassium fractions were not unreasonable.

Table 20. Effect of Catalyst Composition on Activity and Selectivity

		AP25	AP22	AP24
La_2NO_3 Concentration	g/mL	0.1	0.27	0.45
Iron	wt%	17.2	11.5	13.3
Copper	wt%	0.21	0.13	0.13
Potassium	wt%	0.47	0.96	0.31
Lanthanum	wt%	0.68	0.78	1.17
CO Conversion Fraction	% feed	14.0	14.6	12.6
CO Conversion Rate	mol CO/kg cat-hr	11.1	10.7	10.1
Light Gas Selectivity	% CO to HC	14.1	11.5	12.6
Liquid Hydrocarbon Productivity	g hydrocarbon/kg cat-hr	29.9	22	24.8
Wax Hydrocarbon Productivity	g hydrocarbon/kg cat-hr	17.5	28.8	12.5
Aqueous Productivity	g hydrocarbon/kg cat-hr	72.4	55.0	67.7
Ratio Wax:Liquid Hydrocarbon		0.58	1.31	0.50

61

AP22 was the best performing catalyst with the lowest selectivity to light gases and the most productive of heavy hydrocarbons. Conversely, AP24 had the poorest selectivity closely followed by AP25. The activity as measured by carbon monoxide conversion rate was roughly the same for all three batches. The differences in product selectivity between the catalyst batches can be explained by a couple different possibilities, each of which require more data to be proven. The ratio of potassium to iron is four times higher in AP22 because of a smaller weight fraction of iron and much more potassium than the other two batches. Potassium, like lanthanum, is added to the catalyst to decrease acidity, so the significantly improved selectivity of AP22 could very well be due to this. AP25 has a slightly higher ratio of potassium to iron than AP24, and although the light gas selectivity is slightly higher for AP25, it produced more wax than AP24, which lends further support to the effect of potassium on product selectivity.

The other possibility revolves around the original scope of the study on differing amounts of lanthanum. Other researchers have observed that a small amount of lanthanum improves catalyst activity and selectivity, but the effect is not linear, and at a point, an excess of lanthanum will begin to hinder the FT reaction. It is possible that an optimal amount of lanthanum was achieved in AP22, but too much was applied to AP24, which negatively impacted product selectivity. However, it was expected that this deleterious level of lanthanum would be closer to 3%–5%, not 1.1%. Also, the amounts of lanthanum between AP22 and 25 were nearly negligible, yet a rather large difference in product selectivity was observed. The likelihood of potassium composition being the more important variable in this study seems to be greater than that of lanthanum, although more data are required to make a definitive conclusion.

Commercial Catalyst Testing

During the course of the reporting period, a relationship was built with a commercial catalyst supplier through collaboration on other projects, and the supplier agreed to send samples of its developmental FT catalysts for the purposes of providing a baseline to EERC catalyst performance. Two catalysts were supplied: an iron pellet and a cobalt pellet. The cobalt pellet was later ground into a powder and tested as recommended by the supplier. Under an agreement with the supplier, a detailed composition of the catalyst was not determined, but upon visual examination, it appeared that the iron pellet was unsupported. It likely was prepared by forming an iron precipitate and extruding the powder into pellets. The cobalt pellet appeared to be a supported catalyst, but the support material and composition of cobalt on the support are unknown.

The iron catalyst was of greatest interest for this activity as it would be the most relevant benchmark even though it is an unsupported catalyst. The activation procedure for the iron pellets was provided by the supplier, but the operating conditions such as reaction temperature, pressure, and syngas composition were the same as the other EERC catalyst trials. The results of the iron pellet trial are shown in Table 21. The catalyst activity as measured by CO conversion rate is slightly higher when compared to the EERC iron catalyst batch AP22, and selectivity to light gases is a little lower. The major difference between the iron catalysts is the selectivity to heavier hydrocarbons. The supplier's iron pellet produced 70% more waxes by weight, and the ratio of waxes to liquid hydrocarbons is significantly higher. The improvement in product selectivity can be attributed to the inherent difference between supported and unsupported

Table 21. Results of Commercial Supplier Catalyst Trials

		AP22	Fe Pellet	Co Pellet	Co Powder
CO Conversion Fraction	% feed	14.6	19.0	39.1	40.7
CO Conversion Rate	mol CO/kg cat-hr	10.7	12.0	11.5	23.3
Light Gas Selectivity	% CO to hydrocarbon	11.5	10.1	40.1	13.0
Liquid HC Productivity	g hydrocarbon/kg cat-hr	22	19.6	53.8	120.4
Wax HC Productivity	g hydrocarbon/kg cat-hr	28.8	48.9	14.3	120.2
Aqueous Productivity	g hydrocarbon/kg cat-hr	55.0	33.2	198.8	391.2
Ratio Wax:Liquid HC		1.31	2.45	0.27	1.0

catalysts. The EERC catalyst uses a porous alumina support, which increases the surface acidity of the catalyst. This, in turn, reduces the selectivity to heavy hydrocarbons.

The cobalt catalysts were tested at the request of the supplier. The catalyst was received in pellet form. It was loaded into the reactor and activated under flowing hydrogen per the supplier's procedures. Syngas was fed to the reactor in 2:1 hydrogen to carbon monoxide ratio. Reactor temperature was maintained at 220°C with pressures at 300 psi. The cobalt pellet did not perform well. In general, cobalt catalysts are much more active than iron, but in this case the activity was relatively the same as the iron catalysts. Product selectivity was very poor, with light gas selectivity near 40%, and wax production was very marginal as well.

On review of these results, the catalyst supplier recommended to grind the cobalt pellets and sieve the powder to between 50 and 100 µm. The cobalt powder was diluted with Pyrex glass powder in a 2:1 ratio in order to better control heat generation in the reactor. Activation and operating conditions were maintained the same as the cobalt pellet. The cobalt powder activity and product selectivity were dramatically improved. CO conversion rate doubled, light gas selectivity dropped to 13%, and wax productivity increased nearly 8.5 times. Clearly, in pellet form, the FT reaction was severely diffusion limited, which caused the CO conversion rate to be cut in half and the product selectivity to be significantly shifted toward lighter hydrocarbons. Unfortunately, catalyst in powder form cannot be used in large-scale fixed-bed reactors because of large pressure drops, so the cobalt catalyst requires pelletization in order not to compromise diffusion.

Conclusions

In order to demonstrate coal-/biomass-to-liquids technology, the EERC developed an iron-based catalyst to fill a large-scale FT reactor system. Several process variables in catalyst composition, storage protocol, and preparation methods were identified to ensure optimal catalyst activity and product selectivity. Coal and biomass were converted to syngas using a fluidized-bed gasifier. The syngas was cleaned to remove environmental pollutants and catalyst poisons. Clean syngas was fed to the large-scale FT reactor that was loaded with EERC derived

catalyst, and liquid hydrocarbons and waxes were produced. The product hydrocarbons were then upgraded into SPK that is compatible with military-grade jet fuel JP-8.

Subtask 2.2.2 – Hydrotreated Renewable Jet Fuel Process Development

The EERC, under contract to DARPA (Defense Advanced Research Projects Agency), developed a technology pathway for converting renewable TAGs (triacylglycerides) such as crop oil, algal oil, animal fats, and waste grease to jet fuel and other liquid fuels. These alternative fuels have chemical and physical properties identical to their petroleum-derived counterparts. Unique from traditional transesterification-based biodiesel technologies, the EERC catalytic hydrodeoxygenation and isomerization (CHI) process yields an oxygen-free hydrocarbon mixture that when distilled produces renewable versions of naphtha, jet fuel, and diesel that can be fully integrated with the current U.S. petroleum fuel infrastructure. In addition to being renewable and fungible, renewable oil-based fuel produced using the CHI technology contains very low levels of sulfur. Sulfur is increasingly being eliminated from petroleum-derived fuels in order to meet strict U.S. Environmental Protection Agency limits. The sub-ppm levels of sulfur present in CHI-based fuels provide a significant advantage to petroleum refiners looking for alternatives to reducing sulfur content in fuel.

Research activities at the EERC have resulted in the production of hundreds of gallons of hydrocarbon samples from a variety of waste fats and oils, and crop oils, including soybean, canola, coconut, cuphea, camelina, crambe, and corn. The primary end product generated via CHI from all of these feedstocks has been aviation fuel (JP-8) that complies with Appendix B of the military specification MIL-DTL 83133F. However, oxygen-free hydrocarbon produced from the CHI technology can readily be converted into any of several petrochemical intermediates used to produce surfactants or plastics in addition to gasoline, jet fuel, or diesel. A general block flow diagram outlining the CHI process is presented in Figure 39.

In order to advance the technology and support implementation of distributed renewable jet fuel production, additional research is necessary to optimize the process. Research conducted under this contract during the past year focused on optimizing the hydrodeoxygenation (HDO) step operating conditions and evaluating intermediate product characteristics to support future reactor design and pilot-scale demonstration.

Process Chemistry

The HDO reactor converts triglyceride feedstock into hydrocarbon products. By-products of the reaction include water, carbon dioxide, carbon monoxide, and propane. The reaction is heterogeneous and involves the fixed-bed catalyst particle, liquid triglyceride, and gaseous hydrogen. The reaction proceeds by one of three reaction pathways shown in Figure 40. The three reaction pathways are decarboxylation, decarbonylation, and reduction. The decarboxylation reaction produces hydrocarbon, carbon dioxide, and propane. The decarbonylation reaction produces hydrocarbon, carbon monoxide, propane, and water. The reduction reaction produces hydrocarbon, propane, and water. In order of increasing hydrogen consumption, the reactions are ranked: 1) decarboxylation, 2) decarbonylation, and 3) reduction.
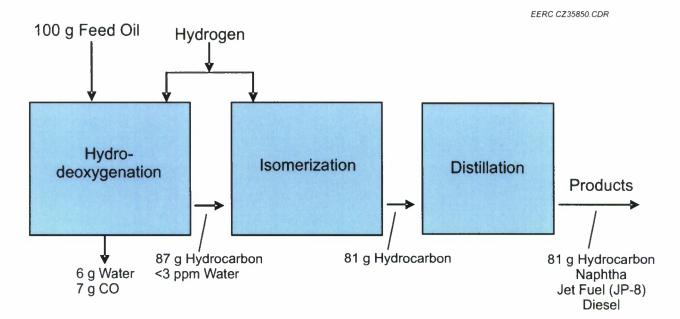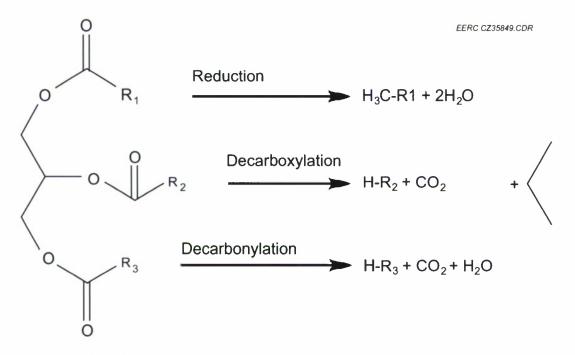
Figure 39. CHI process block flow diagram.

Figure 40. The three deoxygenation reactions that occur in the HDO reactor.

65

Because the triglyceride's glycerol backbone is removed during the HDO step, there is an inherent loss of mass that dictates the maximum theoretical conversion. For example, a theoretical triglyceride molecule consisting of a glycerol backbone and three saturated heptadecane side chains would have a maximum conversion of triglyceride to hydrocarbon of 81 mass%, assuming that only decarbonylation and decarboxylation occurred. The theoretical maximum conversion value varies depending on molecular weight of the triglyceride feedstock, reaction pathway, and degree of saturation. Free fatty acids have a higher theoretical maximum conversion because the glycerol backbone has previously been removed; therefore, only the fatty acid functionality would be removed by the HDO reactor.

Experimental Apparatus

The HDO reactor system consists of a liquid feed pump, a hydrogen gas inlet line, two tubular reactors filled with catalyst, and a product collection system. Both reactors are typically brought online for large sample production runs; however, for certain HDO parametric experiments, only one of the tubular reactors is utilized, and the other is isolated. A picture of the HDO reactor system, taken during its construction, is shown as Figure 41.

The ability to process a variety of triglyceride feedstocks is economically advantageous to a commercial-scale fuel production plant. In order to understand the effect of feedstock composition on product composition, six different feedstocks were processed. Total mass conversion of liquid feedstock to liquid product (water and hydrocarbon), liquid composition (mass% water, mass% hydrocarbon), and hydrocarbon composition (density, acid concentration, water concentration) were measured.

Figure 41. HDO reactor system.

66

Because of the length of the weeklong, continuous test, it was recognized that there could be drift in the data because of possible catalyst deactivation. To measure catalyst deactivation, the reactor was started up on canola oil, and after processing three different feedstocks, canola oil was processed again midrun, before the remaining two feedstocks were processed. There was no difference between the start-up canola-HDO product and the midrun canola-HDO product, so it was assumed that catalyst activity was constant throughout testing. GSC was utilized to ensure steady state was achieved before samples of each product were collected for analysis.

Feedstock Effect on Product Composition and Quality

Mass conversion of liquid feedstock to liquid product ranged from 88 mass% to 99 mass%. Tests using fatty acid feedstocks resulted in greater mass conversion efficiency because fatty acid molecules do not have the glycerol backbone that triglycerides do. The mass conversions for each feedstock, as well as the product composition (%water/%hydrocarbon), are shown in Table 22.

All feedstocks produced a fuel with hydrocarbon chain lengths ranging from C-5 (pentane) to C-24 (tetracosane); however, the abundance of each hydrocarbon component varied. Fuel produced from canola oil feedstock, as shown in Figure 42, comprised mainly C-16 (hexadecane), 17 (heptadecane), and 18 (octadecane) hydrocarbons. The fuel produced from corn oil, Figure 43, was similar to the canola-derived fuel; however, it contained a slightly higher concentration of C-16 hydrocarbon components. As shown in Figures 44 and 45, the fuel derived from the fatty acids was very similar to the fuel derived from corn oil, with a majority of the hydrocarbon components in the C-16 to C-18 range. The camelina oil-derived fuel, Figure 46, differed from the previous fuels and contained higher concentrations of hydrocarbons in the C-19 (nonadecane) to C-20 (isocane) range with a moderate amount of C-22 (docosane) present. The crambe oil-derived fuel, Figure 47, was similar to camelina oil; however, it contained less C-20 hydrocarbons and significantly higher C-21 (heneicosane) and C-22 components.

Operational Parameters' Effect on Product Composition and Quality

Experiments investigating operational parameter effects on product composition and quality were carried out using the continuous tubular reactor (CTR) reactor system.

Table 22. Mass Conversion and Product Composition When Processing Various Feedstocks

Feedstock	Liquid Components			Fuel Phase Characteristics		
	Mass Conv., %	Fuel Phase, %	Water Phase, %	Density, g/mL	Acid, mg KOH/g	Water, ppm
Canola Oil (start-up)	88	90	10	0.782	0.020	49
Corn Oil	92	90	10	0.785	0.029	37
Crambe Oil	90	90	10	0.778	0.012	77
Canola Oil (midrun)					0.014	37
Soy Fatty Acid 1	98	89	11	0.783	0.026	41
Soy Fatty Acid 2	99	89	11	0.785	0.033	48
Camelina Oil	94	90	10	0.801	0.044	49

Figure 42. GC chromatogram showing hydrocarbon distribution of canola oil-derived fuel.

Figure 43. GC chromatogram showing hydrocarbon distribution of corn oil-derived fuel.

Figure 44. GC chromatogram showing hydrocarbon distribution of fatty acid 1-derived fuel.

Figure 45. GC chromatogram showing hydrocarbon distribution of fatty acid 2-derived fuel.
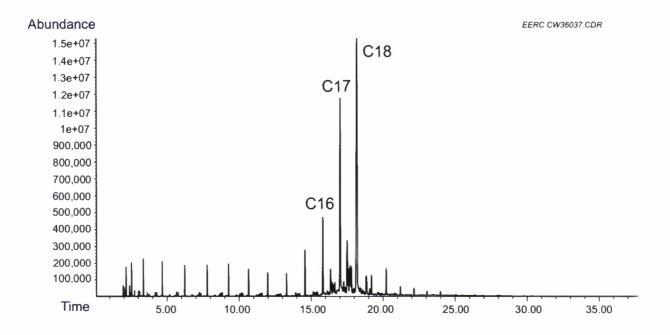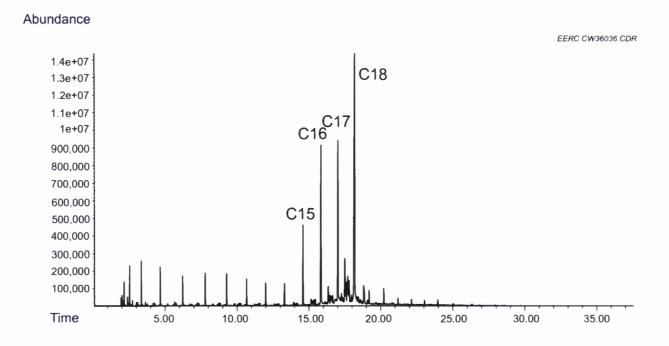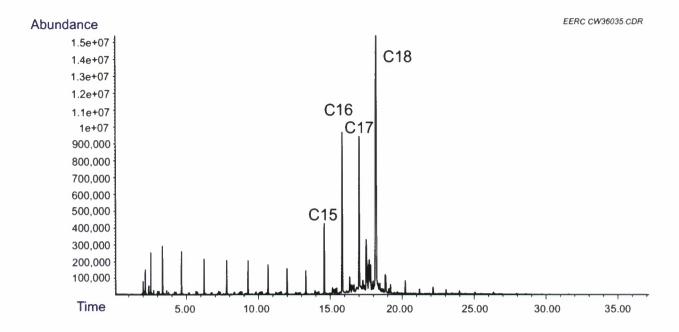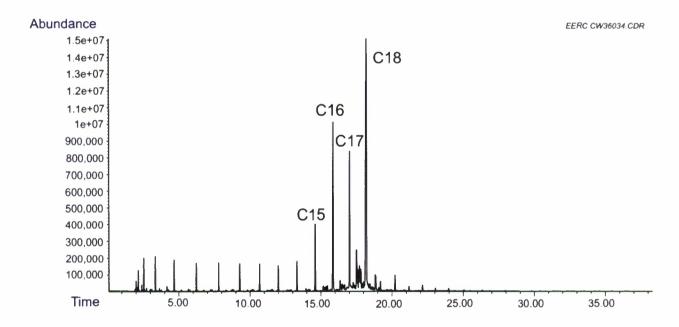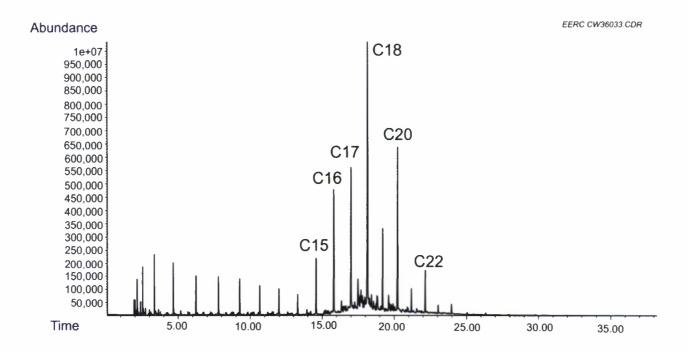
69

Figure 46. GC chromatogram showing hydrocarbon distribution of camelina oil-derived fuel.
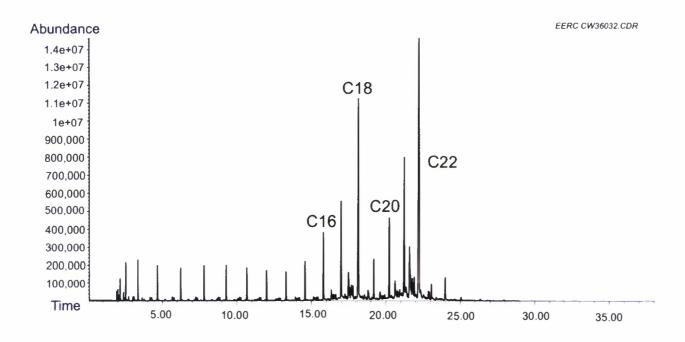
Figure 47. GC chromatogram showing hydrocarbon distribution of crambe oil-derived fuel.

Feedstock flow rate was investigated using both reactors in series while holding temperature, hydrogen flow rate, and pressure constant conditions. Differences in product quality were not discernible by looking at GC results. Therefore, the acid number, determined by titration and reported in mg KOH/g fuel, was utilized to measure changes in product quality. Soy fatty acid feedstock was initially fed to the CTR reactor system. Flow rate was incrementally increased, and the initial acid number was measured. The acid number at 1 L/hr was 0.024 mg KOH/g fuel and increased linearly with flow rate up to 3.5 L/hr, where the acid number was 0.1 mg KOH/g fuel. Above a certain flow rate, the acid number increased exponentially. A maximum flow rate at which a relatively low acid number (0.142 mg KOH/g fuel) could be achieved was found. Results from variable flow rate experiments are shown in Figure 48.

Pressure experiments were conducted in one of the CTR reactors with a canola oil feedstock. Temperature, feedstock flow rate, and hydrogen flow rate were all held constant. Initially, pressure was set and the reactor was run for 6 hours to ensure steady state. Then, the pressure was decreased incrementally while steady-state acid concentration was measured in the hydrocarbon product. Data from these experiments showed that pressure should be kept above a certain set point in order to maintain a low acid number (<0.2 mg KOH/g fuel) in the hydrocarbon product. Results from variable pressure experiments are shown in Figure 49.

The next parameter investigated was hydrogen flow rate. Tests were conducted by maintaining a constant feedstock flow rate, pressure, and temperature while hydrogen flow rate was varied between 30–50 scfh. Results from variable hydrogen flow rate experiments are shown in Figure 50.
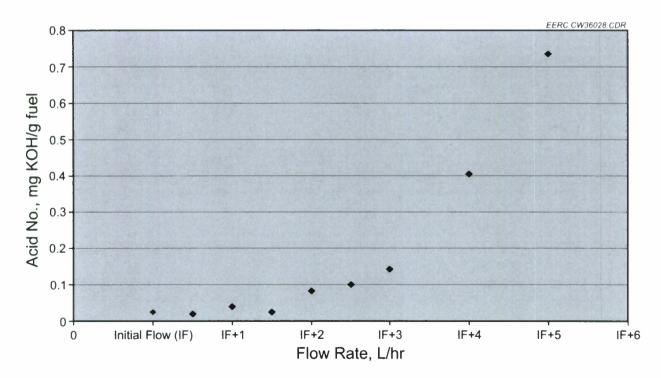
Figure 48. The effect of soy fatty acid feedstock flow rate on hydrocarbon product acid concentration in an HDO reactor.

71
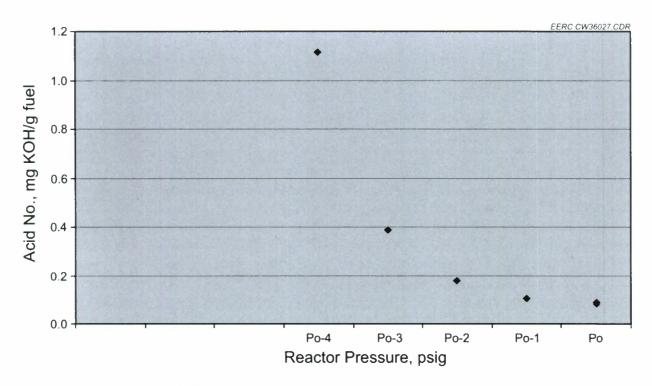
Figure 49. The effect of reactor pressure on hydrocarbon product
acid concentration in an HDO reactor.
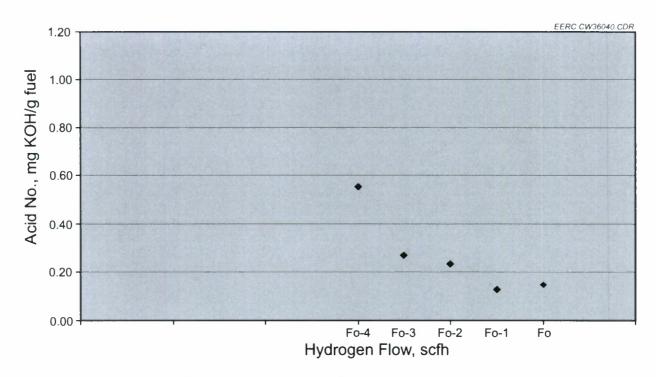
Figure 50. The effect of hydrogen flow rate on hydrocarbon product
acid concentration in an HDO reactor.

HDO Kinetic Rate Data

The purpose of the kinetic rate data experiments was to determine the reaction order, with respect to hydrogen partial pressure and fatty acid feed concentration, in a tubular catalytic HDO reactor. This information is useful for process scale-up and provides a better understanding of the HDO reaction.

Experimental Setup

EERC's small continuous reactor (SCR) was loaded with 1.2 g of HDO catalyst. The reactor vessel was loaded with glass beads in the area below and above the catalyst bed. The top thermocouple point in the SCR's 4-point thermocouple was located in the catalyst bed for accurate temperature monitoring and control. Figure 51 shows a schematic of the SCR reactor configuration. Figure 52 shows a picture of the SCR system.

Background and Theory

The small catalyst bed loaded into the SCR reactor tube constituted a differential reactor. A differential reactor is "normally used to determine the rate of reaction as a function of either concentration or partial pressure. It consists of a tube containing a very small amount of catalyst usually arranged in the form of a thin wafer or disc" (Fogler, 1999). Because the HDO catalyst comes in pellet form, a wafer was not used in these experiments. Instead, the catalyst bed was kept small enough to constitute a differential reactor, but large enough to prevent channeling

EERC CW36038.CDR

1.2 g of HDO Catalyst. The top thermocouple point was in the catalyst bed.

Glass Beads

½"

¾" Tube
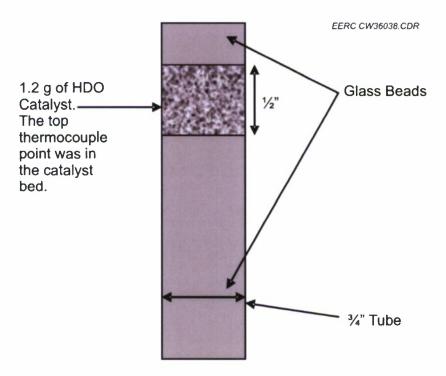
Figure 51. Schematic of the differential reactor used in kinetic rate data experiments.

Figure 52. Small continuous reactor system utilized for kinetic rate data experiment.

around the catalyst bed. A drawing of the differential reactor and accompanying mass balance equations are shown in Figure 53 and Equations 1 through 4, respectively (Fogler, 1999).

$$\begin{bmatrix} Flow \\ Rate \\ In \end{bmatrix} - \begin{bmatrix} Flow \\ Rate \\ Out \end{bmatrix} + \begin{bmatrix} Rate \\ of \\ Generation \end{bmatrix} = \begin{bmatrix} Rate \\ of \\ Accumulation \end{bmatrix} \qquad \text{Eq. 1}$$

$$[F_{AO}] - [F_{Ae}] + \left[\left(\frac{Rate\_of\_\mathrm{Re}action}{Mass\_of\_Catalyst} \right) * Mass\_of\_Catalyst \right] = 0 \qquad \text{Eq. 2}$$

$$F_{AO} - F_{Ae} + (r'_A) * (W) = 0 \qquad \text{Eq. 3}$$

$$-r'_A = \frac{F_{AO} - F_{Ae}}{W} \qquad \text{Eq. 4}$$

Where: F_{AO} = molar flow rate of fatty acid at the inlet
F_{Ae} = molar flow rate of fatty acid at the outlet
-r'_A = rate of disappearance of fatty acid per mass of catalyst
W = weight of hydrodeoxygenation catalyst (1.2g)

74
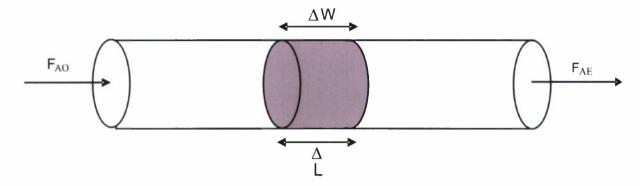
Figure 53. Schematic of a differential reactor. The catalyst bed is kept small, and inlet and outlet concentrations are measured to determine reaction rates.

Rate Order with Respect to Hydrogen

The following rate law was proposed to model the reaction rate of fatty acid conversion to hydrocarbons on the catalyst:

$$r' = k[\text{fatty acid}]^a[\text{hydrogen}]^b \qquad \text{Eq. 5}$$

where: r' is the rate at which acid reactant is consumed
$\quad$ a = rate order with respect to fatty acid concentration
$\quad$ b = rate order with respect to hydrogen concentration

At constant fatty acid concentration in the feed:

$$r' = k'[\text{hydrogen}]^b \qquad \text{Eq. 6}$$

Because hydrogen concentration is related to the hydrogen partial pressure in the reactor:

$$r' = k''(PH_2)^b \qquad \text{Eq. 7}$$

Equation 7 was used to determine the reaction rate order with respect to hydrogen partial pressure. The experimental design used to gather hydrogen rate data is shown in Table 23. The feed for hydrogen experiments was 5 mass% fatty acids and 95% Norpar-15. Norpar-15 is a commercially available blend of normal paraffins, concentrated around C-15 (pentadecane). The molar flow rate of fatty acid at the reactor inlet and outlet were determined by titration and known flow rate. Experiments were run in random order to minimize possible error introduced by measurement drift, catalyst aging, etc.

Equation 7 was manipulated in order to graphically determine the reaction order with respect to hydrogen (superscript "b" in Eq. 7). Taking the natural log of both sides of Eq. 7 gives:

Table 23. Hydrogen Rate Data Experimental Design and Results

Run Order	H₂ Pressure, psi	Acid In, gmole/min	Acid Out, gmole/min	r', (gmolAcid)/(gcat*min)	Conversion
5	300	0.00028	0.000139044	0.0001153	50%
2	450	0.00028	0.000107855	0.0001413	61%
3	600	0.00028	0.000110086	0.0001395	60%
1	750	0.00028	0.000100416	0.0001475	64%
4	900	0.00028	0.000103162	0.0001452	63%

$$\ln(r') = \ln(k) + (b)\ln(PH2) \qquad \text{Eq. 8}$$

Equation 8 is in the form of the equation for a straight line ($y = mx + b$). The natural log of the reaction rate, r', was plotted on the y-axis with the natural log of hydrogen pressure on the x-axis. The slope was then "b" in Equation 8, the reaction order with respect to hydrogen.

The results from hydrogen rate data experiments are shown in Figure 54, and the reaction order with respect to hydrogen was determined to be 0.2. However, the 450 psi data point appeared to be an outlier. The R^2 value for the fitted line was 0.77.

Two additional data points were collected at a later date to investigate whether the 450 psi data point was an outlier because of experimental error or some unknown phenomena that occurs at lower pressure. The two additional data points were taken at 400 and 450 psi. Results are shown in Figure 55. The two additional data points are shown as red boxes. Because the additional data fell much closer to the trended line, the initial 450 psi data point was dubbed an
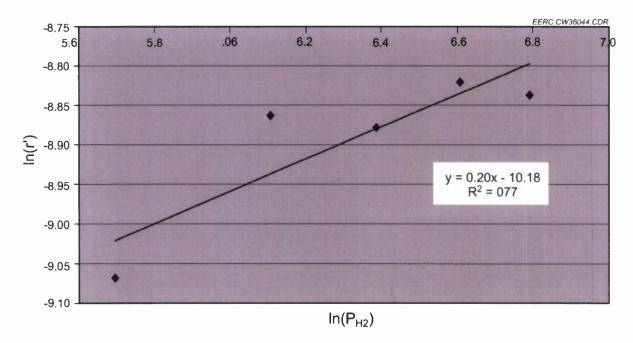
Figure 54. Results from the first five hydrogen rate data experiments.

76
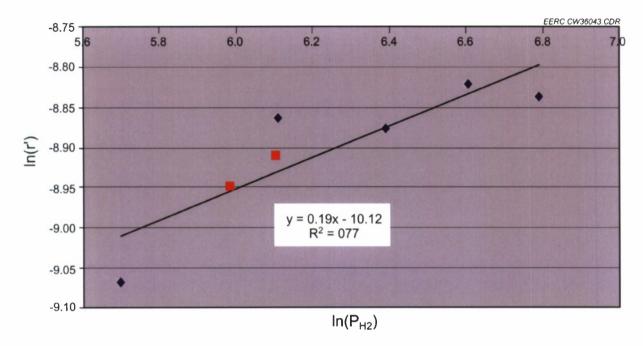
Figure 55. Results from the two additional data points at lower pressure supported the hypothesis that the initial 450 psi data point was an outlier due to experimental error.

outlier due to experimental error. Removing the outlier gave the results shown in Figure 56. The reaction rate order with respect to hydrogen was still found to be 0.2; however, the trended line was a better fit, with an R^2 of 0.88.

Rate Order with Respect to Fatty Acid Concentration

After the rate order was determined with respect to hydrogen, experiments were designed and conducted to determine the reaction rate order with respect to fatty acid concentration. At constant hydrogen pressure, the reaction rate equation (Eq. 5) reduces to:

$$r' = k'''[fatty\ acid]^a \qquad \text{Eq. 9}$$

As in the hydrogen experiments, taking the natural log of both sides of Eq. 9 gives the equation for a straight line which can then be used to extract the rate order with respect to fatty acid concentration. This equation is shown as Eq. 10.

$$\ln(r') = \ln(k) + (a)\ln[fatty\ acid] \qquad \text{Eq. 10}$$

The feed mixture of fatty acids and Norpar-15 was varied according to the experimental design shown in Table 24. The run order was again randomized to minimize errors due to drift, catalyst poisoning, etc.

The results from these experiments were fitted very well ($R^2 = 1$) with the trended line in Figure 57, strongly supporting the assumption of a power law rate mechanism. The reaction rate with respect to fatty acid concentration was found to be approximately first order (0.92).
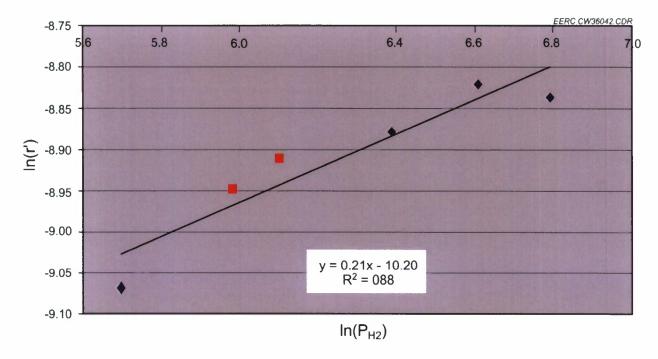
Figure 56. After removing the outlier, the rate order with respect to hydrogen was still found to be 0.2; however, the trend line fitted the data better (R^2 = 0.88).

Table 24. Soy Fatty Acid Concentration Rate Data Experimental Design and Results

Run Order	[fatty acid] mass%	Acid In gmole/min	Acid Out gmole/min	r' (gmolAcid)/(gcat*min)	Conversion
1	1%	0.0000552	0.0000190	0.0000302	66%
3	2%	0.0001105	0.0000393	0.0000594	64%
2	3%	0.0001660	0.0000629	0.0000860	62%
5	4%	0.0002217	0.0000931	0.0001071	58%
4	5%	0.0002774	0.0001153	0.0001351	58%

Conclusion

These experimental results suggest that the HDO reaction is first order with respect to fatty acid feed concentration and fractional order (0.2) with respect to hydrogen partial pressure. The model is shown in Equation 11.

$$r' = k[\text{fatty acid}]^1[\text{hydrogen}]^{0.2}$$ Eq. 11

Where: r' = the rate at which fatty acid is consumed (g mol Acid/[g Catalyst*min])

78
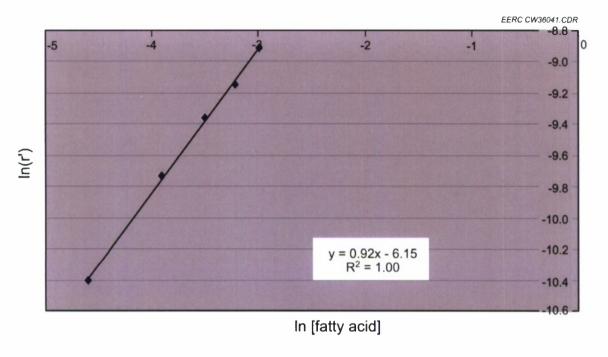
Figure 57. Results from experiments that varied the concentration of fatty acid showed that the reaction rate order with respect to fatty acid concentration was approximately first order.

Isomerization – Intermediate Product Analysis

In order to produce a broad distribution of highly isomerized hydrocarbons that can later be distilled into naptha, jet, and diesel fractions, the hydrodeoxygenated product from the HDO reactor is dried and fed to an isomerization/cracking reactor. The isomerization reactor contains a different catalyst than the HDO reactor. Typically, hydrocarbon product is run through the isomerization reactor multiple times in order to achieve the necessary ratio of straight-chain and branched-chain hydrocarbons. Once sufficient isomerization has been achieved, the product is distilled to provide naphtha, jet fuel, and diesel fuel samples.

Pilot Plant Integration into Existing Refinery

Scaling up the renewable fuel process for integration at an existing refinery is an attractive commercial option when compared to a stand-alone bio-fuels plant capable of producing specification-compliant fuel from renewable feedstock. The CHI process can be optimally tailored to produce a high cetane, low-sulfur hydrocarbon that can be further processed by existing refinery operations into finished fuel. This scenario takes advantage of existing petroleum refining and distribution infrastructure while providing valuable high-cetane, low-sulfur, and renewable hydrocarbon blendstock to the refinery.

To aid in evaluating the value of an integrated CHI-based process with petroleum refining operations, the EERC conducted a series of experiments to produce a variety of hydrocarbon chemical intermediates and fully fungible, drop-in-compatible liquid fuels from a renewable oil feedstock. Canola oil was processed using the CHI technology, and samples of hydrocarbon

were collected from each stage of the process. These samples were analyzed by a contract fuel laboratory to determine physical and chemical properties. Results from these tests are representative of work conducted over the past 2 years in which a variety of feedstocks, including oils from soybean, corn, camelina, canola, crambe, and algae, as well as waste oils, were processed using the CHI technology to produce jet fuel, diesel, and naphtha. Data from these experiments will be used to further evaluate the best integration strategy and pilot plant design basis for the CHI process.

The intermediate renewable hydrocarbon streams have sulfur contents less than 3 ppm and cetane values ranging from 56 to 79. Cetane number trended downward with increased isomerization/cracking. This observation is in agreement with literature reports on cetane number (Santana et al., 2006; Lapidus et al., 2008). Freezing point decreased with increased isomerization. This is the main reason why a high level of isomerization is required to produce a jet fuel that meets specifications. Specific gravity decreased with increased isomerization/cracking. Tables 25 and 26 show fuel analysis results for canola oil, hydrodeoxygenated canola oil (HDO), incrementally isomerized products, and product distillate fractions.

Table 25. Fuel Analysis Results

	Canola	HDO	Isom 1	Isom 2	Isom 3	Isom 4	Isom 5	Isom 6	Naphtha	Jet	Distillate Bottoms
Vol% Aromatics		16.7	1.2	3.4	1.6	1.9	0.8	0.8	NA	0.5	1.8
Vol% Olefins		9.9	0.2	0.7	0.6	1.9	0.5	0.3	0.04	0.5	1.8
Vol% Saturates		73.4	98.6	95.9	97.8	96.2	98.7	99	NA	98.9	96.4
API Gravity @ 60°F		46.9	48.6	49.8	50.9	51.7	53.3	55.2	67.3	53	48.6
Specific Gravity	0.916	0.7936	0.7857	0.7805	0.7758	0.7724	0.7657	0.7579	0.7118	0.7669	0.7857
IBP, °F		140.5	142.5	144.9	149.2	149.2	135.9	145.4	114.6	287.4	450
FBP, °F		752.2	705.6	607.3	608.5	586	568.8	547.9	374.7	523	562.3
Flash, °F	315	<68	<68	68	<68	<68	<68	<70	NA	102	222.8
Freezing, °F		60.8	32	28.4	8.6	-4	-22	-41.8	NA	-79.8	NA
Cloud Smoke, °F		59	42.8	28.4	8.6	-2.2	-29.2	-43.6	NA	<-76	-25.78
Smoke, mm		25	25	25	25	25	25	NA	NA	22	NA
Water Content, ppm		49	41	40	34	15	23	39	47	52	<10
Nitrogen, ppm	<3	<1	<1	<1	<1	2	<1	<1	<1	<1	<1
Sulfur, ppm	3.287										
Sulfur, mg/kg		<3	<3	<3	<3	3.4	<3	<3	<3	<3	<3
Cetane		74.3	76.7	77.8	78.9	64.4	62.3	56.3	NA	56.3	73.8
Viscosity @ 104°F (cst)		0.9800	1.3240	1.0270	0.8995	0.8281	0.5650	0.8011	NA	0.6298	1.0660
Viscosity @ 25°C (mPa*s)	57.569										

Subtask 2.3 – Development of Modular Systems for Distributed Fuels and Energy

Introduction

Military facilities and the personnel stationed there, like any other "community," have requirements for performance of its daily operation. These needs fall into two categories:

Table 26. Metals Content of Canola-Oil Derived Fuel (all samples) – Most Metals Were Nondetectable (<5 ppb) Except:

Metal	Ranges, ppb
Aluminum	24–386
Boron	40–50
Calcium	20–24
Iron	10–13
Lead	100–110
Magnesium	26–38
Silicon	120–226
Titanium	6–8
Zinc	7–14

personnel subsistence and mission-specific requirements. Personnel subsistence needs include electricity, water for consumption and washing, sewer systems (both septic and storm), and heating and cooling. The requirements to carry out a mission, although facility-specific, include electricity, water, and fuel needs (both ground and air vehicles).

Figure 58 provides a simplified diagram of the utility inputs and outputs of the facility as a whole.

The U.S. Department of Defense (DoD) and, equally, each armed services branch, is aggressively evaluating the energy and fuel usage at military facilities for a variety of reasons, including vulnerability, sustainability, and environmental impact (i.e., carbon footprint) to name a few. With this focus in mind, the EERC performed a brief evaluation of specific technologies targeted at the production of fuels and/or energy. The technologies evaluated included biomass gasification coupled with IC engine, biomass gasification coupled with synthetic natural gas production, biomass gasification coupled with the FT process, and CHI. Each of these technologies is discussed in greater detail in the following sections, but Table 27 provides a summary of the technology and primary end product.
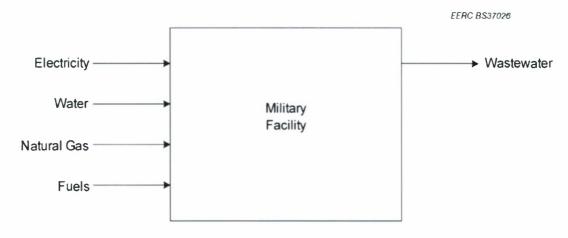
EERC BS37026

Figure 58. Military facility utility inputs/outputs.

Table 27. Summary of Technology Processes

Feedstock	Technology Process	Primary End Product
Biomass	Gasification w/SNG[1] production and IC engine	Electricity
Biomass	Gasification w/SNG production	Natural Gas, Propane
Biomass	Gasification w/FT process	JP-8, Gasoline, Diesel
Renewable-Derived Oils	CHI	JP-8, Gasoline, Diesel

[1] Synthetic natural gas.

Biomass Gasification

Gasification of biomass is the initial step in three of the processes evaluated and, therefore, is discussed in greater detail in this section. Biomass can be gasified into a syngas that can then be converted into electricity, synthetic natural gas, or liquid fuels. This report presents a mass and energy balance for each scenario. Depending on the unique needs at a given military installation, one form of energy may be more desirable than another. The energy efficiency of producing syngas, electricity, synthetic natural gas, and liquid fuels from biomass will be discussed.

According to a National Renewable Energy Laboratory (NREL) subcontractor report (NREL, 2004), the energy efficiency for syngas production from a rice straw gasifier is 70%, where energy efficiency is defined as the energy content of the product syngas divided by the total energy inputs.

Biomass Gasification to Syngas

The NREL report (NREL, 2004) describes experimental results from a 4.8-ton-per-day biomass gasifier. That report is summarized in the simplified block diagram, shown as Figure 59. Inputs, outputs, and energy efficiency are shown in Table 28.

For the purpose of clarity and consistency, the Btu content of the feedstock input for each of the processes discussed in the following section was normalized to a common Btu content of 100 MMBtu, while ratioing the energy input and resulting output proportionally.

Biomass Gasification to Electricity

Biomass-derived syngas can be used in an electrical generator. The average thermal efficiency for a modern IC engine operating on syngas fuel with an energy content $\geq$ 300 Btu/ft^3 is 40%. The biomass to electricity scenario is shown in Figure 60. The overall system efficiency of converting biomass to electricity equates to 28%.

Biomass Gasification to Synthetic Natural Gas

As an alternative to producing electricity, SNG could also be produced from bio-derived syngas. An analysis was conducted, based on wood gasification, by Jurascik et al. (2009). The analysis calculated the efficiency of gasifying a wood feedstock and subsequently converting the

Energy Input
12.5 MMBtu/day

Biomass
54.2 MMBtu/day

Biomass Gasifier

$C + H_2O \rightarrow H_2 + CO$

η=70%

47 MMBtu/day of
322 Btu/ft³ Syngas

Composition (mole%)
Hydrogen, 63%
Carbon Monoxide, 12%
Methane, 7%
>C1 Hydrocarbon, 2%
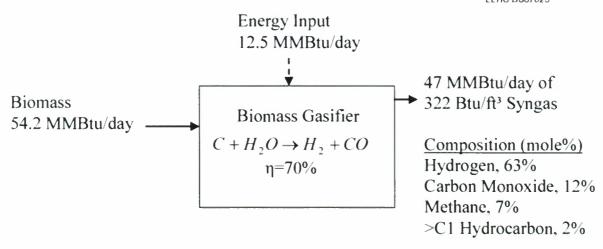
Figure 59. Simplified block flow diagram of a rice straw biomass gasifier.

Table 28. Biomass Gasification Data (NREL, 2004)

Stream Name	Mass per Day, lb	Heating Value, MMBtu	Energy Efficiency
Rice Straw	9600	54.2	
Natural Gas	–	9.76	
Electricity	–	2.71	(47/[54.2+9.76+2.71])=70%
Water (steam)	1728		
Syngas	9886	47	

Energy Input
23 MMBtu

Biomass
100 MMBtu
(9 tons)

Biomass Gasifier
Coupled with an
IC Engine
η = 28%

Electricity
35 MMBtu
(10.255 kWh)

Figure 60. Block diagram for electricity production from biomass.

syngas to SNG. Assuming that 10% of the woody biomass was not converted to syngas and remained as char, the efficiency, defined as the energy contained in SNG divided by total energy inputs, was 54.2%. The overall efficiency of converting biomass to SNG equates to 61%. The block flow diagram in Figure 61 shows the energy balance for such a system.

Biomass Gasification to Liquid Fuels

The Center for Energy and Environmental Studies at Princeton University studied the energy balance for a system that converts biomass into liquid fuels (Larson and Jin, 1999). The study found the overall efficiency of converting biomass to liquid products to be 49%. The liquid products were 25%, by energy, naphtha (C_5-C_9), 50% kerosene (C_{10}-C_{12}), and 25% diesel (C_{13}-C_{18}). A block flow diagram of the biomass F-T process, on the basis of 100 MMBtu of biomass feedstock, is shown in Figure 62.

Catalytic Hydrodeoxygenation–Isomerization

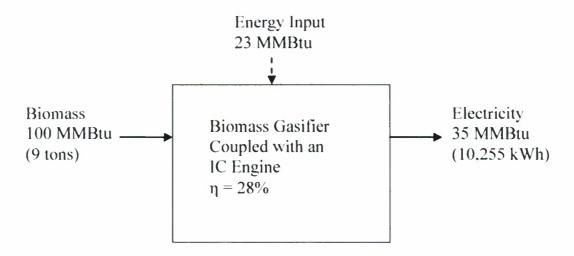The CHI technology utilizes catalyst, heat, and pressure to react hydrogen and renewable TAG to form hydrocarbon products. The TAG can come from crop oils, algal oils, or animal fats. Multiple TAG and fatty acid feedstocks have been assessed at the EERC and converted into specification-compliant fuels. By varying the degree of processing and the distillation cut points, it is possible to provide a slate of fuel products. Typically, JP-8-grade SPK has been the desired end product for EERC fuel production efforts. The renewable SPK product is then blended with ~20% aromatics to produce a specification-compliant JP-8. Aromatics are blended to increase the
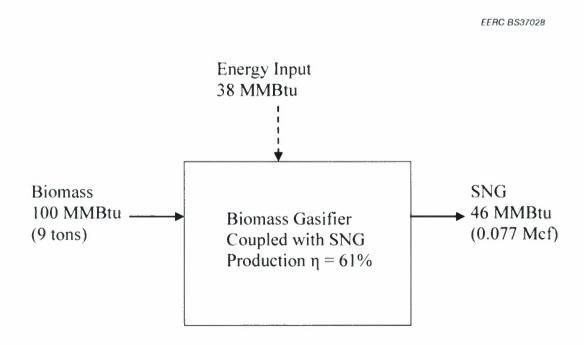
EERC BS37028

Figure 61. Block diagram for SNG production from biomass.

Energy Input
4 MMBtu

Biomass
100 MMBtu
(9 tons)

Biomass Gasifier
Coupled with FT
Process η = 49%

50 MMBtu
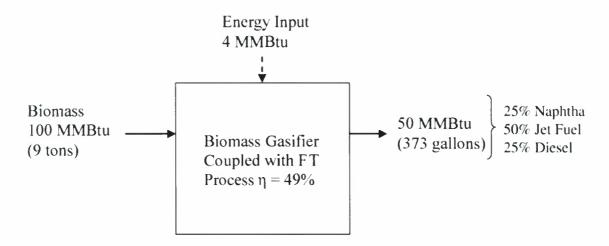(373 gallons)

25% Naphtha
50% Jet Fuel
25% Diesel

Figure 62. Block diagram for liquid fuels production from biomass.

physical density of the fuel and for their lubricity properties. Figure 63 shows the inputs and outputs of the CHI process.

By varying the degree of processing in the CHI unit and changing the distillation parameters, it is possible to optimize the process for a different desired product (example: maximize naphtha or maximize diesel).
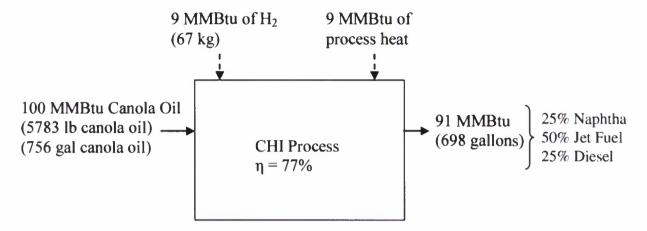
Oils that have been processed include soybean oil, canola oil, corn oil, crambe oil, camelina oil, soy fatty acids, coconut oil, palm oil, yellow grease, fatty acids from animal fats, and various algal oils. Feedstock flexibility is a major process advantage and allows the CHI technology to utilize the most convenient and/or inexpensive TAG source available.

When selecting a modular energy production system, it is important to consider the system's utility requirements. The CHI process requires four process inputs: TAG feedstock, hydrogen, cooling water, and electricity. Steam could be used instead of electricity for some process heating requirements if it is available and less expensive. The major product from the CHI process is liquid hydrocarbon fuel (i.e., naphtha, jet fuel, diesel fuel). Light gases (methane, ethane, propane, carbon dioxide, carbon monoxide) are also produced along the water from the reduction reaction. The light gas stream can be used for heating. The produced water would likely have to be treated before disposal.

Technology Summary

Biomass and renewably derived oils are a suitable feedstock for the production of electricity, SNG, and/or liquid fuels. In order of increasing efficiency, the four processes are ranked: electricity production from biomass, liquid fuels production from biomass, SNG production from biomass, and CHI. These technologies vary in technical maturity and scalability and would each require detailed technical and economic evaluation on a case-by-case basis.

9 MMBtu of H₂
(67 kg)

9 MMBtu of
process heat

100 MMBtu Canola Oil
(5783 lb canola oil)
(756 gal canola oil)

CHI Process
η = 77%

91 MMBtu
(698 gallons)

25% Naphtha
50% Jet Fuel
25% Diesel

*Note: A specification-compliant JP-8 requires ~80% jet range isoparaffins, from the CHI process, and ~20% blended aromatics.

Figure 63. Inputs and outputs for the CHI unit that converts crop or algal oils into fuel products.

Grand Forks Air Force Base – North Dakota

Introduction

In an effort to perform a brief technology evaluation to put the scale of these processes in perspective, the EERC requested and obtained information from GFAFB in North Dakota. The information was related to fuel and utility commodity usage for both mission-critical operations and personnel subsistence requirements.

Facility Information

Information in this section serves as the basis for all technology evaluations and feasibilities. GFAFB is located in northeastern North Dakota and performs its mission with approximately 3200 personnel. The closest town is Emerado, North Dakota (population: 500). The nearest population center is Grand Forks, North Dakota, with a population of approximately 50,000 people. A summary of GFAFB utility use is provided in Figure 64.

Total electrical usage at the GFAFB is approximately 61,000 MWh annually for the entire installation, with a peak electrical demand of slightly greater than 11 MW. Electricity for the facility is provided by Nodak Rural Electric Cooperative, a distribution utility under Minnkota Power Cooperative.

GFAFB primarily utilizes natural gas for heating which is provided by a local utility (Xcel Energy). Some natural gas is used to generate steam for humidification (steam requirements are covered in a later section). Annual consumption of natural gas is approximately 327,000 Mcf.
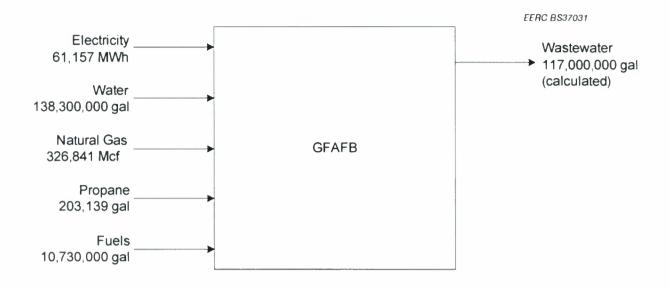
Figure 64. GFAFB utility inputs/outputs.

The peak demand month is January since natural gas demand was primarily for space heating. GFAFB indicated that a natural gas steam generator is operated on the facility, and the steam is used for humidification. Propane use is limited to space heating and amounts to approximately 203,000 gallons annually.

The water supply for GFAFB is provided under contract with the local rural water district (Agassiz Water Users, Inc.) and the city of Grand Forks. The annual water consumption at GFAFB is approximately 138 million gallons per year (MGY) or 378,000 gallons per day (gpd). Peak water demand occurs in August with a peak daily demand of slightly more than 1 million gallons.

GFAFB operates and maintains its own wastewater treatment facility to manage wastewater discharge from the facility. Information regarding the wastewater treatment facility was not provided. Using accepted estimates for per capita discharge, total wastewater discharge would be approximately 320,000 gpd or 117 MGY, assuming 100 gallons per capita per day for the 3200 base personnel.

The GFAFB current mission is to provide refueling support to the U.S. Air Force with a fleet of KC-135 Stratotankers. The annual fuel usage for the GFAFB consists of 10,580,000 gallons of JP-8, 87,000 gallons of gasoline, and 63,000 gallons of diesel fuel (No. 1). It should be noted that the GFAFB mission is currently changing to one of unmanned aerial vehicles (UAV), but for the purposes of this report and given the availability of data, analysis was performed on the GFAFB's mission at the time of writing and does not included fuel usage of the UAV mission.

GFAFB Technology Evaluation. Each process evaluated for the GFAFB focused on a primary target end product and is shown in Table 29. In some cases, such as the FT and CHI

Table 29. Technology Evaluation

Target Product	Applicable Technology	GFAFB Usage	Feedstock Required
Electricity	Biomass gasification with SNG production and IC engine	61,157 MWh/yr	53,000 tons/yr biomass
Natural Gas	Biomass gasification with SNG production	326,841 Mcf/yr	38,000,000 tons/yr biomass
Propane	Biomass gasification with SNG production	203,139 gal/yr	2000 tons/yr biomass
JP-8	Biomass gasification with FT process	10.58 Mg/yr	509,000 tons/yr biomass
Diesel	Biomass gasification with FT process	0.063 Mg/yr	6100 tons/yr biomass
JP-8	CHI	10.58 Mg/yr	84,000 tons/yr canola oil
Diesel	CHI	0.063 Mg/yr	2500 tons/yr canola oil

processes, other usable end products are produced in addition to the target product. The "nontarget" end products are not shown in Table 29 but are discussed in the process summaries below.

Biomass Gasification to Electricity. Based on the information presented in previous sections, gasifying biomass to produce syngas that is, in turn, burned in an IC engine at GFAFB would result in the following scenario. Approximately 53,000 tons of biomass would be required to be gasified a year to meet the annual GFAFB electrical usage of approximately 61,000 MWh.

Biomass Gasification to Synthetic Natural Gas. The biomass gasification to SNG scenario was analyzed for displacement of two different currently used products: natural gas and propane. A system to displace the natural gas usage (327,000 Mcf) at the GFAFB would require greater than 38 million tons, while a system operated to displace propane usage (200,000 gallons) would require approximately 2000 tons.

Biomass Gasification to FT Liquids. To meet the JP-8 demand at the GFAFB (11,000,000 gallons) would require operation of a biomass gasification to FT liquids system capable of processing of approximately 509,000 tons of biomass, resulting in 5 million gallons of both naptha and diesel. A summary of biomass gasification to FT is provided in Table 30.

Table 30. Summary of Biomass Gasification to FT Scenarios

Target Product	Target Quantity	Feedstock Required	By-Product	By-Product Quantity
JP-8	10,580,000 gal	509,000 tons of biomass	Naphtha	5,000,000 gal
			Diesel	5,000,000 gal
Diesel	63,000 gal	6000 tons of biomass	JP-8	127,000 gal
			Naphtha	63,000 gal

This same process operated to displace diesel demand would require 6000 tons of biomass gasified annually and would also produce 63,000 gallons of naptha and 127,000 gallons of JP-8.

CHI Process to Fuels. The CHI process operation can be adjusted to selectively produce a greater percentage of the target fuel. In testing performed at the EERC, the CHI was operated to maximize JP-8 production which resulted in an end product mixture of 33% naptha, 52% JP-8, and 13% diesel. Scaling this system up to meet GFAFB's annual JP-8 demand of approximately 11,000,000 gallons would require a system capable of processing approximately 84,000 tons of renewably derived oil (in this case, canola oil) annually. In addition, approximately 2,000,000 kg of hydrogen would also be required as a process input. As by-products, the system would also produce approximately 7 million gallons of naptha and 3 million gallons of diesel a year.

Operating the CHI process to maximize diesel production would result in an end product fuel of approximately 20% naptha, 40% JP-8, and 40% diesel. A 40% diesel scenario would require approximately 2500 tons a year of canola oil and would result in approximately 63,000 gallons of JP-8 and 32,000 gallons of naptha. This scenario would require approximately 15,000 kg of hydrogen a year. Table 31 summarizes these scenarios.

Table 31. Summary of CHI Scenarios

Target Product	Target Quantity	Feedstock Required	By-Product	By-Product Quantity
JP-8	10,580,000 gal	84,000 tons of canola oil	Naphtha Diesel	7,000,000 gal 3,000,000 gal
Diesel	63,000 gal	2500 tons of canola oil	JP-8 Naphtha	63,000 gal 32,000 gal

Summary of GFAFB Evaluation. Although several technologies can be utilized to displace energy and fuels utilized at GFAFB, only a few appear remotely reasonable from an economic feasibility, scale, and feedstock resource perspective: 1) propane displacement using biomass gasification, 2) diesel production using biomass gasification to FT, and 3) diesel displacement using CHI. The scale and cost of the other process scenarios make them unlikely to be implementable at GFAFB.

The evaluation of GFAFB scenarios was performed as a cursory review of available technologies and their potential implementation. To fully determine both technical and economic feasibility, a thorough analysis would be required.

Task 3 – Project Management and Reporting

This task facilitated management of the entire project, *Production of JP-8-Based Hydrogen and Advanced Tactical Fuels for the U.S. Military,* under Cooperative Agreement No. W9132T-08-2-0014. Chris J. Zygarlicke was the overall project manager and worked primarily with principal investigators in charge of major technical activities in Tasks 1 and 2. Responsibilities of Task 3 included all project management such as tracking deliverables and budgets, monthly

and quarterly reporting, final reporting, internal project meetings, project review meetings with U.S. Army ERDC's CERL staff, and strategic studies. Strategic studies involved developing new ideas and providing forward planning and new technical ideas that enhance the overall goals of this project, working on critical publications and resource assessments, and networking with other researchers and project managers to gain collaborative relationships and valuable technical information. The project had a period of performance from July 1, 2008, to December 24, 2009.

An initial internal meeting was held with all principal investigators involved in the new project and milestones, and project experimental plans were discussed and compared with proposal plans. Work was done to finalize the contract with the ERDC CERL and to justify foreign nationals working on the project. Discussions were held with contract specialists both at the EERC and CERL to determine reporting and other requirements for the project.

The kickoff meeting was held at the Tank Automotive Research, Design, and Engineering Center (TARDEC) facilities in Warren, Michigan, on October 14, 2008. Present were Chris Zygarlicke; EERC principal investigator leads including Bruce Folkedahl, John Hurley, and Ben Oster; Frank Holcomb from CERL; and Harold Sanborn, Patsy Muzzell, and several other individuals from TARDEC who stopped in during the course of the meeting for collaborative and information sharing purposes. The meeting agenda included an overview of EERC projects in energy and fuels that relate to military applications, a general review of progress of the current FY07 project, plans for the new FY08 project, and various presentations by TARDEC personnel on their current work related to military power and fuels. Principal investigators for Task 1 described their work plan for hydrogen production and purification technology development and vehicle development and demonstration. Lead investigators for Task 2 discussed plans to develop alternative (nonpetroleum) feedstock-based technologies for production of advanced tactical fuels with JP8 drop-in compatibility and improved properties for use as hydrogen feedstocks. Reporting, publications, and collaborations with other DoD agencies and researchers were also discussed. Since then a collaborative relationship has continued with Ms. Muzzell and her team regarding FT and catalytically cracked hydrotreated diesel and jet fuels.

During this reporting period, Dr. Chang Sohn from ERDC CERL became the primary contact for this project, and a conference call was held between all project principal investigators, Chris Zygarlicke, Frank Holcomb, and Dr. Sohn to introduce the project and provide technical background. Dr. Sohn also visited the EERC on May 6, 2009, to get further acquainted with the project, to get to know EERC engineers, and to tour pilot and analytical facilities, especially those being developed and used in the project. Technical activities on the recently completed FY2007 and current FY2008 projects were summarized in a PowerPoint presentation, and a full 1-day agenda was organized to review the project with Dr. Sohn. Discussions were also held with Dr. Chang Sohn on supplying more detailed information from the University of North Dakota (UND) billing office along with monthly and quarterly reports, regarding costs for labor, fringe benefits, and supplies/equipment. The EERC worked with the billing office at UND and accommodated this additional information.

Although a hydrogen vehicle demonstration was not part of this FY08 project, several management-level discussions were held concerning the future of demonstrating hydrogen fuel cell vehicles, with great interest in providing continued support but not designing and building

such systems. Strategic planning and management were also applied toward finding a reasonable solution to ePower not delivering on two fully functional hydrogen fuel cell-powered utility vehicles for CERL and Robins Air Force Base (AFB). EERC upper management sent letters to ePower bringing to its attention that Robins AFB and APTO had rejected the Toolcat fuel cell-powered MPUV that ePower had delivered as part of a separate contract with CERL; a contract that, although not appropriated through the EERC, was being executed through the EERC. Scott Slyfield and his staff at APTO determined that the vehicle did not meet the specification developed between ePower and APTO, and as such, APTO asked that the vehicle be removed from Robins AFB. The EERC then worked with California Motors, APTO, and CERL to define a corrective action plan that would satisfy the requirements of the scope of work within the short amount of time remaining on the contract (April 26, 2009). California Motors was unable to repair or modify the existing Toolcat such that the contracted statement of work could be met. Alternatives for providing APTO with a functioning fuel cell electric vehicle were pursued. EERC disassembled the Toolcat to conduct a system/component inventory and was able to reassemble the vehicle to at least get the system to mobilize and start and stop safely. The vehicle was still not satisfactory according to what ePower was supposed to deliver; therefore, the EERC submitted a request for contract modification to CERL to eliminate the delivery of the two Bobcat vehicles and add delivery of a new fuel cell-powered forklift. Frank Holcomb gave approval, and the EERC procured, tested, and delivered a Hyster forklift with a Hydrogenics fuel cell pack. APTO confirmed that the vehicle was performing flawlessly at Robins AFB, and the contract was considered complete.

Several meetings and conferences were attended and participated in by EERC to broaden applicability of technologies being developed in hydrogen, distributed generation and advanced tactical fuels; to network with other researchers and project managers; to gain collaborative working relationships and cost-share partners; and to simply gain valuable technical information that could benefit the technical research activities. An invited presentation and abstract entitled "Biofuels and Bioenergy on U.S. Military Bases" were presented at the U.S. Army Corps of Engineers Net-Zero Energy (NZE) Installation and Deployed Bases 2-day Workshop on February 2–4, 2009, in Colorado Springs. The event had about 140 in attendance, including representatives from U.S. military or defense research departments and defense contractors. Discussions were held with several DoD and nonfederal contractors on potential EERC support research in areas related to energy efficiency and renewable energy for military installations in addition to current work that is focused on hydrogen, distributed generation, and advanced fuels production. Other potential EERC areas of research support that could aid military installations include heating, cooling, materials, design, combined heat and power facilities (CHP), renewable energy systems, microgrids and all many aspects of energy efficiency, building efficiency, and communitywide renewable energy and energy efficiency integration which may be of future benefit to ERDC CERL.

Several good potential collaborative contacts were made with commercial industry, researchers, and military personnel at the Renewable Energy World conference in Las Vegas, Nevada, March 10–12, 2009, and at the National Hydrogen Association Conference and Hydrogen Expo, March 30 – April 3, 2009. The particular collaborative areas are related to energy efficiency, renewable energy, communitywide renewable energy and energy efficiency

integration, fuel cell systems, and hydrogen production. Many of these systems have applications for military installations.

Discussions were held in several round-table meetings at the National Hydrogen Association's (NHA's) Annual Conference and Expo in Columbia, South Carolina, on March 30 – April 3, 2009. Informal presentations, addresses, and discussions were employed to facilitate ideas and programs between the NHA and universities to advance hydrogen production and applications, including military applications.

A presentation related to EERC work in developing oil seed energy crops for conversion to hydrocarbon fuels for military and commercial use was given at the Biomass '09 International Conference and Tradeshow in Portland, Oregon, on April 28–30, 2009.

Meetings and presentations on coal and biomass conversion to FT liquid fuels, biomass combustion and gasification for power production, municipal waste to power, and hydrogen production were attended and facilitated at the 34th International Technical Conference on Coal Utilization & Fuel Systems in Clearwater, Florida, on May 31 – June 4, 2009. A particular emphasis of discussion and information gathering was directed toward indirect and direct coal and biomass liquefaction for fuel development and catalyst production and catalytic processes for gas-to-liquid fuel production. A follow-on planning meeting was attended in Des Plaines, Illinois, to develop panel discussions, tutorials, and keynote addresses that address needs for liquid and gaseous alternative fuels and hydrogen from coal or coal–biomass mixtures for the 35th International Technical Conference on Clean Coal & Fuel Systems that will take place in June 2010. The meetings included a tour of gasification and fuel development research at Gas Technology Institute.

Numerous discussions were held with key experts working in thermochemical approaches to biomass-to-liquid technologies at the tcbiomass2009 conference in Chicago. Especially pertinent to EERC work were discussions related to converting biomass to pyrolysis liquids or synthetic gases, with subsequent conversion to hydrocarbon fuels or ethanol. A trip report was prepared for principal investigators for review of certain presentations, meetings, discussions, and posters. Of particular interest to the EERC was the gas cleanup technology developed by Research Triangle Institute (RTI) (United States) and Energieonderzoek Centrum Nederland (Netherlands Energy Research Foundation) for biomass gasification systems similar to the gasifier designs worked on by the EERC for the CERL project. Potential collaborations may ensue.

Work was done to help facilitate the 4th Biomass Summit: Feedstock, Cofiring, Finance, and Investment in Washington, D.C., held in October 2009, an important venue for discussing real-world biomass fuels and power with applicability to federal and military agencies, financial entities, and industry. Especially pertinent was the sustainability of biomass feedstocks to military installations for power production.

A summit meeting was attended in nearby Fargo, North Dakota, on August 12, 2009, that was put together by Senator Byron Dorgan and involved several national labs, the U.S. Department of Energy, and the National Science Foundation. It was called the Sustainable

Energy Innovations Summit and involved discussions on new developments in the production of jet and vehicle alternative fuels, hydrogen, and sustainable energy and marketable products in general. Also, at the EERC, discussions were held with Mr. Jay Otten, Manager, Technology and Innovation at BASF Corporation – Wayandotte, Michigan. Although primarily in the chemicals business, BASF has been helpful to the EERC CERL projects in supplying materials and expertise. Discussions centered on catalysts for direct and indirect liquefaction of coal and biomass to diesel and jet fuel products; potential production of engine additives, green diesel experience and technology developments in Europe, and cellulose biofuels in general. Discussions were held with Tesoro at the EERC with regard to potential military interests in green diesel and renewable jet fuel production from biobased feedstocks. Finally, fruitful discussions were held with Select Engineering Services (SES) to possibly supply research, development, and technical service work as collaborators with SES on upcoming contractor projects SES may have with TARDEC.

Task 3 facilitated and managed all reporting activities, including quarterly reports and a semiannual report. Also, a project management plan was prepared for ERDC CERL as part of contractual reporting requirements which contained project objectives, work tasks, milestones, and the overall schedule. All reports were prepared and formatted in accordance with U.S. Army Corps of Engineers ERDC Technical Report Guidelines.

In the area strategic studies and publications, a special ERDC/CERL technical report was initiated and completed to a draft copy. The technical report is entitled "Development and Demonstration of Hydrogen Production and Purification Systems for U.S. Military Fuel Cell Vehicles." It was reviewed internally by four EERC principal investigators and Chris J. Zygarlicke. The report summarizes activities to date related to the development of the high-pressure hydrogen production, purification, refueling, and vehicle demonstration work. A copy of the draft report will be given to ERDC CERL for review and inclusion, if possible, of an ERDC CERL author. The document should be completed, finalized, and published in the next few months.

A second major strategic studies effort involved work done to put together a biomass resource and characterization assessment for the contiguous United States. In addition to funds from this project, funds from an industrial partner supported the effort. The final report entitled "Identification and Characterization of Biomass Sources in the United States" is provided in Appendix C. The aim of the report was to determine the current and future availability of agricultural and forest residues, energy crops, and urban residuals as biomass sources in the United States for power and fuels. The study included some data on the chemical and physical properties of those sources and information on national land ownership, climate zones, and biomass-growing conditions. The project produced a detailed report that included county-by-county biomass resource types and estimates and also included some biomass properties data. The large dataset collected as a result of this study will be used to evaluate the feasibility of specific biomass utilization opportunities. One conclusion drawn from the study is that there is no single ideal biomass source. While some sources may have ideal combustion and cofiring properties, such as wood, other sources are optimal feedstocks for fuel production, such as corn or soybeans. In addition, no type of biomass is uniformly available across the United States or even within individual states.

The best source for a particular energy production scenario will depend on multiple factors that will need to be assessed on a case-by-case basis. These factors include the following:

- Local resource availability
- Resource costs
- Resource physical and chemical properties and intrinsic fuel values
- Plant size, feed ratio with coal (for cofiring scenarios)
- Resource processing requirements (drying, shredding, pulverizing, separating), storage options
- Local geography and climate (which will impact biomass properties)
- Availability of process utilities for conditioning as-received resources

When specific biomass utilization applications are considered, it is imperative to verify the information on a local level and test the specific biomass source to be used. Each application will also require a thorough technoeconomic assessment and analysis of available feedstocks prior to a candidate biomass being selected for energy generation or product development.

Finally, this management task was heavily involved in all of the day-to-day contract negotiations that took place related to obtaining approval for foreign nationals to work on the project, securing changes to budget structures for purchasing equipment necessary for technical research, securing no-cost project extensions, securing cost-share funding, and other such project and contract modifications.

REFERENCES

Fogler, S.H. *Elements of Chemical Reaction Engineering*, 3rd Ed.; Prentice-Hall: Upper Saddle River, NJ, 1999; Ch. 5.

Juraščík, M.; Sues, A.; Ptasinski, K.J., Exergy Analysis of Synthetic Natural Gas Production Method from Biomass. *J. Energy* **2009**, *7*, 31.

Lapidusa, A.L.; Bavykin, V.M.; Smolenskii, E.A.; Chuvaeva, I.V. Cetane Numbers of Hydrocarbons as a Function of Their Molecular Structure. *Doklady Chem.* **2008**, *420*, (2), 150–155.

Larson, E.; Jin, H. Biomass Conversion to Fischer–Tropsch Liquids: Preliminary Energy Balances. In *Proceedings of the 4th Biomass Conference of the Americas*; Elsevier Science, Ltd., Oxford, UK, 1999.

Patel, N.M.; Paul, P.J.; Mukunda, H.S.; Dasappa, S., Combustion Studies on Concentrated Distillery Effluent. In *Twenty-Sixth Symposium (International) on Combustion*; The Combustion Institute, Pittsburgh, PA, 1996; 2479–2485.

Santana, R.C.; Do, P.T.; Santikunaporn, M.; Alvarez, W.E.; Taylor, J.D.; Sughrue, E.L.; Resasco, D.E. Evaluation of Different Reaction Strategies for the Improvement of Cetane Number in Diesel Fuels. *Fuel* **2006**, *85 (5–6)*, 643–656.

TSS Consultants. *Gridley Ethanol Demonstration Project Utilizing Biomass Gasification Technology: Pilot Plant Gasifier and Syngas Conversion Testing*; TSS Consultants for the City of Gridley, CA Report; August 2002–June 2004, NREL/SR-510-37581, 2005.

Zygarlicke, C.J.; Hurley, J.P.; Aulich, T.R.; Folkedahl, B.C. *Production of JP-8-Based Hydrogen and Advanced Tactical Fuels for the U.S. Military*; Final Report for U.S. Army Corps of Engineers Engineer Research and Development Center Cooperative Agreement No. W9132T-05-2-0024; Energy & Environmental Research Center: Grand Forks, ND, Aug 2009.

APPENDIX A

JOURNAL OF FUEL CELL SCIENCE AND TECHNOLOGY

JOURNAL OF FUEL CELL SCIENCE AND TECHNOLOGY

APPENDIX B

MIL-DTL-83133F

DETAIL SPECIFICATION

TURBINE FUEL, AVIATION, KEROSENE TYPE,
JP-8 (NATO F-34), NATO F-35, and JP-8+100 (NATO F-37)

This specification is approved for use by all Departments and Agencies of the Department of Defense.

AMSC N/A   FSC 9130

MIL-DTL-83133F

1. SCOPE

1.1 <u>Scope</u>. This specification covers three grades of kerosene type aviation turbine fuel, JP-8 (NATO F-34), NATO F-35, and JP-8+100 (NATO F-37). This specification was thoroughly reviewed as a part of acquisition reform. While most of the requirements were converted to performance terms, not all requirements could be converted due to the military-unique nature of the product (see 6.1) and the need for compatibility with deployed systems. The issuance of this specification as "detail" is not intended to constrain technology advances in future systems.

1.2 <u>Classification</u>. Aviation turbine fuel will be of the following grades, as specified (see 6.2).

Grade	NATO Code No.	Description
JP-8	F-34	Kerosene type turbine fuel which will contain a static dissipator additive, corrosion inhibitor/lubricity improver, and fuel system icing inhibitor, and may contain antioxidant and metal deactivator.
	F-35	Kerosene type turbine fuel which will contain a static dissipator additive, may contain antioxidant, corrosion inhibitor/lubricity improver, and metal deactivator but will not contain fuel system icing inhibitor.
JP-8+100	F-37	JP-8 type kerosene turbine fuel which contains thermal stability improver additive (NATO S-1749) as described in 3.3.6.

2. APPLICABLE DOCUMENTS

2.1 <u>General</u>. The documents listed in this section are specified in sections 3, 4, or 5 of this specification. This section does not include documents cited in other sections of this specification or recommended for additional information or as examples. While every effort has been made to ensure the completeness of this list, document users are cautioned that they must meet all specified requirements of documents cited in sections 3, 4, or 5 of this specification, whether or not they are listed.

2.2 <u>Government documents</u>.

2.2.1 <u>Specifications, standards, and handbooks</u>. The following specifications, standards, and handbooks form a part of this document to the extent specified herein. Unless otherwise specified, the issues of these documents are those cited in the solicitation or contract.

DEPARTMENT OF DEFENSE SPECIFICATIONS

MIL-DTL-5624	Turbine Fuel, Aviation, Grades JP-4 and JP-5
MIL-PRF-25017	Inhibitor, Corrosion/Lubricity Improver, Fuel Soluble
MIL-DTL-85470	Inhibitor, Icing, Fuel System, High Flash NATO Code Number S-1745

DEPARTMENT OF DEFENSE STANDARDS

MIL-STD-290   Packaging of Petroleum and Related Products

QUALIFIED PRODUCTS LIST

QPL-25017   Inhibitor, Corrosion/Lubricity Improver, Fuel Soluble

(Copies of these documents are available from the Standardization Document Order Desk, 700 Robbins Avenue, Building 4D, Philadelphia PA 19111-5094 or online at http://assist.daps.dla.mil)

2.3 Non-government publications. The following documents form a part of this document to the extent specified herein. Unless otherwise specified, the issues of these documents are those cited in the solicitation or contract.

ASTM International

ASTM D 56	Standard Test Method for Flash Point by Tag Closed Cup Tester (DoD Adopted)
ASTM D 86	Standard Test Method for Distillation of Petroleum Products at Atmospheric Pressure (DoD Adopted)
ASTM D 93	Standard Test Methods for Flash Point by Pensky-Martens Closed Cup Tester (DoD Adopted)
ASTM D 129	Standard Test Method for Sulfur in Petroleum Products (General Bomb Method) (DoD Adopted)
ASTM D 130	Standard Test Method for Corrosiveness to Copper from Petroleum Products by Copper Strip Test (DoD Adopted)
ASTM D 156	Standard Test Method for Saybolt Color of Petroleum Products (Saybolt Chromometer Method) (DoD Adopted)
ASTM D 381	Standard Test Method for Gum Content in Fuels by Jet Evaporation (DoD Adopted)
ASTM D 445	Standard Test Method for Kinematic Viscosity of Transparent and Opaque Liquids (and the Calculation of Dynamic Viscosity) (DoD Adopted)
ASTM D 976	Standard Test Methods for Calculated Cetane Index of Distillate Fuels (DoD Adopted)
ASTM D 1094	Standard Test Method for Water Reaction of Aviation Fuels (DoD Adopted)
ASTM D 1266	Standard Test Method for Sulfur in Petroleum Products (Lamp Method) (DoD Adopted)
ASTM D 1298	Standard Test Method for Density, Relative Density (Specific Gravity), or API Gravity of Crude Petroleum and Liquid Petroleum Products by Hydrometer Method (DoD Adopted)
ASTM D 1319	Standard Test Method for Hydrocarbon Types in Liquid Petroleum Products by Fluorescent Indicator Adsorption (DoD Adopted)
ASTM D 1322	Standard Test Method for Smoke Point of Kerosine and Aviation Turbine Fuels (DoD Adopted)
ASTM D 1840	Standard Test Method for Naphthalene Hydrocarbons in Aviation

Turbine Fuels by Ultraviolet Spectrophotometry (DoD Adopted)

ASTM D 2276	Standard Test Method for Particulate Contaminant in Aviation Fuel by Line Sampling (DoD Adopted)
ASTM D 2386	Standard Test Method for Freezing Point of Aviation Fuels (DoD Adopted)
ASTM D 2622	Standard Test Method for Sulfur in Petroleum Products by Wavelength Dispersive X-Ray Fluorescence Spectrometry (DoD Adopted)
ASTM D 2624	Standard Test Methods for Electrical Conductivity of Aviation and Distillate Fuels (DoD Adopted)
ASTM D 2887	Standard Test Method for Boiling Range Distribution of Petroleum Fractions by Gas Chromatography (DoD Adopted)
ASTM D 3120	Standard Test Method for Trace Quantities of Sulfur in Light Liquid Petroleum Hydrocarbons by Oxidative Microcoulometry (DoD Adopted)
ASTM D 3227	Standard Test Method for (Thiol Mercaptan) Sulfur in Gasoline, Kerosine, Aviation Turbine, and Distillate Fuels (Potentiometric Method) (DoD Adopted)
ASTM D 3241	Standard Test Method for Thermal Oxidation Stability of Aviation Turbine Fuels (JFTOT Procedure) (DoD Adopted)
ASTM D 3242	Standard Test Method for Acidity in Aviation Turbine Fuel (DoD Adopted)
ASTM D 3338	Standard Test Method for Estimation of Net Heat of Combustion of Aviation Fuels (DoD Adopted)
ASTM D 3343	Standard Test Method for Estimation of Hydrogen Content of Aviation Fuels (DoD Adopted)
ASTM D 3701	Standard Test Method for Hydrogen Content of Aviation Turbine Fuels by Low Resolution Nuclear Magnetic Resonance Spectrometry (DoD Adopted)
ASTM D 3828	Standard Test Methods For Flash Point by Small Scale Closed Cup Tester (DoD Adopted)
ASTM D 3948	Standard Test Method for Determining Water Separation Characteristics of Aviation Turbine Fuels by Portable Separometer (DoD Adopted)
ASTM D 4052	Standard Test Method for Density and Relative Density of Liquids by Digital Density Meter (DoD Adopted)
ASTM D 4057	Standard Practice for Manual Sampling of Petroleum and Petroleum Products (DoD Adopted)
ASTM D 4177	Standard Practice for Automatic Sampling of Petroleum and Petroleum Products (DoD Adopted)
ASTM D 4294	Standard Test Method for Sulfur in Petroleum and Petroleum Products by Energy-Dispersive X-Ray Fluorescence Spectrometry (DoD Adopted)
ASTM D 4306	Standard Practice for Aviation Fuel Sample Containers for Tests Affected by Trace Contamination (DoD Adopted)
ASTM D 4529	Standard Test Method for Estimation of Net Heat of Combustion of Aviation Fuels
ASTM D 4737	Standard Test Method for Calculated Cetane Index by Four Variable Equation

ASTM D 4809	Standard Test Method for Heat of Combustion of Liquid Hydrocarbon Fuels by Bomb Calorimeter (Precision Method) (DoD Adopted)
ASTM D 4952	Standard Test Method for Qualitative Analysis for Active Sulfur Species in Fuels and Solvents (Doctor Test) (DoD Adopted)
ASTM D 5001	Standard Test Method for Measurement of Lubricity of Aviation Turbine Fuels by the Ball-on-Cylinder Lubricity Evaluator (BOCLE)
ASTM D 5006	Standard Test Method for Measurement of Fuel System Icing Inhibitors (Ether Type) in Aviation Fuels (DoD Adopted)
ASTM D 5186	Standard Test Method for Determination of the Aromatic Content and Polynuclear Aromatic Content of Diesel Fuels and Aviation Turbine Fuels by Supercritical Fluid Chromatography
ASTM D 5452	Standard Test Method for Particulate Contamination in Aviation Fuels by Laboratory Filtration (DoD Adopted)
ASTM D 5453	Standard Test Method for Determination of Total Sulfur in Light Hydrocarbons, Spark Ignition Engine Fuel, Diesel Engine Fuel, and Engine Oil by Ultraviolet Fluorescence
ASTM D 5972	Standard Test Method for Freezing Point of Aviation Fuels (Automatic Phase Transition Method)
ASTM D 6045	Standard Test Method for Color of Petroleum Products by the Automatic Tristimulus Method
ASTM D 7153	Standard Test Method for Freezing Point of Aviation Fuels (Automatic Laser Method)
ASTM D 7154	Standard Test Method for Freezing Point of Aviation Fuels (Automatic Fiber Optical Method)
ASTM D 7224	Standard Test Method for Determining Water Separation Characteristics of Kerosine-type Aviation Turbine Fuels Containing Additives by Portable Separometer
ASTM E 29	Standard Practice for Using Significant Digits in Test Data to Determine Conformance with the Specifications (DoD Adopted)
IEEE/ASTM SI 10	American National Standard for Use of the International System of Units (SI): The Modern Metric System (DoD Adopted)

(Copies of these documents are available at ASTM International, 100 Barr Harbor Drive, PO Box C700, West Conshohocken PA 19428-2959. Electronic copies of ASTM standards may be obtained from http://www.astm.org)

2.4 Order of precedence. In the event of a conflict between the text of this document and the references cited herein (except for related specification sheets), the text of this document takes precedence. Nothing in this document, however, supersedes applicable laws and regulations unless a specific exemption has been obtained.

3. REQUIREMENTS

3.1 <u>Materials</u>. Fuel supplied under this specification shall be refined hydrocarbon distillate fuel oils containing additives in accordance with 3.3. The feedstock from which the fuel is refined shall be crude oils derived from petroleum, tar sands, oil shale, or mixtures thereof.

3.1.1 <u>Materials for Blending</u>. With the approval of both the procuring activity and the applicable fuel technical authorities listed below, up to 50 volume % of the finished fuel may consist solely of Synthetic Paraffinic Kerosene (SPK) derived from a Fischer-Tropsch (FT) process meeting requirements of <u>Appendix A</u>. Finished fuel shall contain additives in accordance with 3.3. During the platform certification/approval process, JP-8 containing SPK will be designated JP-8/SPK.

Procuring Activity: Product Technology and Standardization, DESC, 8725 John J. Kingman Road, Fort Belvoir, VA 22060

Cognizant activity for the Navy and Marine Corps: Naval Fuels and Lubricants Cross Functional Team, AIR-4.4.1, Building 2360, 22229 Elmer Road, Patuxent River, MD 20670-1534.

Cognizant activity for the Air Force: Fuels Certification Office, 77th Monohan Street, Area B, Wright-Patterson AFB, OH 45433-7017.

Cognizant activities for the Army:

Army Ground: US Army TARDEC/RDECOM, 6501 E. 11 Mile Road, AMSRD-TAR-D (MS-110), Warren, MI 48397-5000.

Army Aviation: US Army RDECOM, Attn: AMSRD-AMR-AE-P, Building 4488, Room C-211, Redstone Arsenal, AL 35898-5000

3.1.2 <u>Non-FT Materials</u>. The use of synthetic blending materials represents a potential departure from experience and from the key assumptions which form the basis for fuel property requirements. It is the long-term goal of this specification to fully encompass fuels derived from synthetic materials and non-conventional sources once they have been defined but, this is only partially complete. Until this is accomplished, specific fuel formulations from synthetic materials or non-conventional sources may be submitted to AFRL/RZTG, Bldg 490, 1790 Loop Road N, WPAFB, OH 45433 to begin evaluation of compliance with the intent of this specification.

3.2 <u>Chemical and physical requirements</u>. The chemical and physical properties of a finished fuel containing only the materials described in 3.1 shall conform to the requirements listed in <u>Table 1</u>.

3.2.1 <u>Chemical and physical requirements of blended finished fuels</u>. The chemical and physical properties of a finished fuel blend containing any amount of synthetic SPK as described in 3.1.1 shall conform to the requirements listed in <u>Table 2</u>.

3.3 <u>Additives</u>. The type and amount of each additive used shall be made available when requested by the procuring activity or user (6.2.d). The only additives approved for use are those referenced in this specification.

3.3.1 <u>Antioxidants</u>. Immediately after processing and before the fuel is exposed to the atmosphere (such as during rundown into feed/batch tankage), an approved antioxidant (3.3.1.1) shall be blended into the fuel in order to prevent the formation of gums and peroxides after manufacture. The concentration of the antioxidant to be added shall be:

a. Not less than 17.2 milligrams (mg) nor more than 24.0 mg of active ingredient per liter (L) of fuel (6.0 to 8.4 lb/1000 barrels) to all JP-8 fuel that contains blending stocks that have been hydrogen treated or were manufactured from a Fischer-Tropsch process.

b. At the option of the supplier, not more than 24.0 mg of active ingredient per liter of fuel (8.4 lb/1000 barrels) may be added to JP-8 fuels that do not contain hydrogen treated blending stocks nor Fischer-Tropsch products.

3.3.1.1 Antioxidant formulations. The following antioxidant formulations are approved:

a.   2,6-di-tert-butyl-4-methylphenol

b.   6-tert-butyl-2,4-dimethylphenol

c.   2,6-di-tert-butylphenol

d.   75 percent min-2,6-di-tert-butylphenol
     25 percent max tert-butylphenols and tri-tert-butylphenols

e.   72 percent min 6-tert-butyl-2,4-dimethylphenol
     28 percent max tert-butyl-methylphenols and tert-butyl-dimethylphenols

f.   55 percent min 2,4-dimethyl-6-tert-butylphenol and
     15 percent min 2,6-di-tert-butyl-4-methylphenol and
     30 percent max mixed methyl and dimethyl tert-butylphenols

3.3.2 Metal deactivator. A metal deactivator, N,N'-disalycylidene-1,2-propanediamine, may be blended into the fuel. The concentration of active material used on initial batching of the fuel at the refinery shall not exceed 2.0 mg/L. Cumulative addition of metal deactivator when redoping the fuel, shall not exceed 5.7 mg/L. Metal deactivator additive shall not be used in JP-8 unless the supplier has obtained written consent from the procuring activity and user.

3.3.3 Static dissipater additive. An additive shall be blended into the fuel in sufficient concentration to increase the conductivity of the fuel at the point of injection to within the range specified in Table 1 for fuel offered in accordance with 3.1 or as specified in Table 2 for finished fuel when allowed per 3.1.1. The point of injection of the additive shall be determined by agreement between the purchasing authority and the supplier. The following electrical conductivity additive is approved: Stadis® 450 marketed by Innospec Fuel Specialties LLC (formerly Octel Starreon LLC), Newark, DE 19702.

3.3.4 Corrosion inhibitor/lubricity improver additive. A corrosion inhibitor/lubricity improver (CI/LI) additive conforming to MIL-PRF-25017 shall be blended into the F-34 (JP-8) grade fuel by the contractor. The CI/LI additive is optional for F-35. The amount added shall be equal to or greater than the minimum effective concentration and shall not exceed the maximum allowable concentration listed in the latest revision of QPL-25017. The contractor or transporting agency, or both, shall maintain and upon request shall make available to the Government evidence that the CI/LI additives used are equal in every respect to the qualification products listed in QPL-25017. The point of injection of the CI/LI additive shall be determined by agreement between the purchasing authority and the supplier.

TABLE 1. _Chemical and physical requirements and test methods_.

Property	Min	Max	Test Methods ASTM Standards
Color, Saybolt [1]			D 156 [2] or D 6045
Total acid number, mg KOH/gm		0.015	D 3242
Aromatics, vol percent		25.0	D 1319
Sulfur, total, mass percent		0.30	D 129, D 1266, D 2622, D 3120, D 4294 [2], or D 5453
Sulfur mercaptan, mass percent or		0.002	D 3227
Doctor test		negative	D 4952
Distillation temperature, °C [3] (D 2887 limits given in parentheses) Initial boiling point [1]			D 86 [2] or D 2887
10 percent recovered		205 (186)	
20 percent recovered [1]			
50 percent recovered [1]			
90 percent recovered [1]			
Final boiling point		300 (330)	
Residue, vol percent		1.5	
Loss, vol percent		1.5	
Flash point, °C [4]	38		D 56, D 93 [2], or D 3828
Density			D 1298 or D 4052 [2]
Density, kg/L at 15°C or	0.775	0.840	
Gravity, API at 60°F	37.0	51.0	
Freezing point, °C		-47	D 2386 [2], D 5972, D 7153, or D 7154
Viscosity, at -20°C, mm²/s		8.0	D 445
Net heat of combustion, MJ/kg	42.8		D 3338, D 4529, or D 4809 [2]
Hydrogen content, mass percent	13.4		D 3343 or D 3701 [2]
Smoke point, mm, or	25.0		D 1322
Smoke point, mm, and	19.0		D 1322
Naphthalenes, vol percent		3.0	D 1840
Calculated cetane index [1]			D 976 [5] or D 4737
Copper strip corrosion, 2 hr at 100°C (212°F)		No. 1	D 130
Thermal stability			D 3241 [6]
change in pressure drop, mm Hg		25	
heater tube deposit, visual rating		<3 [7]	

TABLE 1. *Chemical and physical requirements and test methods* – *Continued*

Property	Min	Max	Test Methods ASTM Standards
Existent gum, mg/100 mL		7.0	D 381
Particulate matter, mg/L [8]		1.0	D 2276 or D 5452 [2]
Filtration time, minutes [8]		15	
Water reaction interface rating		1 b	D 1094
Water separation index [9]			D 3948 or D 7224 [2]
Fuel system icing inhibitor, vol percent	0.10	0.15	D 5006 [10]
Fuel electrical conductivity, pS/m [11]			D 2624

NOTES:

1. To be reported – not limited.
2. Referee Test Method.
3. A condenser temperature of 0° to 4°C (32° to 40°F) shall be used for the distillation by ASTM D 86.
4. ASTM D 56 may give results up to 1°C (2°F) below the ASTM D 93 results. ASTM D 3828 may give results up to 1.7°C (3°F) below the ASTM D 93 results. Method IP170 is also permitted.
5. Mid-boiling temperature may be obtained by either ASTM D 86 or ASTM D 2887 to perform the cetane index calculation. ASTM D 86 values should be corrected to standard barometric pressure.
6. See 4.5.3 for ASTM D 3241 test conditions and test limitations.
7. Peacock or Abnormal color deposits result in a failure.
8. A minimum sample size of 3.79 liters (1 gallon) shall be filtered. Filtration time will be determined in accordance with procedure in Appendix B. This procedure may also be used for the determination of particulate matter as an alternate to ASTM D 2276 or ASTM D 5452.
9. The minimum microseparometer rating using a Micro-Separometer (MSEP) shall be as follows:

JP-8 Additives	MSEP Rating, min.
Antioxidant (AO)*, Metal Deactivator (MDA)*	90
AO*, MDA*, and Fuel System Icing Inhibitor (FSII)	85
AO*, MDA*, and Corrosion Inhibitor/Lubricity Improver (CI/LI)	80
AO*, MDA*, FSII and CI/LI)	70

*Even though the presence or absence does not change these limits, samples submitted for specification or conformance testing shall contain the same additives present in the refinery batch. Regardless of which minimum the refiner selects to meet, the refiner shall report the MSEP rating on a laboratory hand blend of the fuel with all additives required by the specification.

10. Test shall be performed in accordance with ASTM D 5006 using the DiEGME scale of the refractometer.
11. The conductivity must be between 150 and 600 pS/m for F-34 (JP-8) and between 50 and 600 pS/m for F-35, at ambient temperature or 29.4°C (85°F), whichever is lower, unless otherwise directed by the procuring activity. In the case of JP-8+100, JP-8 with the thermal stability improver additive (see 3.3.6), the conductivity limit must be between 150 to 700 pS/m at ambient temperature or 29.4°C (85°F), whichever is lower, unless otherwise directed by the procuring activity.

**TABLE 2. *Chemical and physical requirements and test methods*
*for JP-8 with up to 50 percent SPK blend component***

Property	Min	Max	Test Methods ASTM Standards
Color, Saybolt [1]			D 156 [2] or D 6045
Total acid number, mg KOH/gm		0.015	D 3242
Aromatics, vol percent	8.0	25.0	D 1319
Olefins, vol percent		5.0	D 1319
Sulfur, total, mass percent		0.30	D 129, D 1266, D 2622, D 3120, D 4294 [2], or D 5453
Sulfur mercaptan, mass percent or		0.002	D 3227
Doctor test		negative	D 4952
Distillation temperature, °C [3]			D 86
Initial boiling point [1]			
10 percent recovered (T10)	157	205	
20 percent recovered [1]			
50 percent recovered (T50)	168	229	
90 percent recovered (T90)	183	262	
Final boiling point		300	
T50 – T10	15		
T90 – T10	40		
Residue, vol percent		1.5	
Loss, vol percent		1.5	
Flash point, °C [4]	38	68	D 56, D 93 [2], or D 3828
Density			D 1298 or D 4052 [2]
Density, kg/L at 15°C or	0.775	0.840	
Gravity, API at 60°F	37.0	51.0	
Freezing point, °C		-47	D 2386 [2], D 5972, D 7153, or D 7154
Viscosity, at -20°C, mm^2/s		8.0	D 445
Net heat of combustion, MJ/kg	42.8		D 3338, D 4529, or D 4809 [2]
Hydrogen content, mass percent	13.4		D 3343 or D 3701 [2]
Smoke point, mm, or	25.0		D 1322
Smoke point, mm, and	19.0		D 1322
Naphthalenes, vol percent		3.0	D 1840
Calculated cetane index [1]			D 976 [5] or D 4737
Copper strip corrosion, 2 hr at 100°C (212°F)		No. 1	D 130
Thermal stability			D 3241 [6]
change in pressure drop, mm Hg		25	
heater tube deposit, visual rating		<3 [7]	

TABLE 2. _Chemical and physical requirements and test methods_
for JP-8 with up to 50 percent SPK blend component – Continued

Property	Min	Max	Test Methods ASTM Standards
Existent gum, mg/100 mL		7.0	D 381
Particulate matter, mg/L [8]		1.0	D 2276 or D 5452 [2]
Filtration time, minutes [8]		15	
Water reaction interface rating		1 b	D 1094
Water separation index [9]			D 3948 or D 7224 [2]
Fuel system icing inhibitor, vol percent	0.10	0.15	D 5006 [10]
Fuel electrical conductivity, pS/m [11]			D 2624
Lubricity, wear scar diameter, mm		0.85	D 5001

NOTES:

1. To be reported – not limited.
2. Referee Test Method.
3. A condenser temperature of 0° to 4°C (32° to 40°F) shall be used for the distillation by ASTM D 86.
4. ASTM D 56 may give results up to 1°C (2°F) below the ASTM D 93 results. ASTM D 3828 may give results up to 1.7°C (3°F) below the ASTM D 93 results. Method IP170 is also permitted.
5. Mid-boiling temperature may be obtained by ASTM D 86 to perform the cetane index calculation. ASTM D 86 values should be corrected to standard barometric pressure.
6. See 4.5.3 for ASTM D 3241 test conditions and test limitations.
7. Peacock or Abnormal color deposits result in a failure.
8. A minimum sample size of 3.79 liters (1 gallon) shall be filtered. Filtration time will be determined in accordance with procedure in Appendix B. This procedure may also be used for the determination of particulate matter as an alternate to ASTM D 2276 or ASTM D 5452.
9. The minimum microseparometer rating using a Micro-Separometer (MSEP) shall be as follows:

JP-8 Additives	MSEP Rating, min.
Antioxidant (AO)*, Metal Deactivator (MDA)*	90
AO*, MDA*, and Fuel System Icing Inhibitor (FSII)	85
AO*, MDA*, and Corrosion Inhibitor/Lubricity Improver (CI/LI)	80
AO*, MDA*, FSII and CI/LI)	70

*Even though the presence or absence does not change these limits, samples submitted for specification or conformance testing shall contain the same additives present in the refinery batch. Regardless of which minimum the refiner selects to meet, the refiner shall report the MSEP rating on a laboratory hand blend of the fuel with all additives required by the specification.

10. Test shall be performed in accordance with ASTM D 5006 using the DiEGME scale of the refractometer.
11. The conductivity must be between 150 and 600 pS/m for F-34 (JP-8) and between 50 and 600 pS/m for F-35, at ambient temperature or 29.4°C (85°F), whichever is lower, unless otherwise directed by the procuring activity. In the case of JP-8+100, JP-8 with the thermal stability improver additive (see 3.3.6), the conductivity limit must be between 150 to 700 pS/m at ambient temperature or 29.4°C (85°F), whichever is lower, unless otherwise directed by the procuring activity.

     3.3.5 Fuel system icing inhibitor. The use of a fuel system icing inhibitor shall be mandatory for JP-8 and shall conform to MIL-DTL-85470. The point of injection of the additive for JP-8 shall be determined by agreement between the purchasing authority and the supplier. The fuel system icing inhibitor is not to be added to NATO F-35 unless so directed by the purchasing authority.

3.3.6 <u>Thermal stability improver additive</u>. Due to logistic concerns, personnel at the operating location shall request written approval from the cognizant activity to add a thermal stability improver additive to the fuel. If approval is given, the concentration of the additive and location of injection shall be specified by the cognizant service activity listed below. For USAF aircraft, this approval does not override the single manager's authority for specifying allowed/disallowed fuels. JP-8 fuel with an approved thermal stability improver additive at the required concentration shall be designated as JP-8+100. Thermal stability improver additive shall not be used in JP-8 without approval, in writing, from:

Cognizant activity for the Navy and Marine Corps: Naval Fuels and Lubricants Cross Functional Team, AIR-4.4.1, Building 2360, 22229 Elmer Road, Patuxent River, MD 20670-1534.

Cognizant activity for the Air Force: HQ Air Force Petroleum Agency, HQ AFPET/AFT, 2430 C Street, Building 70, Area B, Wright-Patterson AFB 45433-7632.

Cognizant activities for the Army:

Army Ground: US Army TARDEC/RDECOM, 6501 E. 11 Mile Road, AMSRD-TAR-D (MS-110), Warren, MI 48397-5000.

Army Aviation: US Army RDECOM, Attn: AMSRD-AMR-AE-P, Building 4488, Room C-211, Redstone Arsenal, AL 35898-5000

3.3.6.1 <u>Qualified additives</u>. Qualified thermal stability improver additives are listed in <u>Table 3</u>.

TABLE 3. *Qualified thermal stability improver additives*.

Additive Name	Qualification Reference	Manufacturer
SPEC AID 8Q462	AFRL/PRSF Ltr, 9 Dec 97	GE Water & Process Technologies 9669 Grogan Mill Road The Woodlands, TX 77380
AeroShell Performance Additive 101	AFRL/PRSF Ltr, 13 Jan 98	Shell Aviation Limited Shell Centre York Road London, UK SE1 7NA

3.3.7 <u>Premixing of additives</u>. Additives shall not be premixed with other additives before injection into the fuel so as to prevent possible reactions among the concentrated forms of different additives.

3.4 <u>Workmanship</u>. At the time of Government acceptance, the finished fuel or finished fuel blend shall be visually free from undissolved water, sediment or suspended matter, and shall be clear and bright. In case of dispute, the fuel shall be clear and bright at 21°C (70°F) and shall contain no more than 1.0 mg/L of particulate matter as required in <u>Table 1</u> for any finished fuel containing only the materials described in 3.1 or, <u>Table 2</u> for finished fuel blends containing any amount of SPK as described in 3.1.1.

3.5 <u>Recycled, recovered, or environmentally preferable materials</u>. Recycled, recovered, or environmentally preferable materials should be used to the maximum extent possible, provided that the material meets or exceeds the operational and maintenance requirements, and promotes economically advantageous life cycle costs.

4. VERIFICATION

4.1 <u>Classification of inspections</u>. The inspection requirements specified herein are classified as quality conformance inspections (see 4.2).

4.2 <u>Qualification inspection conditions</u>. Test for acceptance of individual lots shall consist of tests for all applicable requirements specified in section 3. Quality conformance inspection shall include the test requirements herein.

. 4.2.1 <u>Inspection lot</u>. For acceptance purposes, individual lots shall be examined as specified herein and subjected to tests for all applicable requirements cited in section 3.

4.3 <u>Inspection</u>.

4.3.1 <u>Inspection conditions</u>. Any finished fuel containing only the materials described in 3.1 shall comply with the limiting values specified in <u>Table 1</u> using the cited test methods. Any finished fuel blend containing any amount of SPK as described in 3.1.1 shall comply with the limiting values specified in <u>Table 2</u> using the cited test methods. Any SPK blend component as described in 3.1.1 shall comply with the limiting values specified in <u>Table A-I</u> using the cited test methods. The specified limiting values must not be changed. This precludes any allowance for test method precision and adding or subtracting digits. For the purposes of determining conformance with the specified limiting values, an observed value or a calculated value shall be rounded off "to the nearest unit" in the last right hand place of digits used in expressing the specified limiting value, in accordance with the Rounding-Off Method of ASTM E 29.

4.4 <u>Sampling plans</u>.

4.4.1 <u>Sampling</u>. Each bulk or packaged lot of material shall be sampled for verification of product quality in accordance with ASTM D 4057 or ASTM D 4177, except where individual test procedures contain specific sampling instructions.

4.4.2 <u>Sampling for inspection of filled containers</u>. A random sample of filled containers shall be selected from each lot and shall be subjected to the examination of filled containers as specified in 4.5.1.3.

4.5 <u>Methods of inspection</u>.

4.5.1 <u>Examination of product</u>.

4.5.1.1 <u>Visual inspection</u>. Samples selected in accordance with 4.4.1 shall be visually examined for compliance with 3.4.

4.5.1.2 <u>Examination of empty containers</u>. Before filled, each unit container shall be visually inspected for cleanliness and suitability in accordance with ASTM D 4057.

4.5.1.3 <u>Examination of filled containers</u>. Samples taken as specified in 4.4.2 shall be examined for conformance to MIL-STD-290 with regard to fill, closure, sealing, leakage, packaging, packing, and markings. Any container with one or more defects under the required fill shall be rejected.

4.5.2 <u>Chemical and physical tests</u>. Tests to determine compliance with chemical and physical requirements shall be conducted in accordance with <u>Table 1</u> or <u>Table 2</u> and/or <u>Table A-I</u> as follows. Any finished fuel containing only the materials described in 3.1 shall pass all tests listed in <u>Table 1</u>. Any finished fuel containing any amount of SPK as described in 3.1.1 shall pass all tests listed in <u>Table 2</u>. Any SPK blend component as defined in 3.1.1 shall pass all tests listed in <u>Table A-I</u>. No additional testing shall be required. Requirements contained herein are not subject to corrections for test tolerances. If multiple determinations are made, results falling within any specified repeatability and reproducibility tolerances may be averaged. For rounding off of significant figures, ASTM E 29 shall apply to all tests required by this specification.

4.5.3 <u>Thermal stability tests</u>. The thermal stability test shall be conducted using ASTM D 3241. The heated tube shall be rated visually (see Annex A1 of ASTM D 3241).

4.5.3.1 <u>ASTM D 3241 test conditions</u>.

a.   Heater tube temperature at maximum point: 260°C (500°F).

b.   Fuel system pressure: 3.45 MPa (500 psig).

c.   Fuel flow rate: 3.0 mL/min.

d.   Test duration: 150 minutes.

4.5.3.2 <u>ASTM D 3241 reported data</u>. The following data shall be reported:

a.   Differential pressure in millimeter of mercury at 150 minutes, or time to differential pressure of 25 mm Hg, whichever comes first.

b.   Heater tube deposit visual code rating at the end of the test.

5. PACKAGING

5.1 <u>Packaging</u>. For acquisition purposes, the packaging requirements shall be as specified in the contract or order (see 6.2). When actual packaging of materiel is to be performed by DoD or in-house contractor personnel, these personnel need to contact the responsible packaging activity to ascertain packaging requirements. Packaging requirements are maintained by the Inventory Control Point's packaging activities within the Military Service or Defense Agency, or within the military service's system commands. Packaging data retrieval is available from the managing Military Department's or Defense Agency's automated packaging files, CD-ROM products, or by contacting the responsible packaging activity.

6. NOTES

(This section contains information of a general or explanatory nature that may be helpful, but is not mandatory.)

6.1 <u>Intended use</u>. The fuels covered by this specification are intended for use in aircraft turbine engines. JP-8 contains military unique additives that are required by military weapon systems. This requirement is unique to military aircraft and engine designs. When authorized, JP-8 (F-34) may be used in ground - based turbine and diesel engines. NATO F-35 is intended for commercial aviation, but can be converted to JP-8 (F-34) by the addition of the appropriate additives.

6.2 <u>Acquisition requirements</u>. Acquisition documents must specify the following:

a. Title, number, date of this specification, and grade (type) of fuel.
b. Quantity required and size containers desired.
c. Level of packaging and packing required (see 5.1).
d. Location and injection method for addition of electrical conductivity additive, fuel system icing inhibitor and corrosion inhibitor, as required.

6.3 <u>Conversion of metric units</u>. Units of measure have been converted to the International System of Units (SI) (Metric) in accordance with ASTM SI 10. If test results are obtained in units other than metric or there is a requirement to report dual units, ASTM SI 10, should be used to convert the units.

6.4 <u>Definitions</u>.

6.4.1 <u>Bulk lot</u>. A bulk lot consists of an indefinite quantity of a homogeneous mixture of material offered for acceptance in a single isolated container or manufactured in a single plant run through the same processing equipment, with no change in ingredient material.

6.4.2 <u>Packaged lot</u>. A packaged lot consists of an indefinite number of 208-liter (55-gallon) drums, or smaller unit packages of identical size and type, offered for acceptance and filled from an isolated tank containing a homogeneous mixture of material; or filled with a homogeneous mixture of material run through the same processing equipment with no change in ingredient material.

6.4.3 <u>Homogenous product</u>. A homogeneous product is defined as a product where samples taken at various levels of the batch tank are tested for the defining homogeneous characteristics and all values obtained meet the repeatability precision requirements for that test method.

6.4.4 <u>Synthetic Paraffinic Kerosene (SPK)</u> Kerosene consisting solely of n-paraffins, cyclic-paraffins, and iso-paraffins.

6.4.5 <u>Fischer-Tropsch (FT) Process</u> A catalyzed chemical process in which a synthesis gas consisting of carbon monoxide and hydrogen are converted into liquid hydrocarbons of various forms. Typical catalysts used are based on iron and cobalt.

6.5 <u>Subject term (key word) listing</u>.

Antioxidants
Corrosion inhibitor
Fischer-Tropsch
Flash point
Freezing point
Hydrocarbon distillate fuel
Hydrogen content
Icing inhibitor
Synthetic Paraffinic Kerosene (SPK)
Lubricity improver
Static dissipator
Thermal stability improver

6.6 <u>International agreements</u>. Certain provisions of this specification are the subject of international standardization agreement ASIC AIR STD 15/6, ASIC AIR STD 15/9, NATO STANAG 1135, and NATO STANAG 3747. When amendment, revision, or cancellation of this specification is proposed which will modify the international agreement concerned, the preparing activity will take appropriate action through international standardization channels including departmental standardization offices, to change the agreement or make other appropriate accommodations.

6.7 <u>Material safety data sheet</u>. Contracting officers will identify those activities requiring copies of completed Material Safety Data Sheets prepared in accordance with FED-STD-313. The pertinent Government mailing addresses for submission of data are listed in FED-STD-313.

6.8 <u>Test report.</u> Test data required by 4.5 should be available for the procurement activity and user in the same order as listed in <u>Table 1</u> for materials conforming to 3.2 requirements or as listed in <u>Table 2</u> for materials conforming to 3.2.1 requirements. The Inspection Data on Aviation Turbine Fuels form published in ASTM D 1655 should be used as a guide. Also, the type and amount of additives used should be reported.

6.9 <u>Changes from previous issue</u>. Marginal notations are not used in this revision to identify changes with respect to the previous issue due to the extent of the changes.

MIL-DTL-83133F
APPENDIX A

SYNTHETIC PARAFFINIC KEROSENE (SPK)

A.1 SCOPE

A.1.1 <u>Scope</u>. This Appendix addresses 100 percent SPK derived from manufactured products of a Fischer-Tropsch process (identified in 3.1.1). This Appendix is a mandatory part of the specification. The information contained herein is intended for compliance.

A.2 REQUIREMENTS

A.2.1 <u>Chemical and physical requirements</u>. The chemical and physical requirements of the SPK shall conform to those specified in <u>Table A-I</u>.

A.2.2 <u>Additives</u>.

A.2.2.1 <u>Antioxidants.</u> Addition of antioxidants shall adhere to the criteria specified in 3.3.1.

A.2.2.2 <u>Static dissipater additive (SDA)</u>. If SPK is to be transported prior to blending with refined hydrocarbon distillate fuel, static dissipater additive shall be injected in sufficient concentration to increase the conductivity of the fuel to within the range specified in <u>Table A-I</u>. The point of injection of the additive shall be determined by agreement between the purchasing authority and the supplier. The following electrical conductivity additive is approved: Stadis® 450 marketed by Innospec Fuel Specialties LLC (formerly Octel Starreon LLC), Newark, DE 19702.

TABLE A-I. <u>Chemical and physical requirements and test methods for 100 percent SPK</u>.

Property	Min	Max	Test Method
Aromatics, vol percent		1	D 5186
Sulfur, total, mass percent		0.0015	D 2622, D 3120, or D 5453 [1]
Distillation temperature, °C			D 86
Initial boiling point [2]			
10 percent recovered	157	205	
20 percent recovered [2]			
50 percent recovered	168	229	
90 percent recovered	183	262	
Final boiling point		300	
Residue, vol percent		1.5	
Loss, vol percent		1.5	
Flash point, °C	38	68	D 56, D 93 [1], or D 3828
Density			D 1298 or D 4052 [1]
Density, kg/L at 15°C or	0.751	0.840	
Gravity, API at 60°F	37.0	57.0	

17

MIL-DTL-83133F
APPENDIX A

TABLE A-I. _Chemical and physical requirements and test methods_
for 100 percent SPK - Continued.

Property	Min	Max	Test Method
Freezing point, °C		-47	D 2386 [1] or D 5972
Viscosity at -20°C, mm^2/s		8.0	D 445
Viscosity at 40°C, mm^2/s [2]			D 445
Net heat of combustion, MJ/kg	42.8		D 3338 or D 4809 [1]
Calculated cetane index [2]			D 976 [3] or D 4737
Naphthalenes, vol percent		0.1	D 1840
Thermal stability change in pressure drop, mm Hg		25	D 3241
heater tube deposit, visual rating		<3 [4]	
Particulate matter, mg/L [5]		1.0	D 2276 or D 5452 [1]
Filtration time, minutes [5]		15	
Water separation index			D 3948 or D 7224 [1]
With SDA	70		
Without SDA	85		
Electrical conductivity, pS/m [6]	150	450	D 2624

NOTES:
1. Referee Test Method.
2. To be reported – not limited.
3. Mid-boiling temperature may be obtained by ASTM D 86 to perform the cetane index calculation.
   ASTM D 86 values should be corrected to standard barometric pressure.
4. Peacock or Abnormal color deposits result in a failure.
5. A minimum sample size of 3.79 liters (1 gallon) shall be filtered. Filtration time will be determined in
   accordance with procedure in Appendix B. This procedure may also be used for the determination of
   particulate matter as an alternate to ASTM D 2276 or ASTM D 5452.
6. Electrical Conductivity when required per A.2.2.2 shall be determined at ambient temperature or
   29.4°C (85°F), whichever is lower, unless otherwise directed by the procuring activity.

METHOD FOR DETERMINATION OF FILTRATION TIME AND TOTAL SOLIDS

B.1 SCOPE

B.1.1 <u>Scope</u>. This Appendix describes the method for determining singularly or simultaneously the filterability characteristics and solids contamination of jet fuel. The purpose is to detect and prevent contaminants in jet fuel that can plug and cause rupture of ground filtration equipment, thereby affecting flight reliability of aircraft. This Appendix is a mandatory part of the specification. The information contained herein is intended for compliance.

B.2 METHOD

B.2.1 <u>Summary of method</u>. 3.79 liters (1 gallon) of jet fuel is filtered through a membrane filter in the laboratory. The time required to filter this volume is measured in minutes and solids content is determined gravimetrically.

B.3 APPARATUS

a. Membrane filter: White, plain, 47 mm diameter, nominal pore size 0.8 μm. The membrane filter must be approved by ASTM for use with ASTM D 5452.

b. Filtration apparatus: The apparatus, constructed of stainless steel, consists of a funnel and a funnel base with a filter support such that a membrane filter and a flow reducing washer can be securely held between the sealing surface of the funnel and funnel base (see Figure 2 in ASTM D 5452).

c. Flow reducing washer: A 47-mm diameter flow reducer washer with an effective filtration area of 4.8 cm^2 (Millipore Corporation Part No. XX10 04710).

d. Vacuum flask: A minimum of 4 liters.

e. Vacuum system: That develops in excess of 67.5 kPa (20 inches of mercury) vacuum.

f. Oven: Of the static type (without fan assisted circulation) controlling to 90° ± 5° C (194° ± 9° F).

g. Forceps: Flat-bladed with unserrated nonpointed tips.

h. Dispenser, rinsing solvent (petroleum ether): Containing a 0.45 μm membrane filter in the delivery line. If solvent has been pre-filtered using a 0.45 μm filter then an inline filter is not required.

i. Glass petri dish: Approximately 125 mm in diameter with removable cover.

j. Analytical balance: Single or double pan, the precision standard deviation of which must be 0.07 mg or better.

B.4 PREPARATION

B.4.1 <u>Preparation of apparatus and sample containers</u>. All components of the filtration apparatus (except the vacuum flask), sample containers and caps must be cleaned as described in paragraph 9 of ASTM D 5452. All metal parts of the filtration apparatus are to be electrically bonded and grounded, including the fuel sample container. See ASTM D 5452 for other safety precautions.

B.5 SAMPLING

B.5.1 <u>Sampling</u>. Obtain a representative 3.79 L (1 gallon) sample as directed in paragraph 8 of ASTM D 5452. When sampling from a flowing stream is not possible, an all level sample or an average sample, in accordance with ASTM D 4057 and/or ASTM D 4177 shall be permitted. The 3.79 L (1 gallon) sample container shall be an interior epoxy-coated metal can, a brown glass bottle, or a clear glass bottle protected by suitable means from exposure to light.

B.6 PROCEDURE

B.6.1 <u>Test procedure</u>.

a. Using forceps, place a new membrane (test) filter in a clean petri dish. Place the petri dish with the lid slightly ajar in a 90 ± 5°C oven for 30 minutes. Remove the petri dish from the oven and place it near the balance with the lid slightly ajar, but still protecting the filter from airborne contamination, for 30 minutes.

b. Weigh the test filter. A filter weighing in excess of 90 mg will not be used for time filtration testing.

c. Place a flow reducing washer (required only for time filtration testing) on top of funnel base then place a test filter on top of the reducing washer and secure the funnel to the funnel base.

d. Immediately prior to filtering the fuel, shake the sample to obtain a homogeneous mix and assure that fuel temperature does not exceed 30°C (86°F). Clean the exterior or top portion of the sample container to ensure that no contaminants are introduced. Any free water present in the fuel sample will invalidate the filtration time results by giving an excessive filtration time rating.

e. With the vacuum off, pour approximately 200 mL of fuel into the funnel.

f. Turn vacuum on and record starting time. Continue filtration of the 3.79 liters (1 gallon) sample, periodically shaking the sample container to maintain a homogenous mix. Record the vacuum (kPa or inches of mercury) 1 minute after start and again immediately prior to completion of filtration. Throughout filtration, maintain a sufficient quantity of fuel in the funnel so that the membrane filter is always covered.

g. Report the filtration time in minutes expressed to the nearest whole number. If filtration of the 3.79 liters (1 gallon) is not completed within 30 minutes, the test will be stopped and the volume of the fuel filtered will be measured. In these cases, report filtration time as ">30 minutes" and the total volume of fuel filtered.

h. Report the vacuum (kPa or inches of mercury) as determined from the average of the two readings taken in B.6.f.

i. After recording the filtration time, shut off the vacuum and rinse the sample container with approximately 100 mL of filtered petroleum ether and dispense into the filtration funnel. Turn vacuum on and filter the 100 mL rinse. Turn vacuum off and wash the inside of the funnel with approximately 50 mL of filtered petroleum ether. Turn vacuum on and filter. Repeat the funnel rinse with another 50 mL of petroleum ether but allow the rinse to soak the filter for approximately 30 seconds before turning the vacuum on to filter the rinse. With vacuum on, carefully remove the top funnel and rinse the periphery of the filter by directing a gentle stream of petroleum ether from the solvent dispenser from the edge of the filter toward the center, taking care not to wash contaminants off the filter. Maintain vacuum after final rinse for a few seconds to remove the excess petroleum ether from the filter.

j. Using forceps, carefully remove test filter (from the funnel base and flow reducing washer if present) and place in a clean petri dish. Dry in the oven at 90° ± 5°C (194° ± 9°F) for 30 minutes with the cover on the petri dish slightly ajar. Remove the petri dish from the oven and place it near the balance with the lid slightly ajar, but still protecting the filter from airborne contamination, for 30 minutes. Reweigh the filter.

k. Report the total solids content in mg/liter by using the following formula:

$$\frac{\text{Weight gain of filter in mg}}{3.785} = \text{mg/liter}$$

l. Should the sample exceed the 30-minute filtration time and a portion of the fuel is not filtered, the solids content in mg/liter will be figured as follows: Determine the volume of fuel filtered by subtracting the mL of fuel remaining from 3.785.

$$\frac{\text{Weight gain of filter in mg}}{\text{mL of fuel filtered} \times 0.001} = \text{mg/liter}$$

B.7 Test conditions for filtration time

a. The vacuum should exceed 67.5 kPa (20 inches of mercury) throughout the test. The differential pressure across the filter should exceed 67.5 kPa (20 inches of mercury).

b. The fuel temperature shall be between 18° and 30°C (64° and 86°F). If artificial heat (such as a hot water bath) is used to heat the sample, erroneously high filtration times may occur, but this approach is allowed.

B.8 NOTES

B.8.1 Filtration time. If it is desired to determine the filtration time and not the total solids content, perform the test by omitting steps B.6.1i, B.6.1j, B.6.1k, and B.6.1l.

B.8.2 Total solids. If it is desired to determine the total solids content and not the filtration time, use of the flow reducing washer may be omitted. It is also permissible, but not required, to use a control filter for a specific analysis or a series of analyses. When this is accomplished, the procedures specified in ASTM D 5452 apply.

MIL-DTL-83133F

CONCLUDING MATERIAL

Custodians: Preparing activity:
  Navy – AS   Air Force – 68
  Army – MR   (Project 9130-2007-001)
  Air Force – 68
  DLA – PS

Review activities:
  Army – AR, AV, AT
  Air Force – 11

  Note: The activities listed above were interested in this document as of the date of this document. Since organizations and responsibilities can change, you should verify the currency of the information using the ASSIST Online database at http://assist.daps.dla.mil.

EERC

Energy & Environmental Research Center

APPENDIX C

IDENTIFICATION AND CHARACTERIZATION OF BIOMASS SOURCES IN THE UNITED STATES

IDENTIFICATION AND CHARACTERIZATION OF BIOMASS SOURCES IN THE UNITED STATES

Final Technical Report

Prepared for:

Franklin H. Holcomb
U.S. Army Corps of Engineers
Engineer Research and Development Center

Prepared by:

Tera D. Buckley
Joshua R. Strege
Kerryanne M.B. Leroux
Wesley D. Peck

Energy & Environmental Research Center
University of North Dakota
15 North 23rd Street, Stop 9018
Grand Forks, ND 58202-9018

2009-EERC-09

September 2009

University of
North Dakota
Grand Forks

EERC DISCLAIMER

TABLE OF CONTENTS

TABLE OF CONTENTS (continued)

LIST OF FIGURES

LIST OF TABLES

ACRONYMS AND ABBREVIATIONS

AEO	Annual Energy Outlook
CHN	carbon, hydrogen, nitrogen
CHNOS	carbon, hydrogen, nitrogen, oxygen, sulfur
DOE	Department of Energy
EDS	energy-dispersive spectrometer
EERC	Energy & Environmental Research Center
EIA	Energy Information Administration
EPA	Environmental Protection Agency
FAPRI	Food and Agriculture Policy Research Institute
FIDO	Federal Interagency Databases Online
HHV	higher heating value
LLV	lower heating value
MSW	municipal solid waste
NASS	National Agriculture Statistics Service
NRCS	National Resources Conservation Service
NREL	National Renewable Energy Laboratory
NWRR	Northwestern Wheat and Range Region
ORECCL	Oak Ridge Energy Crop County-Level Database
ORNL	Oak Ridge National Laboratory
POLYSYS	Policy Analysis System
RFS	Renewable Fuel Standard
RPS	renewable portfolio standard
SCI	Soil Conditioning Index
USDA	U.S. Department of Agriculture
WDS	wavelength-dispersive spectrometer
WTE	waste to energy
XRF	x-ray fluorescence

IDENTIFICATION AND CHARACTERIZATION OF BIOMASS SOURCES IN THE UNITED STATES

EXECUTIVE SUMMARY

With funding from Metso Power and the U.S. Army Construction Engineering Research Laboratory, the Energy & Environmental Research Center (EERC) examined the current and future availability of biomass sources in the United States and provided data on the chemical and physical properties of those sources.

Three primary types of biomass are produced in the United States: agriculture, wood, and urban residuals. Agriculture sources include crops, crop and agriculture processing residues, animal waste and by-products, and dedicated energy crops. Wood resources encompass grown forest products and wood-processing residues. Urban residuals, also commonly referred to as municipal solid waste (MSW), includes construction and demolition debris, mixed paper, railroad ties, refuse-derived fuel, residential MSW, scrap tires, and yard waste. The availability of these biomass sources varies with population distribution, climate, and geography. Biomass resources were quantified on a county-level throughout the United States.

To meet the growing demand for biomass energy, more resources need to become available. The amount of energy currently produced from biomass is expected to double by 2030, while the energy consumption on a per capita basis is expected to decrease 0.05% a year. Growth in renewable electricity (excluding hydropower) represents 33% of the growth in electrical demand from 2007 to 2030. Government influences, particularly the federal Renewable Fuel Standard (RFS) and state renewable portfolio standards, are expected to continue to have a large impact on biomass demand. Agriculture production is expected to gradually increase as a result of projected steady domestic and international economic growth, anticipation of continued high crude oil prices, and increased demand for biofuels. Softwood timber harvest is projected to increase in high-productivity regions in the southeast and south-central parts of the United States, with other regions remaining relatively stable. Hardwood is expected to see stable increases in productivity. MSW generation is also expected to climb to over 500 million tons by 2030, from 413 million tons in 2006.

An extensive literature search was conducted to obtain biomass chemical analysis and physical characterization data. Characteristics varied significantly depending on species, geography, climate, and harvest time; therefore, it is imperative to evaluate the specific biomass feedstock to be used for a given application. Despite these variabilities, some general conclusions can be drawn:

- Chlorine appears to be lower for wood and hard processing residues.

- Wood contains slightly less nitrogen on average.

- Nearly half of the combustion ash of grasses and stalk residues are silica oxides; silica is much less prevalent in hard processing residues.

- Hard processing residues have higher levels of potassium than the other biomass types; however, most literature seems to agree that herbaceous plants such as grasses and straws will have significantly greater potassium content.

- Wood contains higher calcium levels on average than the other plant materials evaluated.

- Wood and grasses contain less total alkali than stalk or hard processing residues.

The energy content or heating value of various biomass types was also reported. In general, wood (untreated) and hard processing residues (shells, hulls, and pits) were observed to have a greater energy content than grass and stalk residues (straw, hay, and stover), averaging 8000 Btu/lb. Wood contains less ash on average than other biomass types, although the average moisture content may be slightly higher. Biomass heating values for biomass residues and wastes averaged about 8000 Btu/lb dry and 6500 Btu/lb assuming the average moisture content of 15%. The energy potential of biomass can range from 14,000 Btu/lb, found in scrap tires with nearly no moisture, to 2600 Btu/lb, typical of leaves and grass clippings containing up to 60% water.

The primary conclusion that can be drawn from this study is that there is no single ideal biomass source. While some sources may have ideal combustion and cofiring properties, such as wood, other sources are optimal feedstocks for fuel production, such as corn or soybeans. In addition, no type of biomass is uniformly available across the United States or even within individual states. The best source for a particular energy production scenario will depend on multiple factors that will need to be assessed on a case-by-case basis. These factors include local resource availability; resource costs; resource physical and chemical properties and intrinsic fuel values; plant size; feed ratio with coal (for cofiring scenarios); resource processing requirements (drying, shredding, pulverizing, separating); storage options; local geography and climate (which will impact biomass properties); and availability of process utilities for conditioning as-received resources. When specific biomass utilization applications are considered, it is imperative to verify the information on a local level and test the specific biomass source to be used. Each application will also require a thorough technoeconomic assessment and analysis of available feedstocks prior to a candidate biomass being selected for energy generation or product development.

IDENTIFICATION AND CHARACTERIZATION OF BIOMASS SOURCES IN THE UNITED STATES

INTRODUCTION

Biomass is a renewable fuel derived from organic matter contained in plants and animals. Renewable energy comprises 7% of the total energy consumption in the United States, as reflected in Figure 1. At 53% of the total renewable energy consumption (or 4.45% of the total energy output), biomass is the largest renewable energy resource. Wood and wood-derived fuels supply 60% of the biomass energy consumed, followed by biofuels at 28% and urban residuals at 12% (Energy Information Administration [EIA], 2009b).

According to the EIA Annual Energy Outlook (AEO) 2009 reference case (EIA, 2009a), energy production from biomass sources is projected to double to 8.85% by 2030.[1] This expected increase in biomass energy production is due in a large part to recently enacted policies and concerns over energy security, greenhouse gas emissions, volatile energy prices, and limited fossil fuel resources.
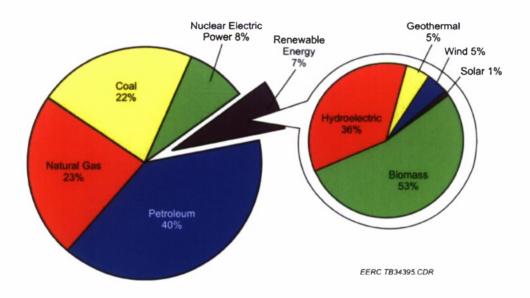

Figure 1. U.S. renewable energy as a share of total primary energy consumption (EIA, 2009b).

---

[1] The EIA AEO 2009 reference case assumed the federal subsidies for renewable generation were to expire as enacted. Their extension would have a large impact on the future of renewable energy generation.

This study seeks to provide an objective evaluation of biomass sources available in the United States. It has four primary sections:

1. Quantification of major biomass resources

2. Calculation of energy content for common biomass types

3. Estimation of projected biomass production yields

4. Presentation of chemical analysis and physical characterization data of biomass resources

Funding for this Energy & Environmental Research Center (EERC) effort was provided by Metso Power, with matching funding from the U.S. Army Construction Engineering Research Laboratory.

QUANTIFICATION OF MAJOR BIOMASS RESOURCES IN THE UNITED STATES

As shown in Figure 2, U.S. biomass resources were classified into three primary categories for this study: agricultural, wood, and urban residuals. The primary categories were further defined into subcategories. The following section presents methods used to obtain county-level data for these subcategories, as well as summary statistics and data limitations. Concentrations of biomass resources varied because of population distribution, climate, and geography.

Agricultural Crops

Agricultural crops are specific goods raised on land for sale to markets such as food, feed, or biofuels and include alfalfa, barley, beans, canola, corn, cotton, flax, forage, oats, peanuts, potatoes, rice, rye, safflower, sorghum, soybeans, sugarbeets, sunflowers, tobacco, wheat, and other vegetable and fruit crops.

National crop acreages and yields by county were obtained from the U.S. Department of Agriculture (USDA) National Agricultural Statistics Service (NASS) database (USDA NASS, 2009a), which is considered to be the definitive source for agriculture production statistics in the United States. Some data sets date back to 1970. NASS records yields on an as-reported basis without making moisture or quality adjustments. Production in counties with less than 1000 acres of a crop are generally combined with other counties in the same Crop Reporting District, and their totals are reported as "other counties" in order to protect the privacy of producers who are distinctive enough in their counties to be clearly identifiable. Summary maps of agriculture crop production by county are provided in Appendix A based on the 2007 Census of Agriculture (USDA, 2009b). Total crop production by county is summarized in Figure 3.
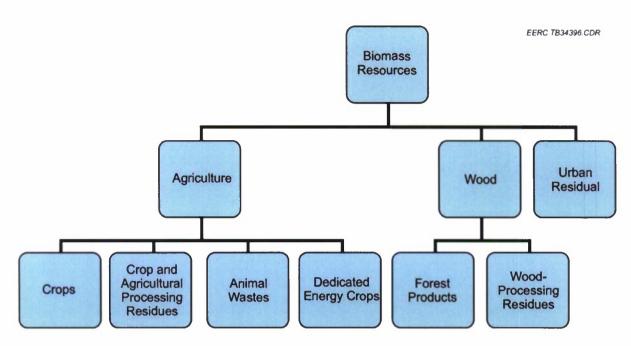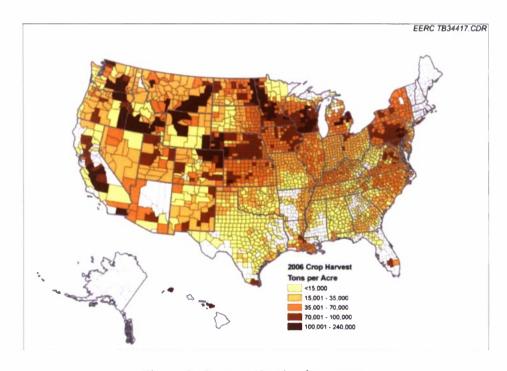
Figure 2. Major biomass resources in the United States.

Figure 3. Crop production by county.

Agricultural Crop and Processing Residues

Crop and agricultural processing residues include wastes from the field, such as leaves, straws, stems, and stalks, as well as processing by-products. Specific residues listed in this category include alfalfa stems; corncobs, stalks, and stover; distillers grains; hay; pits, shells, hulls, and pulp from beet and citrus; straw from barley, flax, mint, oat, rice, and wheat; sunflower stalks; and other vegetable-processing residues. Agricultural crop residues are summarized in Figure 4 by county.

Using nominal industry rules of thumb, common multipliers can be identified or derived for estimating crop and processing residue yields. Factors used are provided in Table 1. These data have been estimated from the Soil Conditioning Index (SCI) RUSLE2 database for all crops except dry edible peas, cigar tobacco, and a few bean varieties (SCI, 2009; National Agronomy Manual, 2002). The conversion factors given are multiplied by the yield of the grain crop to achieve the estimated residual yield. For example, about 1 ton of corn stover can be expected for every ton of corn grain harvested. Likewise, if a chosen acre produced 26 tons of sugar beets, about 1.3 tons of pulp could be expected following sugar processing. A number of crops do not have any usable residues because they have an established market, such as animal feed, or the residue is not harvestable (e.g., stubble or twigs). These include apples, peaches, hay, all types of forage, corn used for silage, and sorghum used for silage. Different residue factors for wheat and barley grown in the Northwestern Wheat and Range Region (NWRR), which includes parts of Washington, Oregon, and Idaho, were also noted.
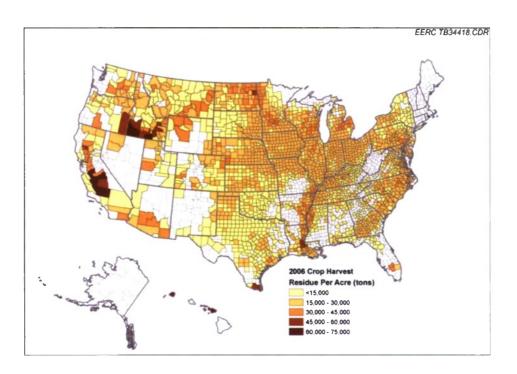

Figure 4. Agricultural crop residues by county.

Table 1. Factors for Yield Estimation of Various Agricultural Residues (SCI, 2009)

Crop Name	Crop Residue, lb/lb	Processing Residue, lb/lb	Comments
Apples	0.0	–	0.03[a]
Barley	1.5	–	
NWRR	1.0	–	1.0 for spring barley, 1.3 for winter barley
Beans, dry edible	1.0	–	
Beans, lima	0.2	–	
Beans, other dry edible	1.0	–	
Beans, pinto	1.0	–	
Canola	2.0	–	
Chickpeas (garbanzo)	2.2	–	
Corn (grain)	1.0	–	AH703[b]
Corn (silage)	0.0	–	0.01[a]
Cotton (American pima and upland)	4.5	–	AH703
Flaxseed	1.3	–	1.3,[c] 1.4-SCI
Forage	0.0	–	
Green Peas for Processing	0.2	–	
Hay	0.0	–	
Lentils	1.2	–	
Mustard	1.2	–	Average for spring and winter residues
Oats	2.0	–	AH703
Peaches	0.0	–	0.03[a]
Peanuts (for nuts)	1.3	–	
Peas, Austrian winter	1.0	–	
Potatoes	0.1	–	value for Irish
Rice	1.0[d]	0.2[c]	
Rye	1.3	–	1.0 for winter, 1.3 for spring, 1.5 for cereal
Safflower	1.5	–	
Snap Beans for Processing	0.4	–	Lower for hand-picked
Sorghum (grain)	1.0	–	AH703[c]
Sorghum (silage)	0.1	–	
Soybeans	1.5	–	AH703 for south
Sugar Beets	0.1	0.05[e]	
Sugarcane for Sugar	0.1	0.3[f]	
Sunflowers	2.2	N/A[g]	
Sweet Corn for Processing	0.3	–	
Sweet Potatoes	0.1	–	
Tobacco, air-cured dark	0.3	–	

Table 1. Factors for Yield Estimation of Various Agriculture Residues (continued)

Crop Name	Crop Residue, lb/lb	Processing Residue, lb/lb	Comments
Tobacco, air-cured light burley	0.1	–	
Tobacco, air-cured light southern	0.1	–	Value for light burley
Tobacco, fire-cured	0.3	–	Value for flue-cured
Tobacco, flue-cured	0.3	–	
Tomatoes for Processing	0.0	–	0.02[a]
Wheat, durum	1.3	–	AH703 for spring wheat
NWRR	1.4	–	
Wheat, other spring	1.3	–	AH703
NWRR	1.4	–	
Wheat, winter	1.7	–	AH703
NWRR	1.4	–	

a Value in parenthesis is reported in SCl RUSLE2 database, taken to be zero for all practical purposes.

b U.S. Department of the Interior, 2009 (noted as AH703).

c Smith et al., 2009

d Summers et al., 2009

e North Dakota sugar beet processor, 2008.

f Austin, 2009.

g Sunflowers used for oil will have processing residues, but the amount of residue generated in processing is unknown.

Animal Wastes

Manure

Animal wastes are manure generated by livestock including beef, dairy, horse, poultry, sheep, and swine. Although NASS does not collect animal waste data, accurate estimates of manure production can be made by multiplying livestock inventories from the Census of Agriculture by manure factors from the National Resources Conservation Service National Engineering Handbook (USDA NRCS, 2009e). An alternative method to estimating manure availability is to use county-level U.S. Department of Energy (DOE) National Renewable Energy Laboratory (NREL) data on methane production from manure management (Milbrandt, 2005).

The state of Minnesota was used as an example to test both methods. The 2005 county-level data from DOE NREL gives methane production rather than manure collection (Milbrandt, 2005). To estimate manure availability, it was assumed that every 100 tons of manure generates 26.7 tons of methane. This is based on the approximate stoichiometry of anaerobic digestion. County-level estimates of manure production in Minnesota were made by multiplying estimated animal weights from the 2007 Census of Agriculture data by appropriate manure production factors. When compared to the estimates made from methane production, it was found that the

estimates made from NASS data were almost 20 times higher than the estimates made from methane production data.

Because the data from NASS, the National Engineering Handbook, and DOE NREL are all considered reliable, the most likely reason for this discrepancy is that only 5% of the available manure in Minnesota is managed for methane production. The remainder is either used as fertilizer or is not collected, especially if it is produced by grazing animals. Neither source of manure is a good candidate for energy production. Fertilizer is too expensive to be used as fuel and is difficult to transport. Furthermore, the qualities that make good fertilizer (high levels of moisture and ash) make poor fuel. Manure from grazing animals is left where it falls, both because it provides nutrients back to the soil and because it is difficult to efficiently collect from the field. Only the manure that is currently collected for methane production could realistically be used for energy production. Figure 5 provides a map of methane produced annually by manure management.

Animal By-Products

Generally, animal fats are products derived from meat-processing facilities and are solid at room temperature. They include tallow from beef processing, lard and choice white grease from pork processing, and poultry fat from poultry processing. It is estimated that U.S. rendering companies produce about 7 billion tons of rendered fat a year, as shown in Table 2 (Eidman, 2007). Production statistics on a state and county level are not readily available and would require contacting approximately 300 rendering facilities serving North America.
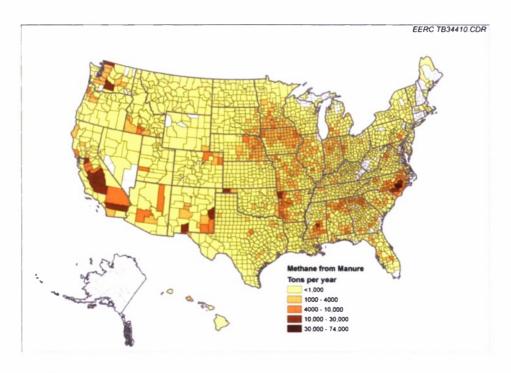

Figure 5. Methane emissions from manure management by county.

Table 2. U.S. Supply of Waste Oil and Animal Fat (Eidman, 2007)

Waste Oil and Animal Fat Type	million tons
Yellow Grease and Other Grease	1.3
Lard	0.5
Edible Tallow	0.9
Inedible Tallow	1.8
Poultry Fat	2.1
Total	6.8

Although there is a large supply of oils and fats in the United States, competing uses for these products keeps supplies tight and prices competitive. About 85% of waste animal fat processed by rendering companies is utilized as animal feed ingredients. Applications for rendered fats in the chemical, metallurgy, rubber, and oleochemical industries account for the second largest market, with over 3000 industrial uses identified. The manufacture of soaps and personal care products remains a major use for animal fats, especially tallow; however, use in biofuel production is increasing (Meeker and Hamilton, 2009). Utilization of rendered fats for biofuel production was estimated at 32.7–87.2 million pounds (3%–8% of total production) in early 2008 (National Renderers Association, 2008).

Dedicated Energy Crops

Dedicated energy crops are raised for the sole purpose of producing energy in the forms of electricity and/or heat and include short-rotation woody crops, like hybrid poplar and willow, and herbaceous crops, like switchgrass, reed canary grass, and miscanthus.

The standard reference for energy crop production potential by county is the Oak Ridge Energy Crop County-Level (ORECCL) Database. This database was prepared in 1996 and gives an estimated upper limit of energy crop production in each county of the United States. Figures 6 and 7 summarize switchgrass and total energy crop yields, respectively.

Figure 7 shows significantly lower energy crop yields in the western United States. This is not due to a lack of data but rather because the ORECCL authors determined that most of the western United States was not suitable for economical energy crop growth. All data are reported as the yield after a 2-year establishment period. If the yield in Year 3 is expected to be less than 2 dry tons/year/acre, the area is designated unsuitable. Some energy crops may still be grown in the western United States, but the sustainable yields will be much lower than in the eastern United States.

It should be noted that ORECCL is no longer publicly available, as an improved database is being developed to account for better measurements and revised economies from the last decade. The new Policy Analysis System (POLYSYS) model is currently being tested at the University of Tennessee Knoxville and should be available to the public before the end of 2009. This model will provide much more realistic estimates for production of various energy crops
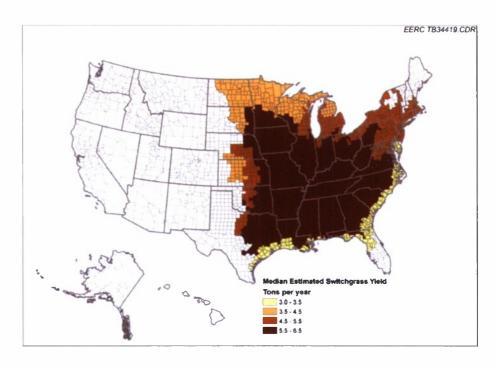
8

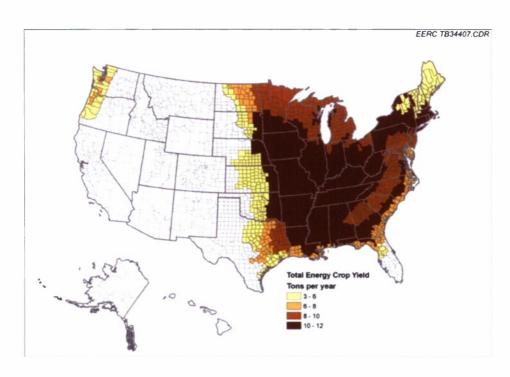Figure 6. Switchgrass crop yield by county.

Figure 7. Total energy crop yield by county.

than any effort the EERC could achieve at this time and will also provide estimates of the effects of crop prices, policies, and other variables on projected energy crop costs and availability. It should also be noted that Oak Ridge National Laboratory (ORNL) published a report presenting estimated switchgrass growing potential at a resolution of 400 m, which is significantly better than county-level resolution (Gunderson et al., 2008). The interested reader is strongly encouraged to examine both the ORNL report and the POLYSYS model when it becomes available.

Forest Products

Specific forest products include all wood grown, such as aspen timber, hardwood timber, softwood timber, brushland, and shrubland. Data on forest products were gleaned from the USDA Forest Service, which performs inventories; collects and analyzes data; and publishes detailed statistics on forest growth, both logging and timber harvesting, and primary wood products industry activities. A rigorous methodology is used to collect and analyze data, updating on a regular basis. The Forest Service statistics are recognized for their completeness and reliability.

Data for this report were generated using the Forest Inventory Database Online (FIDO 2.0) tool (USDA, 2009a). To ensure reliability of the generated data, a comparison was made to data generated for the state of North Dakota using the Forest Service data. The level of detail available from the Forest Service is such that the fate of individual trees of 2-inch-diameter or greater, including exact species, growth, disease, and harvest, can be tracked with time. These data become more manageable when used for statistical purposes such as estimating average hardwood forest cover by county or average yearly wood growth. While the EERC has assembled an incredibly vast data set including all available Forest Service data for multiple years, these data are not included in the report, but can be accessed online at http://fiatools.fs.fed.us/fiadb-downloads/datamart.html or www.ncrs2.fs.fcd.us/4801/FIADB/rpadb_dump/rpadb_dump.htm.

The maps presented in Figures 8–11 summarize the FIDO data and present annual cubic feet of wood produced by living trees per acre of county land (cu ft/acre/year), percent of county land covered by softwood forest, percent of county land covered by hardwood forest, and percent of county land covered by all forest types. Total forest coverage includes mixed forests, not the sum of softwood and hardwood forest coverage. Also, because forest coverage is calculated using statistical estimates based on sample plots, the estimated coverage is greater than 100% in some cases.

This report offers only the total forested land, rather than breaking down the results to show what portion of forested land includes timberland for each county. Many forests (especially in protected areas) may have high yields but cannot realistically be harvested or constitute trees that are not amenable to harvest. Any data older than 2000 will have a higher percentage of timberland, because some forested areas not suitable for timber were not included in measurements.
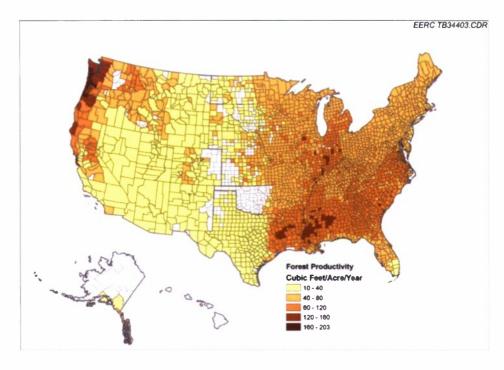
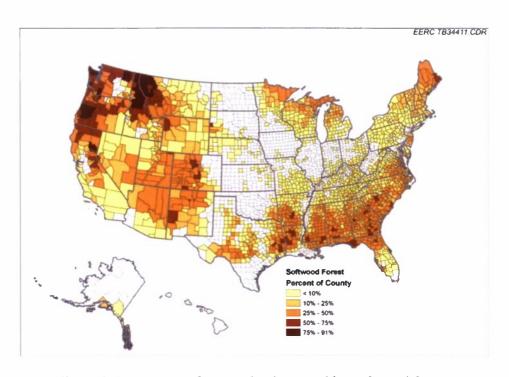Figure 8. Volume of wood produced by living trees.

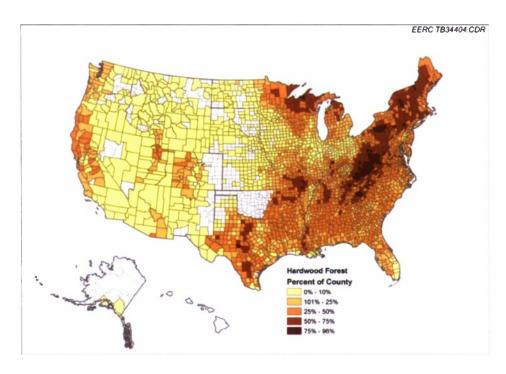Figure 9. Percentage of county land covered by softwood forest.

Figure 10. Percentage of county land covered by hardwood forest.
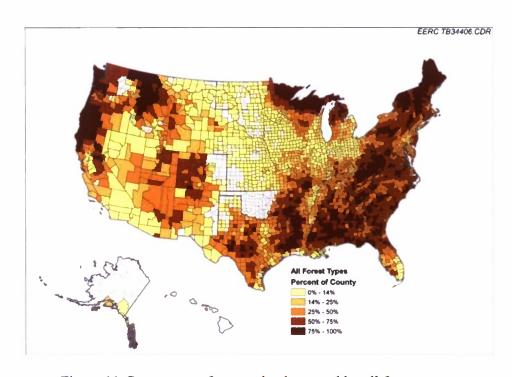

Figure 11. Percentage of county land covered by all forest types.

All forest data were derived on an acre-basis, as reported by the 2000 U.S. Census and does not include any water landcover. Values are reported as a percentage of county land rather than of forested area to avoid inflating the importance of large counties with small but productive forests. One consequence of this approach is that heavily forested, small counties give the false impression of high tree volume. For example, Douglas County, Nevada has high forest coverage per unit area, but the small size of the county means that the total available forest resource is actually quite small.

Although the sampling method used to collect data from tree plots is universal across every state, there are variations in the types of data collected and in the frequency with which data are collected. In many states, limited regional Forest Service personnel cannot complete all samples in a single year, so statewide estimates depend on the results collected over cycles of years. Some states either do not collect or do not report any data. For instance, New Mexico statewide data are available only for 1989 and 1999 through the FIDO interface. Although the raw data downloaded from the Forest Service includes individual plot measurements for later years, these data either cannot be used to represent the full state of New Mexico or are not available to FIDO. Hawaii is the one state in which no data appear to be publicly available for any sample year. As a final note, the standard methods used to sample and report data were changed significantly in the 1990s, so data older than 10 years cannot always be compared to more recent data.

Given these limitations, it was not possible to use consistent data for every state. Where possible, multiyear data with a cycle ending in 2007 were used. When these were not available, multiyear data from within the last 5 years were used. When these were not available, the most recent available single-year data were used. For New Mexico and Oklahoma, the most recent available data were from 1999 and 1993, respectively. For Wyoming, the most recent available data set is from 2000. These years may not reflect all of the changes made to the collection method during the 1990s.

Data used to estimate productivity in Figure 8 are based on weighted averages of forest growth. FIDO only reports classes of growth, with Class 1 representing the highest productivity (>225 cu ft/acre/year) and Class 7 being the lowest (0–19 cu ft/acre/year). Table 3 shows each

Table 3. FIDO Classes of Forestry Growth (USDA, 2009a)

Forest Productivity Class	Description (cu ft/acre/year)	Assumed Average Yield (cu ft/acre/year)
1	225+	250
2	165–224	195
3	120–164	143
4	85–119	103
5	50–84	68
6	20–49	35
7	0–19	10
Unknown Productivity Class		0

class and defined productivity range. The average of each range was used to convert these class categories into values that could estimate county-level average productivity. The average yield for each class was then multiplied by the acres of respective forest classification, summed for the forested area within each county, and divided by the number of total county acres. This gave the approximate yearly growth in cubic feet per acre of county land.

Wood-Processing Residues

Wood-processing residues result from processing timber to create high-value products and include logging residues, primary mill residues (bark, chunks, slabs, edgings, sawdust/shaving), and urban wood waste. Waste from paper and pulp manufacturing is also included in this category.

Reliable information on logging and primary wood product residues is either directly available or can be readily derived from Forest Service data. This leaves a very small amount (~2%) of unused primary mill material available for energy. However, not all types of wood residues or waste are available from the Forest Service database, other government agencies, or other organizations. These other types can be described as wood residues and wastes produced in the secondary wood products industry or further along in the production process.

Residues are also generated at secondary processing mills (e.g., millwork, furniture, flooring, containers, etc.) (ORNL, 2009). Mill residue data were downloaded by state and county from the Forest Service's Timber Product Output database (USDA, 2009b) and are presented in Figure 12. Because primary mill residues tend to be clean, uniform, concentrated, and low in moisture, most of these materials are already used for generating by-products or boiler fuel at the mills. The Forest Service estimates current usage by type as follows:
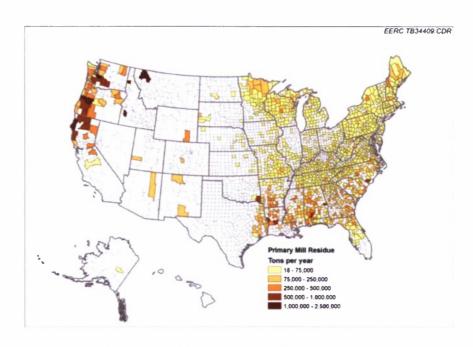

Figure 12. Primary mill residues by county.

14

- Bark – 80% used as fuel and 13% used in products
- Coarse residues – 85% used in products and 13% used as fuel
- Fine residues – 55% used as fuel and 42% used in products

Secondary mill residues include wood scraps and sawdust from woodworking shops—furniture factories, wood container and pallet mills, and wholesale lumberyards. Secondary mill residue data are not collected by the Forest Service or any other federal agency (ORNL, 2009) but were estimated in a 2005 NREL study (Milbrandt, 2005).

The following business categories were included in the Milbrandt (2005) analysis:

- Furniture factories: wood kitchen cabinet and countertop, nonupholstered wood household furniture, wood office furniture, custom architectural woodwork and millwork, and wood window and door manufacturers.

- Millwork: cut stock, resawing lumber and planing, and other millwork (including flooring).

- Truss manufacturing.

- Wood container and pallet manufacturing.

- Lumber, plywood, millwork, and wood panel wholesale companies.

Data on the number and size (number of employees) of businesses were gathered from the U.S. Census Bureau, 2006 County Business Patterns, as shown in Figure 13. According to the Wiltsee study (1998), pallet and lumber companies generate about 300 tons a year, and a small woodworking company typically generates between 5 and 20 tons a year of wood waste.

Urban Residuals

Urban residuals or municipal solid waste (MSW) include construction and demolition debris, mixed paper, railroad ties, refuse-derived fuel (RDF), residential MSW, scrap tires, and yard waste.

The 2008 State of Garbage in America survey, produced by BioCycle (Arsova et al., 2009), provides a picture of how MSW is handled throughout the United States. The survey collected 2006 data from individual states where available. Reported tonnages were adjusted to exclude non-MSW such as construction and demolition debris and industrial waste. The study concluded that of the over 413 million tons of MSW generated, 28.6% is recycled and composted, 6.9% is combusted in waste-to-energy plants, and 64.5% is landfilled. The per capita estimated generation is 1.38 tons/person/year. Figure 14 summarizes MSW tonnage for each state and the percentage of MSW recycled, the percentage used for waste-to-energy (WTE) production, and the percentage landfilled. Appendix B provides the actual MSW tonnage by state based on type of waste and the per capita MSW generation rate based on 2006 population.
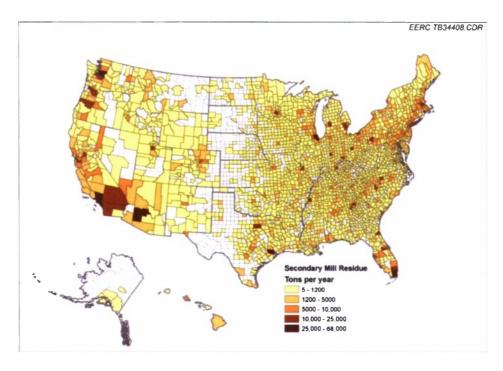
15

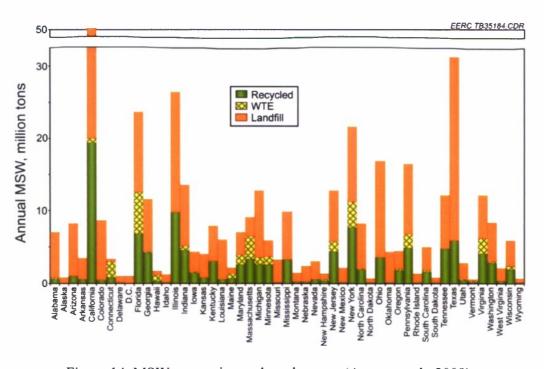Figure 13. Secondary mill residues by county.

Figure 14. MSW generation and use by state (Arsova et al., 2009).

PROJECTED BIOMASS PRODUCTION YIELDS

In determining projected biomass yields, one must heavily consider demand for renewable energy. The forecasted population size coupled with government influences and consumer behavior patterns creates a measureable demand for biomass resources.

Population growth is a key determinant of future energy demand, with fluctuations in energy use per capita resulting from variations in climate and economic factors. The U.S. population is expected to increase 24% from 2007 to 2030; over the same period, energy consumption will increase by only 11% (EIA, 2009a). The result is a decrease in energy consumption per capita at an annual rate of 0.05% per year. The decline in energy consumption is a result of increased interest in energy conservation induced by higher energy prices (EIA, 2009b).

The EIA Early Release Outlook for 2009 anticipates biomass consumption to more than double over the next two decades (2009a), from 2.5 quadrillion Btu of biomass power in 2007 to 5.52 quadrillion Btu by 2030. Rapid growth in the consumption of renewable fuels results mainly from the implementation of the U.S. Environmental Protection Agency's (EPA's) Renewable Fuel Standard (RFS) for transportation fuels and state renewable portfolio standard (RPS) programs for electricity generation. Electricity generation from renewable resources increased in response to minimum renewable generation requirements in more than one-half of the states. Thus growth in renewable electricity (excluding hydropower) represents 33% of the growth in electricity demand between 2007 and 2030. This portion may increase if existing production tax credits scheduled to expire in 2009 are extended, or if policies are implemented to limit greenhouse gas emissions (EIA, 2009a).

The EIA reference case assumed that federal subsidies for renewable generation will expire as enacted, but their extension would have a large impact on renewable generation. Because of the great uncertainties in any energy market projection, particularly in periods of high price volatility or rapid market transformation, the reference case results should not be given undue weight (EIA, 2009b).

Agriculture Production Outlook

The USDA "Agricultural Projections to 2017" report and the Food and Agriculture Policy Research Institute (FAPRI) "2008 U.S. and World Agriculture Outlook Database" provides the most up-to-date and reputable projected agricultural yields (USDA, 2008; FAPRI, 2009). Figures 15 and 16 provide examples of average projected agriculture crop and animal waste production, predicting a gradual increase in overall agriculture production to 2017. Tabular data from both sources is given in Appendix C. The gradual increase in agricultural production across nearly all categories is a result of projected steady domestic and international economic growth. Additionally, the projections reflect continued high crude oil prices and increased demand for biofuels, particularly in the United States and the European Union. It should be noted that the USDA (2008) and FAPRI (2009) sources were generated before the major downturn in the U.S. economy, which will likely influence the agricultural outlook.
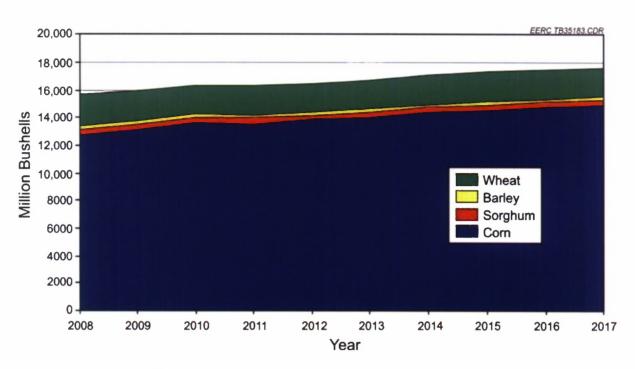
Figure 15. Average projected agriculture crop production to 2017 (USDA, 2008; FAPRI, 2009).
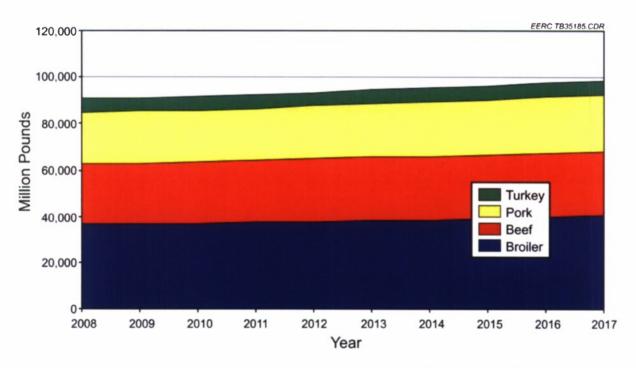

Figure 16. Average projected animal waste production to 2017 (USDA, 2008; FAPRI, 2009).

Although the results were similar, assumptions varied slightly in each source. The projections in both reports are based on macroeconomic conditions, policy, weather, and international developments. Changes in crop varieties, farming practices, prices, and other variables that can impact the area planted, yields, and total production in a given year were not explicitly factored into the analysis of either of these sources, but are implicitly reflected by the historic trends forming the basis for future projections. Both reports assumed no shocks due to abnormal weather, further outbreaks of plant or animal diseases, or other factors affecting global supply or demand. The USDA projections assumed the Farm Security and Rural Investment Act of 2002, the Energy Policy Act of 2005, and the Agricultural Reconciliation Act of 2005 would remain in effect through the projection period. The FAPRI baseline assumed provisions of the Farm Security and Rural Investment Act of 2002 and incorporated the conditions of the Energy Independence and Security Act (signed into law in December 2007).

Wood Production Outlook

Prospective trends in demands and supplies of timber, and the factors that affect these trends, include changes in the U.S. economy, salvage of British Columbia beetle-killed timber, and strength of the U.S. dollar. Other prospective trends that might alter the future timber situation include changes in U.S. timberland area, reductions in southern pine plantation establishment, impacts of climate change on forest productivity, increased restoration thinning on western public lands, and the impact of programs to increase carbon sequestration through afforestation. Data obtained from the USDA Forest Service report "The 2005 RPA Timber Assessment Update" (Haynes et al., 2007) is an update to the "Analysis of the Timber Situation in the United States" report completed in 2003, which reflects these trends.

As shown in Figures 14 and 15, the USDA Forest Service projected increases in softwood and hardwood harvests from forestland in the contiguous states, by region, through 2050. The 2005 update base projection envisions a 38% expansion in total U.S. forest product consumption to 27 billion cubic feet per year by 2020. Softwood timber harvest is projected to increase further in high-productivity regions in the southeast and south-central parts of the United States to meet growing demand in pulpwood; however, other regions will remain relatively stable. Hardwood timber is expected to see stable increases in productivity to 2050 in most regions, again as a result of pulpwood demand. Tabular data for Figures 17 and 18 are presented in Appendix D.

Despite the overall increase expected in timber production, it will not be sufficient to solely meet the demands of the emerging biomass industry. An article in *Biomass Magazine* (Bevill, 2009) by RISI, Inc., titled "The Emerging Biomass Industry: Impact on Woodfiber Markets" examined the availability of woodfiber supply in comparison to the accelerating demands for advanced biofuel production as mandated by the RFS and RPS. It was determined that use of wastewood (including logging residue, sawmill residue, urban waste wood, and short-cycle energy crops such as poplar trees) could contribute up to one-third of the projected demand needed to meet RFS and RPS mandates, doubling overall woodfiber demand by 2023. Thus the current supply of U.S. woodfiber is capable of supporting both the forest products industry and the biomass industry in the short term; however, that supply will be severely strained in the long-term. The combined demand of biomass and forest products would require additional growing
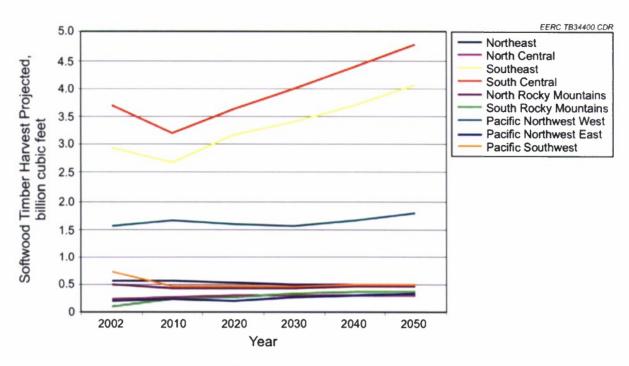
Figure 17. Forest Service softwood timber harvest projections by region 2002–2050 (Haynes et al., 2007).
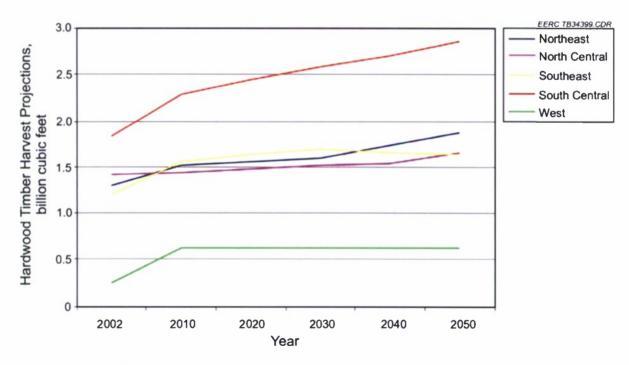

Figure 18. Forest Service hardwood timber harvest projections by region 2002–2050 (Haynes et al., 2007).

stock removals from U.S. forests, putting the nation's forests at risk for depletion. Possible solutions to meet the growing demand include:

1. A massive shift from traditional forest products production.

2. Changes in RFS and RPS mandates.

3. Policy mandates met by greater use of other forms of nonwood biomass, such as dedicated energy crops, and other types of renewable energy, including solar and wind power.

Urban Residues Outlook

Urban residue (or MSW) generation can be directly attributed to population size. MSW generation per capita estimated by state (Arsova et al., 2009) was combined with U.S. population projections by state (U.S. Census Bureau, 2009) to calculate increases in generation of urban residues. Figure 19 depicts national results, estimating over 500 million tons of MSW generated annually, or an increase of 25% from 2006 levels. Current consumption patterns and recycling programs were assumed to remain unchanged. Individual state statistics are available in Appendix E.

Government Influence on Biomass Demand

The increase in energy demand creates a need for biomass energy, but federal and state government initiatives, incentives, and mandates create the immediate demand.
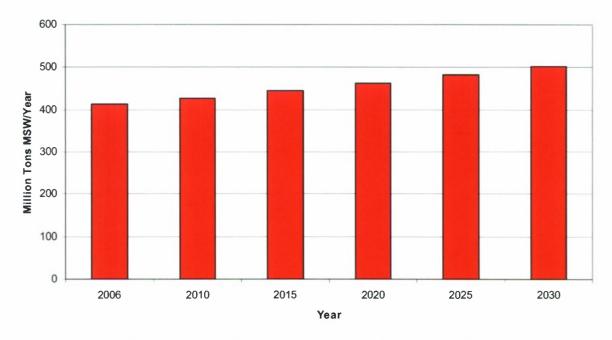

Figure 19. U.S. projected MSW generation to 2030 (U.S. Census Bureau, 2009; Arsova et al., 2009).

21

Perhaps the most influential federal law impacting biomass demand is EPA's RFS, requiring the blending of renewable fuels in transportation fuel. As a result, fuel suppliers blended 9.0 billion gallons of renewable fuel into gasoline in 2008, with annual increases to 36 billion gallons in 2022. The expanded RFS also specifically mandates the use of advanced biofuels, defined as fuels produced from noncorn feedstocks with 50% lower lifecycle greenhouse gas emissions than petroleum fuel, starting in 2009. The RFS creates a guaranteed advanced biofuels market and is expected to continue stimulating biomass growth and consumption.

Tax incentives also provide demand for biomass, such as the $1.00/gallon production tax credit for biodiesel and renewable diesel produced solely from biomass. Diesel fuel created by coprocessing biomass with other feedstocks (e.g., petroleum) is eligible for the $0.50 per gallon tax credit for alternative fuels. These federal tax credits were scheduled to expire on December 31, 2008, but were extended for 1 year through December 31, 2009. The long-term continuation of this tax credit is uncertain.

The passing of the Food, Conservation, and Energy Act of 2008 (H.R. 6124), ("The Farm Bill") assists in the development of agricultural biomass resources. Several grant and loan programs are anticipated, such as the Biomass Crop Assistance Program, which supports sustainably-grown energy crops. These programs will be administered by the USDA and will also impact biomass demand.

In addition to federal programs, 29 states and the District of Columbia (see Figure 20) have implemented regulatory policies (varying by state) requiring the increased production of renewable energy. Many states offer end users tax incentives, in addition to federal incentives, to encourage the use of biomass. To further economic development and the use of state biomass resources, some states also offer grants, or loans to companies willing to locate biomass-based companies within their state.

BIOMASS CHEMICAL ANALYSIS AND PHYSICAL CHARACTERIZATION

An extensive literature search was conducted to obtain biomass chemical analysis and physical characterization data. Major sources included data generated through past EERC biomass research efforts and the U.S. DOE Energy Efficiency and Renewable Energy Biomass Feedstock Composition Database. International biomass composition databases such as the Phyllis Biomass Composition Database; IEA BioBank; and the University of Technology, Vienna, BIOBID database were not used because they were believed to contain mostly data from biomass sources outside the United States. It was discovered that a limited amount of original biomass characterization exists in published literature, oftentimes citing other work without evaluating specific biomass sources. Therefore, differing sample collection, handling, and preparation techniques and scientific methodologies were used to generate the data procured for this study, and values varied widely across regions and states. Because of these variations, it is imperative to evaluate the specific biomass feedstock to be used for a given application.
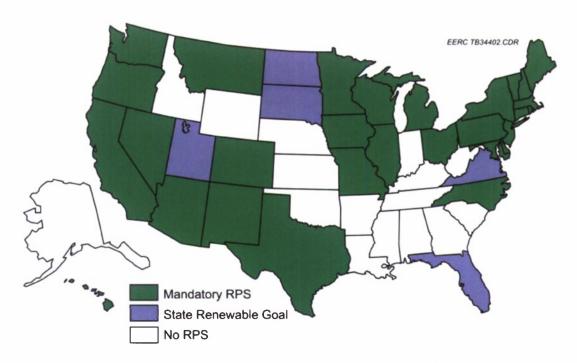
EERC TB34402.CDR

Mandatory RPS
State Renewable Goal
No RPS

Figure 20. States having renewable performance standards (Dick, 2009).

Only samples that are clearly untreated wood, grass, stalk residue (straw, hay, and stover), or hard processing residue (shells, hulls, and pits) are presented in this section. To account for differing collection methods and allow standard comparison, "as-determined" or air-dry moisture content was assumed to represent total moisture, leaving other results (volatiles, ash, Btu/lb, etc.) unadjusted. The correction does not make a great impact as air-dry losses were generally low (<1%). References for external data are noted in Appendix F. Definitions and methods of characterization analyses for the datasets are presented in Appendix G.

The energy content or heating value of wood and hard processing residues was observed to be greater than grass and stalk residues on average. Figure 21 provides a summary of the biomass energy data, displayed as frequency distributions of incremental analytical results. For instance, nearly 45% of the analytical data procured for grasses had energy densities 7000–7500 Btu/lb. The average energy of stalk residue is about 7000 Btu/lb, as well. Wood and hard processing residues tend to be >8000 Btu/lb.

Summaries of proximate, ultimate, and ash oxide data are presented in Figures 22–25 and Table 4 as frequency distributions of analytical results with values given in logarithmic increments. For example, the first column of each graph shows the number of samples found with a given property fraction of <0.1%, while the final column shows the number of samples with content >46%.

23

Figure 21. Summary of biomass heating values (Btu/lb).
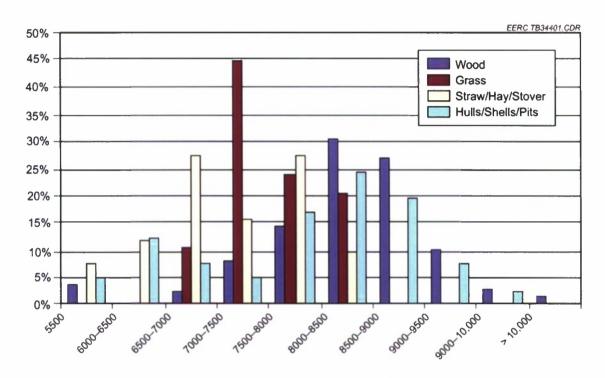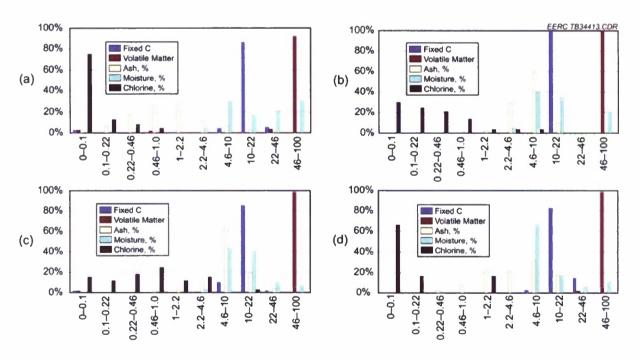

Figure 22. Summaries of proximate analyses: a) wood, b) grasses, c) straw/hay/stover, and d) hulls/shells/pits.
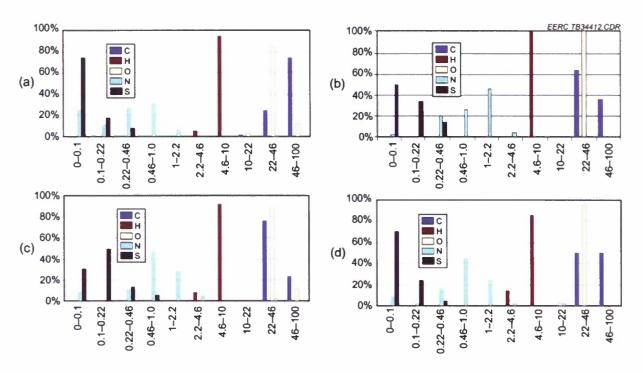
24

Figure 23. Summaries of ultimate analyses: a) wood, b) grasses, c) straw/hay/stover, and
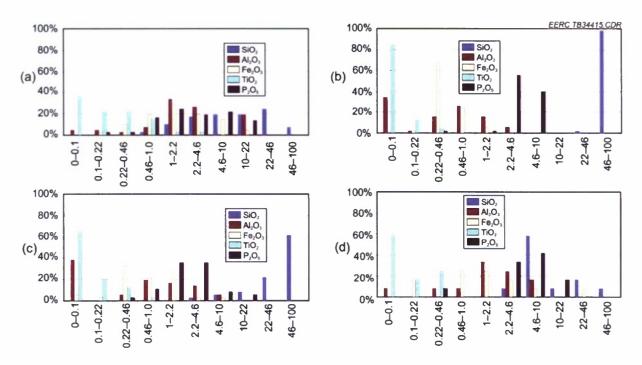d) hulls/shells/pits.

Figure 24. Summaries of major element ash oxide composition (% in ash): a) wood, b) grasses,
c) straw/hay/stover, and d) hulls/shells/pits.
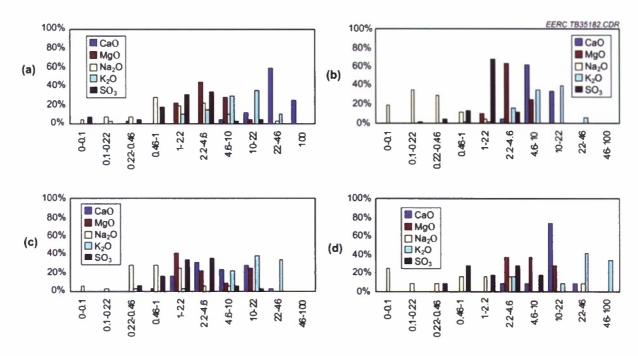
Figure 25. Summaries of major element ash oxide composition (% in ash), continued: a) wood, b) grasses, c) straw/hay/stover, and d) hulls/shells/pits.

Table 4. Estimated Average Elemental Oxide Values (Ash Basis)

	Wood	Grass	Straw/Hay/Stover	Hulls/Shells/Pits
SiO_2	13–24	65–70	43–58	10–26
Al_2O_3	2.6–5.6	0.5–1.0	0.6–1.8	1.9–3.6
Fe_2O_3	1.9–3.7	0.4–0.6	0.6–1.3	1.5–7.7
TiO_2	0.2–0.5	0–0.1	0.1–0.2	0.1–0.2
P_2O_5	3–5	4–5	2–4	5–8
CaO	30–40	8–10	6–10	11–15
MgO	4–6	3–4	3–7	7–9
Na_2O	1.2–3.6	0.2–0.4	0.6–1.9	1.1–6.1
K_2O	8–13	9–13	14–20	28–41
SO_3	1.5–3.0	1.3–1.7	1.8–3.4	1.8–3.0

Figure 22 shows that wood contains less ash on average than other biomass types, although the average moisture content may be slightly higher. Lower ash levels cause less abrasion or agglomeration during combustion. Fixed carbon and volatile matter are similar for the biomass types shown. Chlorine appears to be lower for wood and hard processing residues, with a majority of samples containing less than 0.1%. It can also vary widely in absolute quantity because of its higher solubility, e.g., levels in grasses and stalk range 0–10%. Chlorine is notorious for causing boiler ash deposition and corrosion.

Figure 23 shows the biomass types shown to be similar in ultimate composition. Hard processing residues contain slightly more carbon than stalks or grasses, and wood contains more carbon still. This is to be expected, as it coincides with the higher energy potential from

26

combustion of hard processing residues and wood. Wood also contains slightly less nitrogen on average.

A large majority of the grasses and stalk residue ash characterization data collected contains more than 46% silica (SiO_2), as seen in Figure 24, and more, apparently, in the averaged values shown in Table 4. This is likely the result of silica-based phytoliths in the stalk material of plants. Phytoliths are hardened mineral deposits that are incorporated into the cell walls of plants to add structure and support, and as such, they are common in the stalks of grassy plants. Silica is much less prevalent in hard processing residues, with well more than half of the data collected containing less than 10% silica. Because seeds do not provide support to the plant, they incorporate less phytolithic material. The significant presence of phosphorus in biomass combustion ash (~5% P_2O_5 average) without potential contaminants (e.g., mercury), generates an inert waste and a suitable fertilizer.

Figure 25 shows that hard processing residues have higher levels of potassium than the other biomass types. Potassium is an important nutrient for plants. The large EERC switchgrass data set may have affected potassium averages for grass data, showing similar levels as wood. Most literature seems to agree that herbaceous plants such as grasses and straws will have higher levels of potassium, >20% K_2O in combustion ash. The figures also show that wood contains higher calcium levels on average than the other plant materials shown, as it is more common to find calcium-based phytoliths in wood. Another interesting observation is the relative consistency of magnesium in all biomass types shown, with an average ~5% MgO in combustion ash. Magnesium is the chelated metal in chlorophyll that plants use for photosynthesis. As a result, there is little variance in the magnesium levels.

Many factors can interact with feedstock characteristics, affecting the suitability of biomass as a resource for a given application. For example, wood and grasses contain less total alkali (sodium-Na_2O and potassium-K_2O) than stalk or hard processing residues. High alkali concentrations in feedstock ash can cause slagging or deposits on combustion heat-transfer surfaces. Potassium specifically interacts with silica and alumina material, lowering the ash melting temperature and causing agglomeration issues. Table 4 provides this "slag potential," suggesting wood to be more amenable to combustion than other biomass types.

In addition, transportation costs will likely be the determinant of acceptable moisture or energy content for a given biomass application. A strong inverse relationship exists between moisture content and heating value, shown in Figure 26 for selected biomass samples, suggesting low-moisture feedstocks to be preferable. However, if the radius of procurement for a dry biomass resource is significantly greater than the radius of a wetter feedstock, then the wet biomass may be preferable over a dry biomass because of lower transportation costs per Btu. It is also possible to dry a wet feedstock through process heat recovery. Therefore, all factors should be evaluated when a biomass feedstock is chosen.
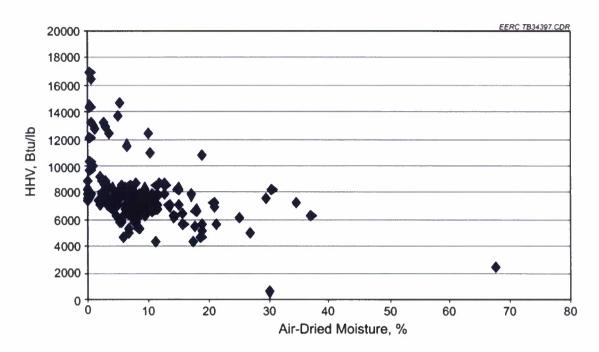
Figure 26. Energy versus moisture for selected biomass samples (HHV = higher heating value).

VIABILITY OF BIOMASS

Geographic and seasonal factors can significantly impact biomass growth. These factors also affect the elemental uptake of plants, which varies between plant species. Thus the plant environment will affect the inorganic content of biomass. This variability is of particular interest for elements that give rise to slagging, fouling, and particulate emissions when the biomass is used as an energy source in combustion systems. However, the extent of the impact of geographic and seasonal factors depends largely on the biomass type.

Studies have been performed on the variability of short rotation woody feedstocks (such as hybrid poplar or willow) and have found minimal compositional variation due to clonal, geographical, and environmental factors, indicating that they are a consistent and stable feedstock for biofuels production (Davis et al., 1995). Compositional variability has also been assessed for herbaceous energy crops. In this case, large differences in composition were found between stems and leaves, with leaves containing much higher concentrations of nonstructural components. The geographic location of where the plants were grown was found to affect the composition even more than differences between varieties (Johnson et al., 1995).

An in-depth study was conducted by the EERC to evaluate the geographic and climatic factors influencing the elemental composition of switchgrass. Factors evaluated included temperature, solar radiation, moisture supply, soil, and time of harvest. The analysis was performed on switchgrass samples from ten different farms in the south-central portion of Iowa (Zygarlicke et al., 2001).

Figure 27 shows variability of switchgrass from two farms in southern Iowa over the course of several months. Note that ash and alkalinity – both features that increase agglomeration tendency – are several times higher in early fall than in mid to late spring. There appears to be a correlation between extra moisture in the spring and the increase in aluminum oxide (Al_2O_3). However, potassium oxide (K_2O) was the lowest in the spring, which will tend to offset the high Al_2O_3 content. Since this trend is the result of seasonal variations, the extent of variation shown will likely also vary by environmental conditions specific to geographical location. (Zygarlicke et al., 2001).

CALCULATION OF ENERGY CONTENT PER ACRE

Biomass energy density or heating values average about 8000 Btu/lb without moisture and 6500 Btu/lb when accounting for the presence of water. Table 5 shows individual heating values on both a dry and wet basis for the major biomass sources defined in the previous sections. The heating values are multiplied by a chosen biomass yield to estimate the potential energy available per acre. Since biomass resources are typically not dried at their location, the heating values adjusted for moisture content were utilized. For example, the energy potential of a region growing hybrid poplar trees would be approximately 120 MMBtu per acre with a yield of 8 tons/acre and an energy density of 2600 Btu/lb on a wet basis.
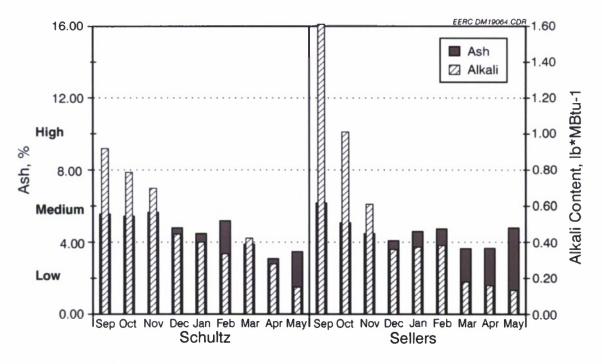

Figure 27. Ash and alkali content for unharvested switchgrass in southern Iowa (Zygarlicke et al., 2001).

Table 5. Typical Energy Content for Various Biomass Types

Biomass Source	Btu/lb, dry	Btu/lb, wet	Ref.*
Agricultural-Based	7700	6500	
Harvest Residuals	*7600*	*6600*	
Wheat Straw	7700	6800	1
Rice Straw	6500	6000	1
Flax Straw	8600	6600	2
Cornstalks (aka stover)	7800	7100	3
Processing Residuals	*8000*	*7300*	
Rice Hulls	6800	6100	1
Sugarcane Bagasse	8200	7300	1
Almond Shells/Hull	8200	7700	1
Olive Pits	9300	8700	1
Sugar Beet Pulp	7300	6600	3
Animal Wastes	*7300*	*4500*	
Poultry Litter	6000	4700	4
Feedlot Wastes	8500	4300	5
Forest Products	7900	5200	
Logging Residuals	*8600*	*4300*	
Cull Trees	8700	4300	6
Tops	8700	4300	6
Dead Wood	8400	4200	6
Small-Diameter Stock	8700	4300	6
Primary Wood-Processing Residuals	*7500*	*5700*	
Sawdust	8600	5800	1
Leaves and Grass Clippings	6500	2600	7
Bark	8800	7900	6, 8
Edgings	6800	6100	6
Slabs	6800	6100	6
Secondary Wood-Processing Residuals	*7700*	*5900*	
Sawdust	8600	5800	1
Edging	6800	6100	6
Urban Wastes	8600	7100	
Residential	*8700*	*7700*	
MSW	7500	6100	9
RDF	6700	6400	1
Mixed Paper	8900	8200	1
Yard Waste	7000	4300	1

Table 5. Typical Energy Content for Various Biomass Types (continued)

Biomass Source	Btu/lb, dry	Btu/lb, wet	Ref.*
Demolition Wood Waste	7900	7200	1
Serap Tires	14,000	14,000	6, 10
Urban and Landscape Residuals	*8500*	*6100*	
Chipped and Unchipped Wood	8500	6300	1
Construction and Demolition Waste	7900	7200	1
Pallets/Serap	8400	4200	6
Railroad Ties	9200	6800	11
Dedicated Energy Crops	8600	7400	
Grasses	*7900*	*7000*	
Switchgrass	7900	7000	1
Native Grasses	7900	7100	1
Trees	*8400*	*6900*	
Willow	8400	7500	1
Cottonwood	8700	5600	12
Hybrid Poplar	8200	7600	1
Others	*9500*	*8400*	
Alfalfa Stems	8000	7300	1
Specialty Crops**	11,000	9500	6

*References:
1. Miles et al., 1995.
2. The Prairie Agricultural Machinery Institute, 2009.
3. Agricultural Utilization Research Institute, 2009.
4. Reardon et al., 2009.
5. Combs, 2009.
6. Center for Energy and Environment, 2007.
7. California Energy Commission, 2008.
8. Ince, 2009.
9. Chang and Davila, 2008.
10. Kentucky Pollution Prevention Center, 2009.
11. Ellis, 2009.
12. FirewoodResource.com, 2009.
**Average of corn, soybeans, and canola.

DISCUSSION

This report aims to provide a comprehensive, up-to-date, quantitative assessment of the availability of various biomass resources, including material quantities as produced on site (e.g., energy crops, agricultural residues, annual forestry growth) and material generated as a by-product of human consumption (e.g., MSW, mill residues, methane from manure management). Data collection methods erred on the side of overreporting rather than underreporting. While the tactic of collecting all available data has led to the compilation of a fairly comprehensive data set, an unavoidable result is that most resources are counted more than once. For example, estimates of annual forestry growth include all wood grown in a year regardless of its purpose or

availability. Some of this wood will be harvested for timber, and its by-product will be mill residues, which are reported in a separate section of the report. Forestry harvest thus impacts mill residue availability. Similarly, energy crops can only be grown in the absence of forests or agricultural crops; therefore, a county cannot yield significant energy crops while maintaining its agricultural and forestry output. These examples demonstrate one of the limits of how these data can be used, and each section must be assessed individually.

The biomass resource assessment quantifies feedstock growth and production on a county-level where available. Although these data are believed to be the most comprehensive and up-to-date available, they are mostly based on estimates and may vary from actual values. Wherever possible, these estimates were made using well-documented standard formulas and techniques.

Many biomass sources are already used in other applications and may not be accessible or economical to use as an energy source. As an example, agricultural residues are generally difficult to harvest and are composted in the field to maintain soil quality. It is unlikely that the total agricultural residues presented can be economically harvested.

Also not reflected in the quantification of biomass sources are new crop species and higher yielding crops that may emerge as the country moves to reduce consumption of fossil fuels by increasing efficiency and use more renewable resources for energy. Dedicated biomass crops for energy, fuels, chemicals, and other bioproducts may develop with sufficient market and government incentives and improved agronomic practices. Waste streams may find some application as commercial products or fuel (as has already happened with fly ash and most food industry processing residues). In the ever-changing world of developing energy technologies, it is impossible to estimate what resources will be valuable for energy production until those resources are discovered. Therefore, continued monitoring of the energy industry is necessary to ensure that the data reported here remain up-to-date.

The chemical and physical analysis data also have limitations. The samples were collected and prepared using different methods, derived from different locations, and tested using different techniques. Analysis of many hundreds of biomass samples shows that biomass properties vary widely, even within the same species. Based on data sets from within the same laboratories or using the same methods, a valid conclusion can be drawn that biomass combustion properties will likely vary dramatically by species, location, and agricultural practices. This is especially true for resources such as MSW that have no well-defined composition.

CONCLUSIONS

The primary conclusion that can be drawn from this study is that there is no single ideal biomass source. While some sources may have ideal combustion and cofiring properties, such as wood, other sources are optimal feedstocks for fuel production, such as corn or soybeans. In addition, no type of biomass is uniformly available across the United States or even within individual states. The best source for a particular energy production scenario will depend on multiple factors that will need to be assessed on a case-by-case basis. These factors include local resource availability; resource costs; resource physical and chemical properties and intrinsic fuel

values; plant size; feed ratio with coal (for cofiring scenarios); resources processing requirements (drying, shredding, pulverizing, separating); storage options; local geography and climate (which will impact biomass properties); and availability of process utilities for conditioning as-received resources. When specific biomass utilization applications are considered, it is imperative to verify the information on a local level and test the specific biomass source to be used. Each application will also require a thorough technoeconomic assessment and analysis of available feedstocks prior to a candidate biomass being selected for energy generation or product development.

REFERENCES

Agricultural Utilization Research Institute (AURI). Agricultural Renewable Solid Fuels Data. AURI Fuels Initiative, http://forum.iburncorn.com/wiki/index.php/BTU_Values (accessed Jan 2009).

Arsova, L.; van Haaren, R.; Goldstein, N.; Kaufman, S.M.; Themelis, N.J. The State of Garbage in America. BioCycle **2008**, *49* (12), 22, www.jgpress.com/archives/_free/001782.html#more (accessed Feb 2009).

Austin, A. Sugarcane Bagasse Could Benefit Brazil Energy Matrix. *Biomass Magazine* **2009**, *Jan*, www.biomassmagazine.com/article.jsp?article_id=2299 (accessed Feb 2009).

Bevill, K. Forest Products Industry Studies Biomass Impact. *Biomass Magazine* **2008**, *Oct* www.biomassmagazine.com/article.jsp?article_id=2074&q=forest%20products%20industr y (accessed Feb 2009).

California Energy Commission. *An Assessment of Biomass Resources in California, 2007*; Draft Report, Contract No. 500-01-016, March 2008.

Center for Energy and Environment. BioPower Evaluation Tool. Minneapolis, MN, 2007.

Chang, N.B.; Davila, E. Municipal Solid Waste Characterizations and Management Strategies for the Lower Rio Grande Valley, Texas. *Waste Management* **2008**, *28*, 776–794.

Combs, S. *The Energy Report. Texas Comptroller of Public Accounts*; May 2008, www.window.state.tx.us/specialrpt/energy/pdf/96-1266EnergyReport.pdf (accessed Feb 2009).

Davis, M.; Johnson, D.; Deutch, S.; Agblevor, F.; Fennell, J.; Ashley, P. Variability in the Composition of Short Rotation Woody Feedstocks. In *Proceedings of the 2nd Biomass Conference of the Americas*; Portland, OR, 1995; pp 216–225.

Dick, R. Biomass Fueled Power Plants – An Overview. Presented at the Minnesota Society of Professional Engineers, 2009.

Eidman, V.R. Commercialization of First Generation Biofuels. Presented Aug 21, 2007.

Ellis, R.P. Biomass-Fueled Power Plants: An Overview. Utility Engineering Corporation, www.ue-corp.com/news/wp_biomass.pdf (accessed Jan 2009).

Energy Information Administration. *Annual Energy Outlook 2009: Early Release Overview*; Jan 2009, www.eia.doe.gov/oiaf/aco/pdf/earlyrelease.pdf (accessed Feb 2009a).

Energy Information Administration. *Annual Energy Review 2007; Renewable Energy Production and Consumption by Primary Energy Source*; www.eia.doe.gov/emeu/aer/renew.html (accessed March 2009b).

FirewoodResource.com. Tree Species for Firewood and Btu Chart. http://firewoodresource.com/species/index.html (accessed Jan 2009).

Food and Agriculture Policy Research Institute (FAPRI). 2008 U.S. and World Agriculture Outlook Database; www.fapri.iastate.edu/tools/outlook.aspx (accessed Feb 2009).

Gunderson, C.A.; Davis, E.B.; Jager, H.I., West, T.O.; Perlack, R.D.; Brandt, C.C.; Wullschleger, S.D.; Baskaran, L.M.; Wilkerson, E.G.; Downing, M.E. *Exploring Potential U.S. Switchgrass Production for Lignocellulosic Ethanol*; Report No. ORNL/TM-2007/183 prepared by Oak Ridge National Laboratory, Oak Ridge, TN, under Contract No. DE-AC05-00OR22725 for the U.S. Department of Energy, Aug 2008.

Haynes, R.W.; Adams, D.M.; Alig, R.J.; Ince, P.J.; Mills, J.R.; Zhou, X. *The 2005 RPA Timber Assessment Update*; PNW-GTR-699. U.S. Department of Agriculture, Forest Service, Pacific Northwest Research Station: Portland, OR, 2007; 212 p.

Ince, P.J. *How to Estimate Recoverable Heat Energy in Wood or Bark Fuels*. Forest Products Laboratory, Forest Service, U.S. Department of Agriculture, General Technical Report FPL 29, 1979, www.fpl.fs.fed.us/documnts/fplgtr/fplgtr29.pdf (accessed Jan 2009).

Johnson, D.; Ashley, P.; Deutch, S.; Davis, M.; Fennell, J. Compositional Variability in Herbaceous Energy Crops. In *Proceedings of the 2nd Biomass Conference of the Americas*; Portland, OR, 1995; pp 267–277.

Kentucky Pollution Prevention Center. Introducing Industrial Solid Waste Reduction. University of Louisville, www.deq.state.mi.us/documents/deq-css-rctap-tm_SolidWaste-att2.pdf (accessed Jan 2009).

Meeker, D.L.; Hamilton, C.R. An Overview of the Rendering Industry. http://nationalrenderers.org/assets/essential_rendering_overview.pdf (accessed Feb 2009).

Milbrandt, A. *A Geographic Perspective on the Current Biomass Resource Availability in the United States*; Final Technical Report NREL/TP-560-39181 Prepared for U.S. Department of Energy under Contract No. DE-AC36-99-GO10337; Dec 2005.
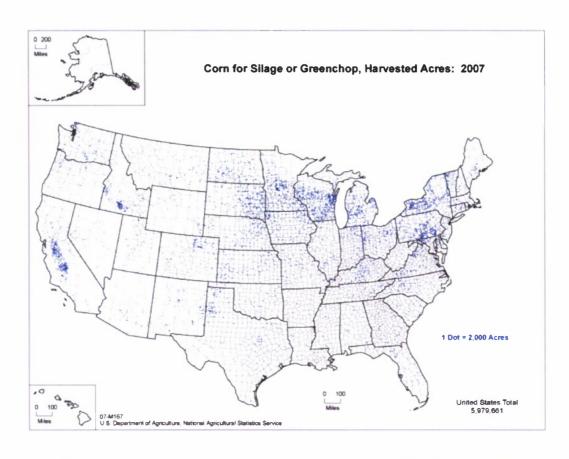
Miles, T.R.; Baxter, L.L.; Bryers, R.W.; Jenkins, B.M.; Oden, L.L. *Alkali Deposits Found in Biomass Power Plants, A Preliminary Investigation*; Summary Report Prepared for National Renewable Energy Laboratory, April 15, 1995.

National Agronomy Manual, 3rd Ed. 190-V-NAM, U.S. Department of Agriculture, National Resources Conservation Service: Washington, DC., Oct 2002.

National Renderers Association. http://nationalrenderers.org (accessed July 2008).

National Weather Service. JetStream – Online School for Weather, www.srh.weather.gov/srh/jetstream/global/climate_max.htm (accessed March 2009).

National Wilderness Institute. Public Land Ownership by State. 1995, www.nrcm.org/documents/publiclandownership.pdf (accessed March 2009).

North Dakota sugar beet processor. Personal Communication, Sept 2008.

Oak Ridge National Laboratory. *Biomass Energy Data Book, Appendix C – Assumptions, Ed. 1*; September 2006, ORNL/TM-2006/571, http://cta.ornl.gov/bedb/appendix_c.shtml (accessed Feb 2009).

Reardon, J.; Lilley, A.; Browne, K.; Beard, K.; Wimberly, J.; Avens, J. *Demonstration of a Small Modular BioPower System Using Poultry Litter*; Community Power Corporation, DOE SBIR Phase-I Final Report; Contract: DE-FG03-01ER83214, Feb 2001, www.osti.gov/bridge/servlets/purl/794292-6l279H/native/794292.pdf (accessed Jan 2009).

Smith, M.; Carlson, S.; Wiedenhoeft, M. *Weed Management in Flax Production, On-Farm Trials – 2005*; Iowa State University, University Extension, Feb 2006, www.valuechains.org/flax/weed%20management%20onfarm%202005.pdf (accessed Feb 2009).

Soil Conditioning Index. SCI Spreadsheet, version 25. sciver25.xls. ftp://ftp-fc.sc.egov.usda.gov/SQI/web/. (accessed March 2009).

Summers, M.D.; Hyde, P.R.; Jenkins, B.M. Yields and Property Variations for Rice Straw in California. University of California, www.brdisolutions.com/pdfs/bcota/abstracts/1/305.pdf (accessed Feb 2009).

The Prairie Agricultural Machinery Institute. Using Straw as a Farm Heating Fuel. ISSN 1188-4770, Group 2 (i), July 1995, www1.agric.gov.ab.ca/$department/deptdocs.nsf/all/eng3127/$file/719.pdf?OpenElement (accessed Jan 2009).

U.S. Census Bureau, Population Division. Interim State Population Projections, 2005, www.census.gov/population/www/projections/projectionsagesex.html (accessed Feb 2009).
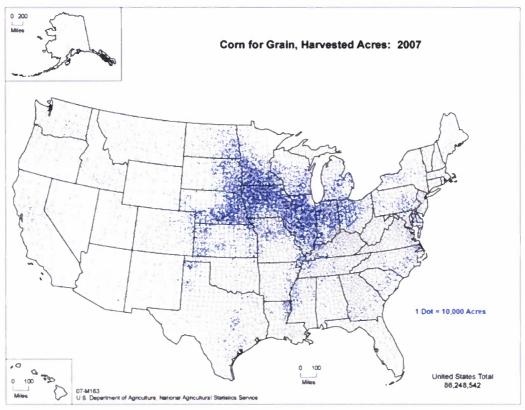
U.S. Department of the Interior, Office of Surface Mining. *Revised Universal Soil Loss Equation (RUSLE) – AH 703, Appendix D*; Parameter Values for Major Agricultural Crops and Tillage Operations, pp 349–361, www.techtransfer.osmre.gov/NTTMainSite/ Library/hbmanual/rusle/ah703apd.pdf (accessed March 2009).

U.S. Department of Agriculture National Agricultural Statistics Service. www.nass.usda.gov/QuickStats/indexbysubject.jsp?Pass_group=Crops+%26+Plants (accessed Jan 2009a).

U.S. Department of Agriculture National Agricultural Statistics Service. 2007 Census of Agriculture, www.agcensus.usda.gov/Publications/2007/Online_Highlights/Ag_Atlas_ Maps/index.asp (accessed March 2009b).

U.S. Department of Agriculture National Resources Conservation Service. National *Engineering Handbook, Part 651, Animal Waste Management, Chapter 4*; 210-VI, NEH-651, June 1999, www.wsi.nrcs.usda.gov/products/W2Q/AWM/handbk.html (accessed Jan 2009c).

U.S. Department of Agriculture. Forest Service Forest Inventory Data Online (FIDO) Tool. www.fia.fs.fed.us (accessed March 2009a).

U.S. Department of Agriculture. Timber Product Output Database. http://srsfia2.fs.fed.us/ php/tpo2/tpo.php (accessed Jan 2009b).

U.S. Department of Agriculture. *USDA Agricultural Projections to 2017, Long-Term Projections Report OCE-2008-1*; Feb 2008.

Wiltsee, G. *Urban Wood Waste Resource Assessment*; Appel Consultant, Inc. Valencia, CA, Nov 1998.

Zygarlicke, C.J.; McCollor, D.P.; Eylands, K.E.; Hetland, M.D.; Musich, M.A.; Crocker, C.R.; Dahl, J.; Laducer, S. *Impacts of Cofiring Biomass with Fossil Fuels*; Final Report (April 1, 1999 – March 31, 2001) for U.S. Department of Energy Contract No. DE-FC26-98FT40320; EERC Publication 2001-EERC-08-03; Energy & Environmental Research Center: Grand Forks, ND, Aug 2001.
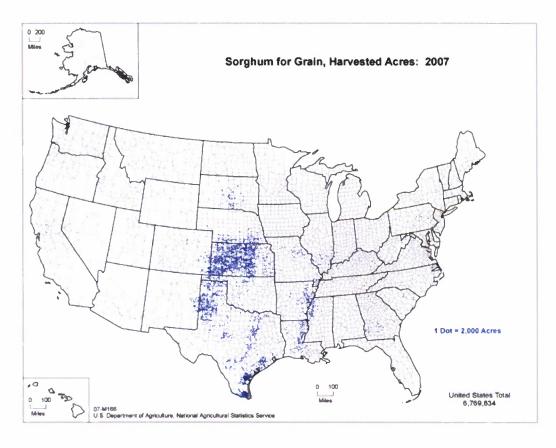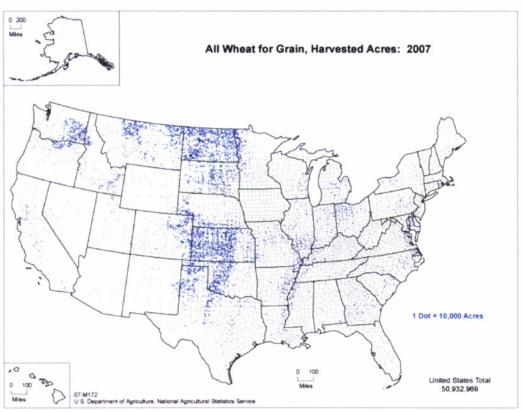
APPENDIX A
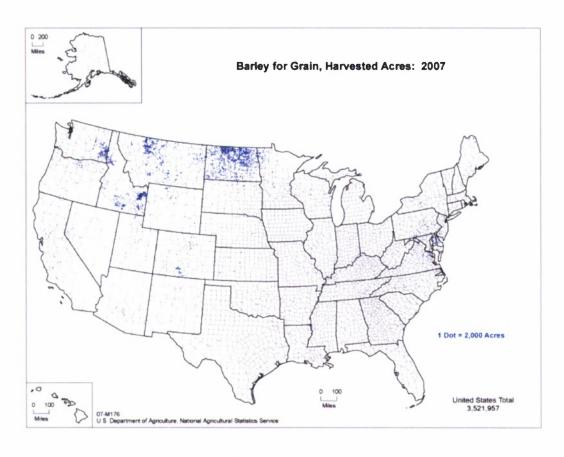
AGRICULTURE CROP YIELDS BY COUNTY – SUMMARY MAPS

Corn for Silage or Greenchop, Harvested Acres: 2007

1 Dot = 2,000 Acres

United States Total
5,979,661

07-M167
U.S. Department of Agriculture, National Agricultural Statistics Service

Corn for Grain, Harvested Acres: 2007

1 Dot = 10,000 Acres

United States Total
86,248,542

07-M163
U.S. Department of Agriculture, National Agricultural Statistics Service

A-1

Sorghum for Grain, Harvested Acres: 2007

1 Dot = 2,000 Acres

United States Total
6,769,634

07-M168
U.S. Department of Agriculture, National Agricultural Statistics Service

All Wheat for Grain, Harvested Acres: 2007

1 Dot = 10,000 Acres

United States Total
50,932,969

07-M172
U.S. Department of Agriculture, National Agricultural Statistics Service

A-2

Barley for Grain, Harvested Acres: 2007

1 Dot = 2,000 Acres

United States Total
3,521,957

07-M176
U.S. Department of Agriculture, National Agricultural Statistics Service

Oats for Grain, Harvested Acres: 2007

1 Dot = 1,000 Acres

United States Total
1,509,149

07-M178
U.S. Department of Agriculture, National Agricultural Statistics Service

A-3

Rice, Harvested Acres: 2007

0 200 Miles

1 Dot = 3,000 Acres

0 100 Miles

0 100 Miles

United States Total
2,758,792

07-M180
U.S. Department of Agriculture, National Agricultural Statistics Service

Sunflower Seed (Oil Varieties), Harvested Acres: 2007

0 200 Miles

1 Dot = 1,000 Acres

0 100 Miles

0 100 Miles

United States Total
1,710,057

07-M182
U.S. Department of Agriculture, National Agricultural Statistics Service

A-4

Sunflower Seed (Non-Oil Varieties), Harvested Acres: 2007

1 Dot = 1,000 Acres

United States Total
290,096

07-M183
U.S. Department of Agriculture, National Agricultural Statistics Service

Canola, Harvested Acres: 2007

1 Dot = 1,000 Acres

United States Total
1,149,682

07-M184
U.S. Department of Agriculture, National Agricultural Statistics Service

A-5

All Cotton, Harvested Acres: 2007

0 200 Miles

0 100 Miles

0 100 Miles

1 Dot = 5,000 Acres

United States Total
10,493,238

07-M185
U.S. Department of Agriculture, National Agricultural Statistics Service

Tobacco, Harvested Acres: 2007

0 200 Miles

0 100 Miles

0 100 Miles

1 Dot = 500 Acres

United States Total
359,846

07-M191
U.S. Department of Agriculture, National Agricultural Statistics Service

A-6

Soybeans for Beans, Harvested Acres: 2007

1 Dot = 10,000 Acres

United States Total
63,915,821

07-M193
U.S. Department of Agriculture, National Agricultural Statistics Service

**Dry Edible Beans, Excluding Limas,
Harvested Acres: 2007**

1 Dot = 2,000 Acres

United States Total
1,455,549

07-M197
U.S. Department of Agriculture, National Agricultural Statistics Service

A-7

Dry Edible Peas, Harvested Acres: 2007

1 Dot = 500 Acres

United States Total
848,874

0 200 Miles

0 100 Miles

07-M198
U.S. Department of Agriculture, National Agricultural Statistics Service

Potatoes, Excluding Sweet Potatoes,
Harvested Acres: 2007

1 Dot = 1,000 Acres

United States Total
1,131,963

0 200 Miles

0 100 Miles

07-M199
U.S. Department of Agriculture, National Agricultural Statistics Service

A-8

Sugarbeets for Sugar, Harvested Acres: 2007

1 Dot = 1,500 Acres

United States Total
1,253,817

07-M201
U.S. Department of Agriculture, National Agricultural Statistics Service

Sugarcane for Sugar, Harvested Acres: 2007

1 Dot = 2,000 Acres

United States Total
846,666

07-M202
U.S. Department of Agriculture, National Agricultural Statistics Service

A-9

Peanuts for Nuts, Harvested Acres: 2007

1 Dot = 1,000 Acres

United States Total
1,200,564

07-M203
U.S. Department of Agriculture, National Agricultural Statistics Service

Forage - Land Used for All Hay and All Haylage,
Grass Silage, and Greenchop, Harvested Acres: 2007

1 Dot = 10,000 Acres

United States Total
61,455,483

07-M204
U.S. Department of Agriculture, National Agricultural Statistics Service

A-10

Hay - All Hay Including Alfalfa, Other Tame,
Small Grain, and Wild, Harvested Acres: 2007

1 Dot = 10,000 Acres

United States Total
58,121,003

07-M206
U.S. Department of Agriculture, National Agricultural Statistics Service

Alfalfa Hay, Harvested Acres: 2007

1 Dot = 5,000 Acres

United States Total
20,244,497

07-M208
U.S. Department of Agriculture, National Agricultural Statistics Service

A-11

Ryegrass Seed, Harvested Acres: 2007

1 Dot = 300 Acres

United States Total
307,722

07-M216
U.S. Department of Agriculture, National Agricultural Statistics Service

Vegetables, Acres Harvested for Sale: 2007

1 Dot = 1,000 Acres

United States Total
4,682,588

07-M217
U.S. Department of Agriculture, National Agricultural Statistics Service

A-12

Total Acres of Land in Orchards: 2007

1 Dot = 1,000 Acres

United States Total
5,039,476

07-M233
U.S. Department of Agriculture, National Agricultural Statistics Service

A-13

EERC

Energy & Environmental Research Center

APPENDIX B

URBAN RESIDUALS GENERATION AND USE BY STATE

State	Population (2006)	Estimated MSW Generation, tons/yr	MSW Recycled, tons/yr	MSW to WTE,[1] tons/yr	MSW Landfilled, tons/yr	Per Capita Estimated Generation, tons/person/yr	Number of MSW Landfills	Number of WTE Plants	Glass, tons/yr	Paper, tons/yr	C&D,[2] tons/yr	Steel, tons/yr	Plastic, tons/yr	Aluminum, tons/yr	Other Metals, tons/yr	Wood, tons/yr	Tires, tons/yr	Organics, tons/yr	Total Other, tons/yr
Alabama	4,590,240	6,996,343	591,608	194,039	6,210,696	1.52	300	1											
Alaska	677,450	765,354	28,646	3,000	733,708	1.13	40	0											
Arizona	6,165,689	8,197,591	1,025,591	0	7,172,000	1.33	62	0											
Arkansas	2,809,111	3,468,842	532,689	35,464	2,900,689	1.23		3	2,646	148,851		72,264	33,876	76,293		55,878	34,508	79,068	5,622
California	36,249,872	49,926,000	19,409,000	591,000	29,926,000	1.38		3											
Colorado	4,766,248	8,690,005	481,598	0	8,208,407	1.82		0	2,557	308,209	4,227		1,076	733	7,457	12	32,022		14,339
Connecticut	3,495,753	3,360,933	830,264	2,158,292	372,377	0.96		6	32,182	460,056		11,959	13,067		75,507			233,029	236,754
Delaware	852,747	988,433	103,150	0	885,283	1.16		0	5,538	14,066		404	876	258					
District of Columbia	585,459	1,031,083	21,142	12,791	997,150	1.76		0											
Florida	18,057,508	23,631,947	6,775,329	5,796,339	11,060,279	1.31	50	11	164,965	1,780,993	2,668,057	312,730	69,425	44,247	2,066,703	1,525,048	607,000	1,440,745	
Georgia	9,342,080	11,549,889	n/a	81,535	7,195,075	1.24	56	1											
Hawaii	1,278,635	1,649,000	410,000	756,000	483,000	1.29		1											
Idaho	1,463,878	1,238,394	99,590	0	1,138,804	0.85	49	0											
Illinois	12,777,042	26,420,364	9,773,194	0	16,647,170	2.07	35	0											
Indiana	6,302,646	13,570,231	4,531,056	569,263	8,469,912	2.15	59	1											
Iowa	2,972,566	4,341,454	1,464,395	54,496	2,822,563	1.46	52	1											
Kansas	2,755,817	4,089,591	817,818	0	3,271,773	1.48	34	0	27,854	267,852		39,435	5,633	5,194	118,749	62,343	12,787	76,592	20,712
Kentucky	4,204,444	7,887,748	2,996,565	63,700	4,827,483	1.88	27	2											
Louisiana	4,243,288	6,051,158	500,000	0	5,551,158	1.43	12	0	4,688	231,326		1,437,226	4,617	12,295	102,751		942,361	258,752	2,546
Maine	1,314,910	2,178,339	695,580	701,811	780,948	1.66	22	4	52,172	286,055	24,830	81,853	15,646	2,185	92,219	94,518	30,678	30,371	9,883
Maryland	5,602,017	7,009,905	2,536,633	1,371,970	3,101,302	1.25	18	9	58,992	938,992	155,967	532,583	34,815		619,247	209,140	29,925	898,777	42,549
Massachusetts	6,434,389	9,160,000	3,410,000	3,100,000	2,650,000	1.42	50	7	420,000	1,240,000	3,060,000		60,000		920,000	6,000		734,000	30,000
Michigan	10,102,322	12,768,089	2,594,940	1,039,389	9,133,760	1.26	21	3	122,274	932,501		24,778	47,845	24,778	406,604	103,837	18,646	179,043	825,937
Minnesota	5,154,586	5,894,933	2,523,635	1,170,841	2,200,457	1.14	17	9											
Mississippi	2,899,112	3,194,368	145,000	0	3,049,368	1.10	21	0											
Missouri	5,837,639	9,939,008	3,183,864	23,300	6,731,844	1.70	21	7											
Montana	946,795	1,430,049	240,510	0	1,189,539	1.51	79	0	1,024	56,698	28,971	135,172	260	1,733				31,135	4,963
Nebraska	1,763,765	2,360,861	260,514	0	2,100,347	1.34	23	0	8,457	231,058		1,935	6,895	8,549					3,620
Nevada	2,492,427	3,007,000	619,000	0	2,388,000	1.21	9	0			304,657								
New Hampshire	1,311,821	1,269,774	406,693	206,873	656,208	0.97	12	2	9,251	50,870		24,909	2,086	823	1,232			30,387	287,135
New Jersey	8,666,075	12,756,058	4,400,000	1,397,094	6,958,964	1.47	33	5	300,521	1,364,156		593,276	75,160	79,474		159,433	37,327	1,723,466	
New Mexico	1,942,302	2,125,052	191,601	0	1,933,451	1.09	27	0	541	88,162		21,528	1,760	3,672			866	65,137	3,935
New York	19,281,988	21,686,509	7,694,160	3,491,700	10,500,649	1.12	40	10	333,181	2,603,911	6,319,191	1,381,104	205,107	60,680	28,382	70,179	39,124	856,642	522,679
North Carolina	8,869,442	8,205,475	1,877,277	107,837	6,220,361	0.93	14	1	51,883	305,615	40,352	7,516	19,373	5,808		60,399	187,273	570,994	69,041
North Dakota	637,460	660,552	83,404	0	577,148	1.04	42	0											
Ohio	11,463,513	16,885,677	3,530,328	0	13,355,349	1.47	38	0	40,112	1,029,617		409,862	43,739	124,485	4,834	193,783	106,772	1,311,497	265,627
Oklahoma	3,577,536	4,394,393	170,000	0	4,224,393	1.23	33	0			14,332								
Oregon	3,691,084	4,426,431	1,820,063	203,103	2,403,265	1.20	48	1	96,619	790,363		339,360	42,412	21,521	8,398	87,645	16,557	391,213	52,959
Pennsylvania	12,402,817	16,496,254	4,868,115	1,951,447	9,666,692	1.33	2	6	57,447	557,578	404,745	19,074	56,625	47,603	1,062,090	191,032	49,730	557,691	2,269,246
Rhode Island	1,061,641	1,351,454	166,962	1,995	1,182,497	1.27	18	1	14,980	57,847		5,696	4,909	1,027				76,242	403
South Carolina	4,330,108	4,974,679	1,510,409	224,506	3,239,764	1.15	15	1	11,090	822,026	1,093,459	4,415	20,379	6,606	190,220	44,127	62,765	604,699	348,779
South Dakota	788,467	861,576	83,476	0	778,100	1.09	34	0											
Tennessee	6,074,913	12,211,686	4,798,402	0	7,413,284	2.01	215	0	5,196	85,387	65,020	10,643	4,274		25,727	369,962	72,902	148,330	5,113
Texas	23,407,629	31,212,927	5,900,000	0	25,312,927	1.33	34	0											
Utah	2,579,535	2,864,492	438,873	123,912	2,301,707	1.11	4	1											
Vermont	620,778	644,226	229,953	47,286	366,987	1.04	60	1											
Virginia	7,640,249	12,210,991	4,140,457	2,135,407	5,935,127	1.60	16	5	39,278	922,024	123,998	1,048,885	30,159	14,951	704,127	296,165	70,210	860,133	237,769
Washington	6,374,910	8,313,340	2,725,310	325,398	5,262,632	1.30	19	3	90,992	570,802	2,295,278	3,217	38,262	623	135,976	289,612	23,528	1,000,040	
West Virginia	1,808,699	2,110,381	337,661	0	1,772,720	1.17	35	0	777	22,165			688		105				
Wisconsin	5,617,744	5,881,023	1,886,545	454,321	3,540,157	1.05	51	2	103,527	921,125	46,000	25,973	29,424	7,959	17,231		31,500	537,600	212,206
Wyoming	512,757	684,690	73,200	0	611,490	1.34		0											

[1] Waste to energy.

[2] Construction and demolition.

EERC
Energy & Environmental Research Center

APPENDIX C

AGRICULTURE PRODUCTION OUTLOOK

USDA Agricultural Projections to 2017 (USDA, 2009)

Item	Unit	2006	2007	2008	2009	2010	2011	2012	2013	2014	2015	2016	2017
Corn Yield	bushels/acre	149.1	153.0	155.3	157.3	159.3	161.3	163.3	165.3	167.3	169.3	171.3	173.3
Corn Production	million bushels	10535	13168	12515	13150	13635	13645	13650	13820	14070	14240	14405	14660
Sorghum Yield	bushels/acre	56.2	76.8	66.1	66.5	67.0	67.4	67.9	68.3	68.8	69.2	69.7	70.1
Sorghum Production	million bushels	278	515	395	365	340	345	340	340	335	340	340	345
Barley Yield	bushels/acre	61.1	60.4	65.0	65.6	66.2	66.8	67.4	68.0	68.6	69.2	69.3	70.4
Barley Production	million bushels	180	212	255	230	200	200	200	205	205	210	210	210
Oats Yield	bushels/acre	59.8	60.9	63.1	63.5	63.9	64.3	64.7	65.1	65.5	65.9	66.3	66.7
Oats Production	million bushels	94	92	100	100	100	105	105	105	105	105	105	105
Wheat Yield	bushels/acre	38.7	40.5	42.5	42.8	43.1	43.4	43.7	44.0	44.3	44.6	44.9	45.2
Wheat Production	million bushels	1812	2067	2350	2185	2140	2120	2100	2110	2110	2125	2120	2135
Rice Yield	lb/acre	6868	7247	7222	7284	7351	7419	7481	7543	7608	7666	7725	7784
Rice Production	million hundredweight	193.7	197.9	201.0	210.0	215.5	221.2	226.8	232.4	236.3	240.0	243.8	247.6
Upland Cotton Yield	lb/acre	806	845	860	875	885	895	905	915	925	935	945	955
Upland Cotton Production	million bales	20.82	18.05	17.40	18.80	19.50	20.10	20.60	20.80	21.20	21.60	22.10	22.50
Soybean Yield	bushels/acre	42.7	41.3	42.1	42.6	43.0	43.5	43.9	44.4	44.8	45.3	45.7	46.2
Soybean Production	thousand tons	3188	2594	2950	2920	2930	2935	2970	3000	3005	3035	3065	3095
Sugarbeet Yield	tons/acre	26.1	25.4	26.3	26.6	26.8	27.1	27.3	27.5	27.7	27.9	28.1	28.3
Sugarbeet Production	million short tons	34.1	31.6	31.6	30.7	30.7	30.4	30.3	30.6	30.9	31.2	31.5	31.8
Sugarcane Yield	tons/acre	33.0	34.7	34.2	34.3	34.5	34.6	34.7	34.8	34.9	35.0	35.1	35.2
Sugarcane Production	million short tons	28.0	28.9	28.6	28.1	25.9	26.0	26.1	26.2	26.3	26.4	26.5	26.6
Citrus Fruit	million lb	23490	20528	24960	25334	25841	26358	27017	27692	28246	28811	29243	29682
Noncitrus Fruit	million lb	40378	40436	40746	41058	41372	41689	42008	42330	42654	42981	43310	43642
Tree Nuts	million lb	3186	3628	3664	3745	3827	3911	3997	4085	4175	4267	4361	4457
Fresh Market Vegetables	million lb	42738	43000	44052	44555	45063	45578	46098	46624	47157	47696	48241	48793
Processing Vegetables	million lb	38915	42800	40500	40865	41232	41603	41978	42356	42737	43121	43510	43901
Potatoes	million lb	44135	44797	45155	45517	45881	46248	46618	46991	47367	47746	48128	48513
Specialty and Minor Vegetables	million lb	8000	8120	8242	8365	8491	8618	8748	8879	9012	9147	9284	9424
Beef, Commercial Production	million lb	26153	26135	26000	25565	25515	26017	26273	26365	26373	26586	26893	27132
Beef, Farm Production	million lb	105	105	105	105	105	105	105	105	105	105	105	105
Pork, Commercial Production	million lb	21055	21754	22265	21884	21866	21737	21904	22230	22623	23004	23372	23756
Pork, Farm Production	million lb	20	20	20	20	20	20	20	20	20	20	20	20
Broiler Production	million lb	35369	35442	36456	36722	36906	37090	37350	37748	38312	38888	39484	40098
Turkey Production	million lb	5612	5815	5862	5863	5879	5896	5910	5946	5998	6076	6176	6306
Dairy Cows	number of cows, 1000 head	9112	9148	9215	9230	9195	9160	9130	9105	9075	9040	9015	8985

FAPRI Agricultural Projections to 2017 (FAPRI, 2008)

Item	Unit	2007	2008	2009	2010	2011	2012	2013	2014	2015	2016	2017
Corn Yield	bushels/acre	151.1	153.5	155.5	157.8	159.9	162.1	164.3	166.4	168.6	170.8	173.0
Corn Production	million bushels	13074	12910	13214	13661	13541	13968	14298	14697	14862	15142	15212
Sorghum Yield	bushels/acre	74.2	64.6	64.6	64.9	65.2	65.4	65.6	65.8	66.1	66.3	66.6
Sorghum Production	million bushels	505	430	371	390	379	382	377	376	373	372	369
Barley Yield	bushels/acre	60.4	62.9	63.5	64.1	64.8	65.4	66.0	66.6	67.3	67.9	68.5
Barley Production	million bushels	212	227	241	239	232	233	232	232	230	229	226
Oats Yield	bushels/acre	60.9	61.9	62.2	62.6	62.9	63.3	63.6	63.9	64.2	64.6	64.9
Oats Production	million bushels	92	81	85	88	88	87	86	84	84	83	83
Wheat Yield	bushels/acre	40.5	42.7	42.9	43.2	43.5	43.9	44.2	44.5	44.9	45.2	45.5
Wheat Production	million bushels	2067	2244	2103	2111	2126	2136	2138	2146	2157	2163	2177
Rice Yield	lb/acre	7185	7074	7161	7216	7282	7332	7396	7451	7511	7571	7634
Rice Production	million hundredweight	197.5	204.3	188.7	204.5	203.9	215.9	215.4	227.2	228.8	230.0	237.1
Upland Cotton Yield	lb/acre	857	830	840	847	855	862	870	877	885	892	900
Upland Cotton Production	million bales	18.21	14.69	17.31	17.09	17.20	16.96	16.81	16.53	16.55	16.55	16.49
Soybean Yield	bushels/acre	41.2	42.5	42.9	43.4	43.8	44.3	44.7	45.1	45.6	46.0	46.5
Soybean Production	thousand tons	2585	2913	3082	3006	3118	3095	3130	3134	3183	3201	3262
Hay Yield	tons/acre	2.44	2.48	2.52	2.54	2.55	2.56	2.57	2.58	2.59	2.61	2.62
Hay Production	million tons	150.3	153.3	154.6	155.1	155.8	156.5	157.2	157.8	158.3	158.8	159.3
Sunflower Seed Yield	lb/acre	1437	1376	1389	1403	1418	1432	1446	1461	1475	1490	1505
Sunflower Seed Production	million lb	2889	2785	2781	2878	2937	2922	2953	2974	3022	3059	3114
Canola Seed Yield	lb/acre	1250	1431	1449	1467	1485	1503	1521	1539	1557	1575	1593
Canola Seed Production	million lb	1454	1933	1872	2125	2150	2110	2197	2252	2321	2388	2481
Peanut Yield	lb/acre	3130	3034	3062	3087	3114	3141	3169	3196	3223	3250	3276
Peanut Production	million lb	3741	3783	3962	4027	3965	4003	4004	3998	4026	4027	4053
Sugarbeet Yield	tons/acre	25.59	23.93	24.14	24.30	24.45	24.61	24.78	24.93	25.10	25.26	25.41
Sugarbeet Production	1,000 tons	31912	26386	28323	28850	28723	28697	29081	28845	29302	29322	29258
Sugarcane Yield	tons/acre	34.99	34.72	34.89	35.20	35.30	35.45	35.80	36.04	36.29	36.51	36.63
Sugarcane Production	1,000 tons	29101	27977	28078	28933	28469	28262	28752	28793	28977	29088	28773
Beef Production	million lb	26515	26465	26811	27388	27861	28336	28455	28485	28482	28440	28450
Pork Production	million lb	21959	22692	22786	22751	22836	23174	23675	24167	24509	24699	24887
Broiler Production	million lb	35492	36354	36812	37119	37583	38059	38531	38989	39525	40104	40741
Turkey Production	million lb	5825	5841	5800	5785	5801	5838	5882	5927	5977	6032	6094
Dairy Cows	number of cows, 1000 thousand head	9153	9245	9186	9187	9195	9199	9196	9184	9171	9161	9156

EERC
Energy & Environmental Research Center

APPENDIX D

WOOD PRODUCTION OUTLOOK

Timber harvests from forest land in the contiguous states, by region, 2002, with projections through 2005

	2002	2010	2020	2030	2040	2050
			Projections			
			Billion cubic feet			
Softwoods:						
Northeast	0.58	0.58	0.53	0.51	0.50	0.51
North Central	0.26	0.28	0.30	0.30	0.30	0.30 a
Southeast	2.92	2.67	3.17	3.41	3.70	4.06
South Central	3.69	3.21	3.64	4.00	4.39	4.79
North Rocky Mountains	0.50	0.44	0.43	0.44	0.46	0.46
South Rocky Mountains	0.10	0.25	0.28	0.32	0.35	0.36
Pacific Northwest West	1.55	1.65	1.58	1.57	1.65	1.78 b
Pacific Northwest East	0.20	0.24	0.20	0.29	0.31	0.34 c
Pacific Southwest	0.72	0.46	0.47	0.47	0.49	0.49 d
Softwoods Total Harvests	10.51	9.77	10.67	11.31	12.15	13.11
Hardwoods:						
Northeast	1.29	1.51	1.55	1.59	1.73	1.87
North Central	1.42	1.43	1.47	1.51	1.53	1.65
Southeast	1.19	1.55	1.63	1.70	1.66	1.64
South Central	1.84	2.28	2.44	2.58	2.70	2.86
West	0.25	0.63	0.62	0.62	0.62	0.62
Hardwoods Total Harvests	5.99	7.40	7.70	7.99	8.24	8.65

a. Includes the Great Plains States: Kansas, Nebraska, North Dakota, and eastern South Dakota.

b. Excludes Alaska. Includes western Oregon and western Washington and is also called the Douglas fir subregion.

c. Includes eastern Oregon and eastern Washington and is also called the ponderosa pine subregion.

d. Excludes Hawaii.

Source: The 2005 RPA Timber Assessment Update

APPENDIX E

URBAN RESIDUES OUTLOOK

State	Census April 1, 2000	Per Capita Estimated Generation (tons/person/yr)*	Projections July 1, 2010	Estimated MSW Generation (tons/yr), 2010	Projections July 1, 2015	Estimated MSW Generation (tons/yr), 2015	Projections July 1, 2020	Estimated MSW Generation (tons/yr), 2020	Projections July 1, 2025	Estimated MSW Generation (tons/yr), 2025	Projections July 1, 2030	Estimated MSW Generation (tons/yr), 2030
Alabama	4,447,100	1.52	4,596,330	6,986,422	4,663,111	7,087,929	4,728,915	7,187,951	4,800,092	7,296,140	4,874,243	7,408,849
Alaska	626,932	1.13	694,109	784,343	732,544	827,775	774,421	875,096	820,881	927,596	867,674	980,472
Arizona	5,130,632	1.33	6,637,381	8,827,717	7,495,238	9,968,667	8,456,448	11,247,076	9,531,537	12,676,944	10,712,397	14,247,488
Arkansas	2,673,400	1.23	2,875,039	3,536,298	2,968,913	3,651,763	3,060,219	3,764,069	3,151,005	3,875,736	3,240,208	3,985,456
California	33,871,648	1.38	38,067,134	52,532,645	40,123,232	55,370,060	42,206,743	58,245,305	44,305,177	61,141,144	46,444,861	64,093,908
Colorado	4,301,261	1.82	4,831,554	8,793,428	5,049,493	9,190,077	5,278,867	9,607,538	5,522,803	10,051,501	5,792,357	10,542,090
Connecticut	3,405,565	0.96	3,577,490	3,434,390	3,635,414	3,489,997	3,675,650	3,528,624	3,691,016	3,543,375	3,688,630	3,541,085
Delaware	783,600	1.16	884,342	1,025,837	927,400	1,075,784	963,209	1,117,322	990,694	1,149,205	1,012,658	1,174,683
District of Columbia	572,059	1.76	529,785	932,422	506,323	891,128	480,540	845,750	455,108	800,990	433,414	762,809
Florida	15,982,378	1.31	19,251,691	25,219,715	21,204,132	27,777,413	23,406,525	30,662,548	25,912,458	33,945,320	28,685,769	37,578,357
Georgia	8,186,453	1.24	9,589,080	11,890,459	10,230,578	12,685,917	10,843,753	13,446,254	11,438,622	14,183,891	12,017,838	14,902,119
Hawaii	1,211,537	1.29	1,340,674	1,729,469	1,385,952	1,787,878	1,412,373	1,821,961	1,438,720	1,855,949	1,466,046	1,891,199
Idaho	1,293,953	0.85	1,517,291	1,289,697	1,630,045	1,385,538	1,741,333	1,480,133	1,852,627	1,574,733	1,969,624	1,674,180
Illinois	12,419,293	2.07	12,916,894	26,737,971	13,097,218	27,111,241	13,236,720	27,400,010	13,340,507	27,614,849	13,432,892	27,806,086
Indiana	6,080,485	2.15	6,392,139	13,743,099	6,517,631	14,012,907	6,627,008	14,248,067	6,721,322	14,450,842	6,810,108	14,641,732
Iowa	2,926,324	1.46	3,009,907	4,394,464	3,026,380	4,418,515	3,020,496	4,409,924	2,993,222	4,370,104	2,955,172	4,314,551
Kansas	2,688,418	1.48	2,805,470	4,152,096	2,852,690	4,221,981	2,890,566	4,278,038	2,919,002	4,320,123	2,940,084	4,351,324
Kentucky	4,041,769	1.88	4,265,117	8,018,420	4,351,188	8,180,233	4,424,431	8,317,930	4,489,662	8,440,565	4,554,998	8,563,396
Louisiana	4,468,976	1.43	4,612,679	6,596,131	4,673,721	6,683,421	4,719,160	6,748,399	4,762,398	6,810,229	4,802,633	6,867,765
Maine	1,274,923	1.66	1,357,134	2,252,842	1,388,878	2,305,537	1,408,665	2,338,384	1,414,402	2,347,907	1,411,097	2,342,421
Maryland	5,296,486	1.25	5,904,970	7,381,213	6,208,392	7,760,490	6,497,626	8,122,033	6,762,732	8,453,415	7,022,251	8,777,814
Massachusetts	6,349,097	1.42	6,649,441	9,442,206	6,758,580	9,597,184	6,855,546	9,734,875	6,938,636	9,852,863	7,012,009	9,957,053
Michigan	9,938,444	1.26	10,428,683	13,140,141	10,599,122	13,354,894	10,695,993	13,476,951	10,713,730	13,499,300	10,694,172	13,474,657
Minnesota	4,919,479	1.14	5,420,636	6,179,525	5,668,211	6,461,761	5,900,769	6,726,877	6,108,787	6,964,017	6,306,130	7,188,988
Mississippi	2,844,658	1.10	2,971,412	3,268,553	3,014,409	3,315,850	3,044,812	3,349,293	3,069,420	3,376,362	3,092,410	3,401,651
Missouri	5,595,211	1.70	5,922,078	10,067,533	6,069,556	10,318,245	6,199,882	10,539,799	6,315,366	10,736,122	6,430,173	10,931,294
Montana	902,195	1.51	968,598	1,462,583	999,489	1,509,228	1,022,735	1,544,330	1,037,387	1,566,454	1,044,898	1,577,796
Nebraska	1,711,263	1.34	1,768,997	2,370,456	1,788,508	2,396,601	1,802,678	2,415,589	1,812,787	2,429,135	1,820,247	2,439,131
Nevada	1,998,257	1.21	2,690,531	3,255,543	3,058,190	3,700,410	3,452,283	4,177,262	3,863,298	4,674,591	4,282,102	5,181,343
New Hampshire	1,235,786	0.97	1,385,560	1,343,993	1,456,679	1,412,979	1,524,751	1,479,008	1,586,348	1,538,758	1,646,471	1,597,077
New Jersey	8,414,350	1.47	9,018,231	13,256,800	9,255,769	13,605,980	9,461,635	13,908,603	9,636,644	14,165,867	9,802,440	14,409,587
New Mexico	1,819,046	1.09	1,980,225	2,158,445	2,041,539	2,225,278	2,084,341	2,271,932	2,106,584	2,296,177	2,099,708	2,288,682

Continued...

State	Census April 1, 2000	Per Capita Estimated Generation (tons/person/yr)*	Projections July 1, 2010	Estimated MSW Generation (tons/yr), 2010	Projections July 1, 2015	Estimated MSW Generation (tons/yr), 2015	Projections July 1, 2020	Estimated MSW Generation (tons/yr), 2020	Projections July 1, 2025	Estimated MSW Generation (tons/yr), 2025	Projections July 1, 2030	Estimated MSW Generation (tons/yr), 2030
New York	18,976,457	1.12	19,443,672	21,776,913	19,546,699	21,892,303	19,576,920	21,926,150	19,540,179	21,885,000	19,477,429	21,814,720
North Carolina	8,049,313	0.93	9,345,823	8,691,615	10,010,770	9,310,016	10,709,289	9,959,639	11,449,153	10,647,712	12,227,739	11,371,797
North Dakota	642,200	1.04	636,623	662,088	635,133	660,538	630,112	655,316	620,777	645,608	606,566	630,829
Ohio	11,353,140	1.47	11,576,181	17,016,986	11,635,446	17,104,106	11,644,058	17,116,765	11,605,738	17,060,435	11,550,528	16,979,276
Oklahoma	3,450,654	1.23	3,591,516	4,417,565	3,661,694	4,503,884	3,735,690	4,594,899	3,820,994	4,699,823	3,913,251	4,813,299
Oregon	3,421,399	1.20	3,790,996	4,549,195	4,012,924	4,815,509	4,260,393	5,112,472	4,536,418	5,443,702	4,833,918	5,800,702
Pennsylvania	12,281,054	1.33	12,584,487	16,737,368	12,710,938	16,905,548	12,787,354	17,007,181	12,801,945	17,026,587	12,768,184	16,981,685
Rhode Island	1,048,319	1.27	1,116,652	1,418,148	1,139,543	1,447,220	1,154,230	1,465,872	1,157,855	1,470,476	1,152,941	1,464,235
South Carolina	4,012,012	1.15	4,446,704	5,113,710	4,642,137	5,338,458	4,822,577	5,545,964	4,989,550	5,737,983	5,148,569	5,920,854
South Dakota	754,844	1.09	786,399	857,175	796,954	868,680	801,939	874,114	801,845	874,011	800,462	872,504
Tennessee	5,689,283	2.01	6,230,852	12,524,013	6,502,017	13,069,054	6,780,670	13,629,147	7,073,125	14,216,981	7,380,634	14,835,074
Texas	20,851,820	1.33	24,648,888	32,783,021	26,585,801	35,359,115	28,634,896	38,084,412	30,865,134	41,050,628	33,317,744	44,312,600
Utah	2,233,169	1.11	2,595,013	2,880,464	2,783,040	3,089,174	2,990,094	3,319,004	3,225,680	3,580,505	3,485,367	3,868,757
Vermont	608,827	1.04	652,512	678,612	673,169	700,096	690,686	718,313	703,288	731,420	711,867	740,342
Virginia	7,078,515	1.60	8,010,245	12,816,392	8,466,864	13,546,982	8,917,395	14,267,832	9,364,304	14,982,886	9,825,019	15,720,030
Washington	5,894,121	1.30	6,541,963	8,504,552	6,950,610	9,035,793	7,432,136	9,661,777	7,996,400	10,395,320	8,624,801	11,212,241
West Virginia	1,808,344	1.17	1,829,141	2,140,095	1,822,758	2,132,627	1,801,112	2,107,301	1,766,435	2,066,729	1,719,959	2,012,352
Wisconsin	5,363,675	1.05	5,727,426	6,013,797	5,882,760	6,176,898	6,004,954	6,305,202	6,088,374	6,392,793	6,150,764	6,458,302
Wyoming	493,782	1.34	519,886	696,647	528,005	707,527	530,948	711,470	529,031	708,902	522,979	700,792
United States	281,421,906	1.38	308,935,581	426,331,102	322,365,787	444,864,786	335,804,546	463,410,273	349,439,199	482,226,095	363,584,435	501,746,520

E-2

EERC

Energy & Environmental Research Center

APPENDIX F

EXTERNAL CHEMICAL ANALYSIS AND PHYSICAL CHARACTERIZATION DATA REFERENCES

EXTERNAL CHEMICAL ANALYSIS AND PHYSICAL CHARACTERIZATION DATA REFERENCES

Alter, H. *Municipal Solid Waste*; Marcel Dekker, Inc.: New York, NY, 1983.

Arola, R.A.; Radcliffe, R.C.; Sturos, J.B. Characterizing Chunkwood. In *Chunkwood: Production, Characterization, and Utilization*; General Technical Report NC-145, U.S. Department of Agriculture, Forest Service, North Central Forest Experiment Station: St. Paul, MN, 1981.

Arola, R.A.; Miyata, E.S. Harvesting Wood for Energy. U.S. Department of Agriculture Forest Service, Research Paper NC-200, North Central Forest Experiment Station, St. Paul, MN, 1981; 25 p.

Bridgeman, T.G.; Jones, J.M.; Shield, I.; Williams, P.T. Torrefaction of Reed Canary Grass, Wheat Straw and Willow to Enhance Solid Fuel Qualities and Combustion Properties. *Fuel* **2008**, 87, 844–856.

California Energy Commission, *An Assessment of Biomass Resources in California, 2007*; Draft Report; Contract No. 500-01-016, March 2008.

Chang, N.B. Davila, E. Municipal Solid Waste Characterizations and Management Strategies for the Lower Rio Grande Valley, Texas. *Waste Management* **2008**, *28*, 776–794.

Clarke, M.; Guidotti, P. Waste Incineration in the Pulp and Paper Industry. *Paper Technology* **1995**, *36*, 26–30.

Dierenfeld, E.S.; Atkinson, S.; Craig, A.M.; Walker, K.C.; Streich, W.J.; Clauss, M. Mineral Concentrations in Serum/Plasma and Liver Tissues of Captive and Free-Ranging Rhinoceros Species. *Zoo Biology* **2005**, *24*.

European Bioenergy Networks. Biomass Co-Firing – An Efficient Way to Reduce Greenhouse Gas Emission, VTT Processes, Finland, March 2003.

Evans, R.J.; Knight R.A.; Onischak, M.; Babu, S.P. *Development of Biomass Gasification to Produce Substitute Fuels*; Report PNL-6518; Pacific Northwest Laboratory (PNL), Richland, 1988; p. 14.

Fasina, O.; Ranatunga, T.; Vaughan, B. Physical and Chemical Characteristics of Biofuel Feedstocks Indigenous to Southeastern United States. Presented at the 2007 ASABE Annual International Meeting, Minneapolis, MN, June 17–20, 2007, Paper No. 076247.

Garcia, R.A.; Rosentrater, K.A. Concentration of Key Elements in North American Meat and Bone Meal. *Biomass and Bioenergy* **2008**, *32*, 887–891.

Guar, S.; Reed, T.B. *Thermal Data for Natural and Synthetic Fuels*; Marcel Dekker, Inc.: New York, NY, 1998.

Hanley, T.A.; McKendrick, J.D. *Seasonal Changes in Chemical Composition and Nutritive Value of Native Forages in a Spruce-Hemlock Forest, Southeastern Alaska*; Res. Pap. PNW-312. Portland, OR; U.S. Department of Agriculture, Forest Service, Pacific Northwest Forest and Range Experiment Station; Nov 1983; 41 p.

Khan, A.A.; de Jong, W.; Jansens, P.J.; Spliethoff, H. Biomass Combustion in Fluidized-Bed Boilers: Potential Problems and Remedies. *Fuel Process. Technol.* **2009**, *90*, 21–50.

Kitani, O.; Hall, C.W. Biomass Handbook; Grodon and Breach Science Publishers Ltd: New York, 1989.

Krotscheck, A.W.; Sixta, H. Characterization of Black Liquor, Chapter 9: Recovery. In *Handbook of Pulp*, Sixta, H., Ed.; Wiley – VCH, Feb 2006.

Kyari, M.; Cunliffe, A.; Williams, P.T. Characterization of Oils, Gases, and Char in Relation to the Pyroloysis of Different Brands of Scrap Automotive Tires, *Energy & Fuels* **2005**, *19* (3), 1165–1173.

Lynd, L.R.; Wyman, C.E.; Gerngross, T.U. Biocommodity Engineering. *Biotechnology Progress,* **1999**, *15*, 777–793.

McDaniel, J. *Biomass Cogasification at Polk Power Station*; Final Technical Report for Tampa Electric Company, May 2002.

McNeil Technologies, Inc. *Biomass Resource Assessment and Utilization Options for Three Counties in Eastern Oregon*; Report for Oregon Department of Energy; Dec 31, 2003.

Miles, T.R.; Miles, T.R., Jr.; Baxter, L.L.; Byers, R.W.; Jenkins, B.W.; Oden, L.L. *Biomass Bioenergy* **1996**, *10*, 125–138.

Miller, B.G.; Pisupati, S.V.; Johnson, D.; Clifford, D.J.; Badger, M.W.; Wasco, R.W.; Falcone Miller, S.; Mitchell, G.D.; Tillman, D. Enhanced Biomass Characterization: A Foster Wheeler Energy Corporation/ Penn State Initiative. www.brdisolutions.com/pdfs/bcota/abstracts/18/z177.pdf (accessed Dec 2008).

Richard, T.; Trautmann, N.; Krasny, M.; Frendeburg, S.; Stuart, C. Substrate Composition Table. Cornell University, Ithaca, NY, http://compost.css.cornell.edu/calc/lignin.noframes.html (accessed Jan 2009).

Thipse, S.S.; Sheng, C.; Booty, M.R.; Magee, R.S.; Bozzelli, J.W. Chemical Makeup and Physical Characterization of Synthetic Fuel and Methods of Heat Content Evaluation for Studies on MWS Incineration, *Fuel* **2002**, *81*, 211–217.

Thy, P.; Grundvig, S.; Jenkins, B. M.; Shiraki, R.; Lesher, C.E. Analytical Controlled Losses of Potassium from Straw Ashes. *Energy Fuels* **2005**, *19* (6), 2571–2574.

Tillman, D.A.; Harding, *N.S. Fuels of Opportunity: Characteristics and Uses in Combustion Systems*; Elsevier, 2004.

Tillman, D.A. *The Combustion of Solid Fuels and Wastes*; Academic Press, Inc.: San Diego, CA, 1991.

Tsamba, A.J.; Yang, W.; Blasiak, W.; Wojtowicz, M.A. Cashew Nut Shells Pyroloysis: Individual Gas Evolution Rates and Yields. *Energy Fuels* **2007**, *21*, 2357–2362.

U.S. Department of Agriculture Soil Conservation Service. *Agriculture Waste Management Field Handbook, Chapter 4: Agricultural Waste Characteristics*; No. 210-AWMFH, 4/92, April 1992.

Valenzuela, M.B.; Jones, C.W.; Agrawal, P.K. Batch Aqueous-Phase Reforming of Woody Biomass. *Energy & Fuels* **2006**, *20* (4), 1744–1752.

Whitely, N.; Ozao, R.; Artiaga, R.; Cao, Y.; Pan, W.-P. Multi–utilization of Chicken Litter as Biomass Source, Part I. Combustion. *Energy Fuels* **2006**, *20* (6), 2660–2665.

EERC

Energy & Environmental Research Center

APPENDIX G

DEFINITIONS AND METHODS OF CHARACTERIZATION ANALYSIS

DEFINITIONS AND METHODS OF CHRATERIZATION ANALYSIS

Various methods are used to determine biomass properties. The list below describes typical methods used for analyzing combustion feedstocks. Analyses may be conducted on an as-determined basis; i.e., samples were air-dried before analysis and the moisture losses were recorded, or reported on an as-received basis, meaning the samples are analyzed without prior drying.

Ash Content – The solid residue that remains after the biomass is utilized for energy production is measured by combusting the biomass in a weighed crucible inside of a laboratory furnace. When performed together with moisture, volatiles, and fixed carbon analyses, the total analysis is called "proximate" analysis.

Ash Melting Behavior – Ash melting behavior was not determined in the sources reviewed.

Bulk Density – Bulk density is the density of the loose fuel or ash. Here, "loose" means that the material has not been packed down, so the density measurement includes any air pockets that may form.

Chlorine Content – The chlorine content of biomass is often measured as part of the CHN analysis by including a chlorine analyzer for the product gas.

C, H, N Content – The carbon (C), hydrogen (H), and nitrogen (N) content of a biomass sample is typically measured by combusting the biomass in a test furnace and analyzing the product gas.

Energy Content/Calorific Value – Energy content is represented on as Btu/lb on a dry weight basis. This may be reported as a higher heating value (HHV) or a lower heating value (LHV), because not all laboratories specify which method is used. HHV measures the amount of energy liberated when fuel at 25°C is combusted, cooled back to 25°C, and all product water is condensed. LHV measures the amount of energy recovered when the combustion gas is only cooled to 150°C, meaning the latent heat of water is not recovered. Energy content is generally reported with the proximate and/or ultimate analysis. In some cases, energy content may not be actually measured, but the calculated calorific value based on proximate and ultimate analysis may be reported.

Fixed Carbon – The combustible portion of the biomass that is not driven off as volatiles is measured by first driving off volatiles, then measuring ash content to determine the amount of fixed carbon remaining in the biomass.

Fluorine Content – Fluorine content was typically not determined in the sources reviewed.

Major Elements (Na, K, Ca, Mg, Si, P, Fe, Al, Ti) – The major elements present in biomass ash are generally determined by x-ray fluorescence (XRF). This technique can be

performed using an electron-dispersive spectrometer (EDS) or a wavelength-dispersive spectrometer (WDS). The EERC's XRF analyzer uses WDS equipped with a rhodium x-ray tube and six analyzing crystals to determine the bulk chemistry of a sample. The sample is usually ground to a powder and pressed into a pellet or fused with a fluxing agent to produce a glass disc. Typically, it is assumed that all major elements are present as oxides in the ash when calculating ash composition. This may not be true if the ash contains significant carbonate, sulfate, or unoxidized material.

Minor Elements (Cd, Ti, Hg, Sb, As, Cr, Co, Cu, Mn, Ni, V, Pb, Sn, Zn) – These and other trace metals can be determined as part of an XRF analysis along with the major elements. However, most laboratories that use XRF for ash analysis (including the EERC) do not report the minor elements by default. As such, they are usually only reported when requested.

Moisture Content – The amount of water remaining in biomass is measured, typically by drying the biomass sample at around 100°C for 2 hours, although exact methods may vary by fuel sample and laboratory.

Oxygen Content – The oxygen content of a biomass sample is typically determined by measuring the weight loss during CHN analysis. It is not actually possible to measure a combustion product for oxygen, but if the CHN content is known and the weight loss is known, then the weight of CHN can be subtracted from the weight loss to give the oxygen by difference.

Size Distribution – The distribution of particle sizes for a fuel or ash sample. May be measured by various techniques depending on the particle-size range and the capabilities of the analytical laboratory.

Sulfur Content – The sulfur content of biomass is often determined as part of the CHN analysis by measuring SO_2. When this is done in conjunction with oxygen analysis, the overall analysis is referred to as CHNOS or "ultimate" analysis.

Ultimate Analysis – The ultimate analysis includes the CHNOS results.

Volatiles – Elements or compounds found in biomass that become a gas under elevated temperatures or pressures are measured by heating the biomass (generally to 950°C) under an inert atmosphere to drive off volatile components without combusting nonvolatile or "fixed" carbon.